SHAPE MEMORY POLYMER COMPOSITES CONTAINING CARBON BASED FILLERS

A THESIS SUBMITTED TO
THE GRADUATE SCHOOL OF NATURAL AND APPLIED SCIENCES
OF
MIDDLE EAST TECHNICAL UNIVERSITY

BY

İREM ŞENGÖR

IN PARTIAL FULFILLMENT OF THE REQUIREMENTS
FOR
THE DEGREE OF MASTER OF SCIENCE
IN
CHEMICAL ENGINEERING

AUGUST 2013

Approval of the thesis:

SHAPE MEMORY POLYMER COMPOSITES CONTAINING CARBON BASED FILLERS

submitted by **İREM ŞENGÖR** in partial fulfillment of the requirements for the degree of **Master of Science in Chemical Engineering Department, Middle East Technical University** by,

Prof. Dr. Canan Özgen
Dean, Graduate School of **Natural and Applied Sciences** _____

Prof. Dr. Deniz Üner
Head of Department, **Chemical Engineering** _____

Prof. Dr. Göknur Bayram
Supervisor, **Chemical Engineering Dept., METU** _____

Assist. Prof. Dr. Özcan Köysüren
Co-supervisor, **Chemical Engineering Dept., KSU** _____

Examining Committee Members:

Prof. Dr. Cevdet Kaynak
Metallurgical and Materials Engineering Dept., METU _____

Prof. Dr. Göknur Bayram
Chemical Engineering Dept., METU _____

Assist. Prof. Dr. Özcan Köysüren
Chemical Engineering Dept., KSU _____

Assoc. Prof. Dr. Arcan Dericioğlu
Metallurgical and Materials Engineering Dept., METU _____

Assist. Prof. Dr. Serkan Kıncal
Chemical Engineering Dept., METU _____

Date: 26.08.2013 _____

I hereby declare that all information in this document has been obtained and presented in accordance with academic rules and ethical conduct. I also declare that, as required by these rules and conduct, I have fully cited and referenced all material and results that are not original to this work.

Name, Last name : İrem Şengör

Signature :

ABSTRACT

SHAPE MEMORY POLYMER COMPOSITES CONTAINING CARBON BASED FILLERS

Şengör, İrem

M.Sc., Department of Chemical Engineering

Supervisor: Prof. Dr. Göknur Bayram

Co-Supervisor: Assist. Prof. Dr. Özcan Köysüren

August 2013, 113 pages

The aim of this dissertation was to produce shape memory polymer nanocomposites using diglycidyl ether of bisphenol A (DGEBA) epoxy resin and isophorone diamine based cyclo-aliphatic curing agent. The polymer matrix was modified with aliphatic and aromatic monomers namely, neopentyl glycol diglycidyl ether (NGDE) and resorcinol diglycidyl ether (RDE). In the formation of composites, carbon black and carbon nanotubes were used separately and also together as hybrid filler. All samples were subjected to mechanical (tensile and impact tests), thermal (DSC analysis), electrical (electrical resistivity test), morphological (SEM analysis) and shape memory characterization tests (bending test).

In consequence of these characterization tests, 15 wt. % monomer containing polymers were found to have superior properties for both NGDE and RDE containing formulations. For CB loaded composites, percolation threshold was found at 1 wt. % loading and for carbon nanotube loaded composites it was found at 0.25 wt. %. In formation of hybrid composites carbon black amount was kept constant as 1 wt. % for all formulations and carbon nanotube amount was varied as 0.25 %, 0.5 % and 1 % by weight. Among these compositions, hybrid composite containing 1 % CB and 0.5 % CNT was found to have better properties for generally all characterization tests. As final composites 15 % NGDE and 15 % RDE were combined with 1 %CB, 0.5 %CNT and 1 % CB - 0.5 % CNT filler compositions.

NGDE containing composites had much lower glass transition temperature compared to RDE containing ones and the composites which did not contain monomer. There was no significant difference in shape recovery values in final composites and these values were calculated in the range between 97-99 %. Same comment can be made for shape fixity property. Composites containing NGDE showed faster shape recovery than the other composites. Electrical shape memory actuation was applied for the sample containing 2

wt. % carbon nanotube only with the application of constant 100 V. Shape recovery was achieved at 49°C, whereas this value was determined as 90°C for thermal actuation.

Finally, cyclic shape memory tests were applied for investigation of performance of neat epoxy and samples of E-15N, E-15N-1CB, E-15N-0.5CNT and E-15N-1CB-0.5CNT. Totally 10 consecutive cycles were applied on each sample. It was found that amount of cycles did not affect shape recovery for any sample. While percent shape fixity decreased by 2-3 % for neat epoxy and E-15N samples and did not change for the other composites. Recovery time was increased continuously for neat epoxy, but did not change for E-15N-0.5CNT and E-15N-1CB-0.5CNT samples.

Keywords: shape memory polymers, carbon nanotube, carbon black, hybrid composites, electrical actuation

ÖZ

KARBON BAZLI DOLGU MADDELERİ İÇEREN ŞEKİL HAFIZALI POLİMER KOMPOZİTLERİ

Şengör, İrem

Yüksek Lisans, Kimya Mühendisliği Bölümü

Tez Yöneticisi: Prof. Dr. Göknur Bayram

Ortak Tez Yöneticisi: Assist. Prof. Dr. Özcan Köysüren

Ağustos 2013, 113 sayfa

Bu çalışmanın amacı diglisidil eter bisfenol A epoksi (DGEBA) reçinesi ve izoforon diamin bazlı siklo-alifatik kürlenme ajanı kullanarak şekil hafızalı polimer nanokompozitleri üretmektir. Polimer matriksi neopentil glikol diglisidil eter (NGDE) ve aromatik risorsinol diglisidil eter (RDE) olarak adlandırılan alifatik ve aromatik monomerler ile modifiye edilmiştir. Kompozitlerin üretiminde karbon siyahı (CB), karbon nanotüp (CNT) ayrı bir şekilde ve beraber hibrit dolgu maddesi olarak kullanılmıştır. Bütün numuneler mekanik (çekme ve darbe testleri), ısıl (DSC analizi), elektriksel (elektriksel özdirenç ölçüm testi), morfolojik (SEM analizi), ve şekil hafıza karakterizasyon (bükme testi) testlerine tabi tutulmuştur.

Karakterizasyon testlerinin sonucunda her iki NGDE ve RDE içeren monomer formülasyonunda kütlece % 15 monomer içeren numunelerin diğerlerine göre daha başarılı özelliklere sahip olduğu bulunmuştur. CB içeren kompozitler için perkolasyon eşiği ağırlıkça % 1 dolgu maddesi miktarında görülmüş, CNT içeren kompozitler için ise bu değer ağırlıkça % 0.25 olarak belirlenmiştir. Hibrit kompozitlerin üretiminde CB miktarı % 1 olarak sabit tutulup, karbon nanotüp miktarı % 0.25, % 0.5 ve % 1 olarak değiştirilmiştir. Bu kompozisyonlar arasında % 1 CB ve % 0.5 CNT içeren hibrit kompozitin genel olarak bütün karakterizasyon testlerine göre diğer numunelerden daha iyi özelliklere sahip olduğu görülmüştür. Final kompozitleri olarak, % 15 NGDE ve % 15 RDE monomerleri % 1 CB, % 0.5 CNT ve % 1CB-% 0.5CNT dolgu maddesi kompozisyonları ile birleştirilmiştir.

NGDE içeren kompozitler, RDE içeren veya monomer içermeyen kompozitlere göre çok daha düşük camsı geçiş sıcaklığına sahiptir. Final kompozitlerinde şekil geri kazanım değerleri arasında fark görülmemiş ve bu değerler % 97-% 99 aralığında hesaplanmıştır. Aynı yorum şekil sabitleme özelliği için de yapılabilir. NGDE içeren kompozitler diğerlerine göre daha hızlı geri kazanımı göstermişlerdir. Elektriksel tetikleme sadece %

2 CNT içeren numune için sabit 100 V'ta uygulanmıştır. Şekil geri kazanımına 49°C'de ulaşılmıştır, bu değer ısıl tetikleme için 90°C olarak belirlenmiştir.

Sonuç olarak, saf epoksi, E-15N, E-15N-1CB, E-15N-0.5CNT ve E-15N-1CB-0.5CNT numunelerinin performans ölçümlerinin incelenmesi için döngüsel şekil hafıza testleri uygulanmıştır. Her numuneye toplamda 10 döngü uygulanmıştır. Döngü sayısının hiçbir numune için şekil geri kazanım değerine etki etmediği belirlenmiştir. Şekil sabitlenme yüzdesi saf epoksi ve E-15N numuneleri için % 2-3 azalırken, diğer kompozitler için değişmemiştir. Şekil geri kazanım süresi saf epoksi numunesi için döngü miktarı ile devamlı artarken, E-15N-0.5CNT ve E-15N-1CB-0.5CNT numuneleri için değişiklik göstermemiştir.

Anahtar kelimeler: şekil hafızalı polimerler, karbon nanotüp, karbon siyahı, hibrit kompozitler, elektriksel tetikleme

To my family

ACKNOWLEDGEMENTS

To begin with, I would like to express my deepest appreciations to my supervisor Prof. Dr. Göknur Bayram for giving unlimited support, patience and advices throughout my study. Without her encouraging attitude it would not be possible for me to study with full motivation and willingness. I will always feel lucky that I had a chance to study with her. I am also grateful to my co-supervisor Assist. Prof. Dr. Özcan Köysüren for his guidance and help during my thesis study.

I would like to thank to Yiğit Genç from IMDB for supplying epoxy polymer and Murat Marmara from Orion Carbons for supplying carbon black for my project. Additionally, I would like to thank to Mihrican Açıkgöz for her supports in the application of DSC analysis.

I wish to thank Nisa Ilgaz and Feride Nur Ersaraç for sharing their experiences with me about the shape memory topic and epoxy polymer. Besides, I wish to thank to my present lab mates Eda Açık, Toufik Baouz, Yüksel Sayın, Miray Yaşar and Erdem Balık for their contributions in conducting my experiments and also for their friendly attitudes. I would sincerely thank to Kübra Yamanel, Ülkü Katırcı, Muzaffer Soyer, Hanen Çiftdoğan, Pelin Aslan, Tutku Gökalp and Ceren Baykal for their unlimited support and kind friendship throughout my life. I would like to express my deepest appreciations to Gülçin Kadıoğlu, Özge Küçüktaşkıran and Burcu Gökbudak for their valuable friendship and especially for not letting me alone in laboratory and accompanying me during most of my experiments. Words will never be enough to state my gratefulness to all my friends for their supports.

I would like to thank to my boss in ASELSAN, Tevfik Yüksel and chief engineers A. Z. Bülent Taşkeli and Muhittin Aday for their tolerance and especially for making me possible to finish my graduate studies. Also I want to acknowledge my co-workers Aslı Boran and Korhan Sezgiker for their support and kind friendship.

Finally, an honourable mention should go to my family; to whom I dedicated this study. I would like to thank to my parents, Şükran and Erol Şengör for their never ending love, patience and unlimited supports which were absolutely a must for me to complete this study with success. I wish to thank to my grandmother Mübeccel Kunak, my uncle Ali Kunak and his wife Aygen Kunak, and my dear cousin Merve Kunak for their everlasting motivations. Certainly I would like to express my most intimate appreciations to my dearest sister Esra Şengör Şenalp and to her husband M. Gürsan Şenalp for always helping and encouraging me in finishing this study, and also supporting me through all my life. Finally, I would like to finish the acknowledgements by thanking my little nephew Ege Şenalp for being born. Every little smile that he showed me were contributions to my motivation.

TABLE OF CONTENTS

LIST OF TABLES

TABLES

LIST OF FIGURES

FIGURES

NOMENCLATURE

A	Area, cm^2
E	Young's Modulus, MPa
F	Force measured during tensile testing, N
G	Gauge length, mm
$\Delta H_{uncured}$	Heat of cure for uncured resin, J/g
ΔH_{cured}	Heat of cure for cured resin, J/g
I	Current, A
L	length, cm
L_i	Instantaneous strain, cm
L_f	Fixed strain, cm
R	Resistance, Ω
R_f	Shape fixity, %
R_r	Shape recovery ratio, %
S	Cross sectional area, cm^2
T_g	Glass transition temperature, °C
TS	Ultimate tensile strength, MPa
t_{rec}	Recovery time, s
V	Voltage, V

Greek Letter

ρ	Volumetric resistivity, Ω.cm
σ	Stress, MPa
σ_y	Stress at yield
ϵ	Strain

τ	Tensile Strength, MPa
$\% \epsilon_{break}$	Elongation at break
θ_f	Fixed angle
θ_i	Initial loading angle
θ_r	Recovered angle

Abbreviations

CB	Carbon Black
CNT	Carbon nanotube
DGEBA	Diglycidyl ether of bisphenol A
DSC	Differential Scanning Calorimetry
MWNT	Multi walled carbon nanotube
NGDE	Neopentyl glycol diglycidyl ether
NTC	Negative temperature coefficient
PTC	Positive temperature coefficient
RDE	Resorcinol diglycidyl ether
SEM	Scanning Electron Microscopy
SWNT	Single walled carbon nanotube

CHAPTER 1

INTRODUCTION

Smart matters are intelligent materials which can change their function upon certain stimulus from the environment **[1]**. Shape memory materials constitute an important example among those intelligent materials. Substances that are able to remember their shape drew considerable attention due to their unique capability of being fixed into a temporary shape, then recovering their original shape with the application of an external effect. Shape memory alloy was first developed in early 1930s and further developed in 1970s. At the present time several different types of shape memory alloys are being produced and used in many application areas like automotive and biomedical applications **[2]**. L. B. Vernon was first to publish a work related to a shape memory effect of a polymer in 1941. Later in 1960s shape memory polyethylene is used in heat shrinkable tubing. The attention drawn to shape memory polymers has been growing day by day since then **[3]**.

Shape memory polymers provide several advantages when compared to shape memory alloys. Having low density, low cost and easy processing features make them versatile among the other types of shape memory materials. Having high elastic deformation, they can be used in greater extent of usage areas like electronics, textile and aerospace industry. It is also possible to tailor the application temperature by using different combination of polymers which offers a broad range of application temperature and the ability to work in the desired temperature range. Some shape memory polymers have also biocompatibility, biodegradability and controlled drug release features, which make them potential candidates for being used in biomedical applications **[3, 4]**.

Shape memory polymers can be used in quite a few applications. Heat shrinking ability of these smart materials lead them to be used in packaging and heat shrink tubings. They are used for protection and insulation for electronic cables. They are able to shrink when heated to proper temperature **[1, 5]**. In biomedical applications shape memory polymers can be used in vascular stents, clot removal, orthodontic wires and many other biomedical devices. Ongoing biocompatibility studies will enhance the applications in biomedicine **[4]**. Shape changing materials are gathering attention also in textile industry. Shape memory polyurethane fabrics, originally increased form at room temperature are able to become smooth when reaches higher temperature. Another example is a fabric which fits on the wearer's body figure without the application of tension. Upon heating, the permanent size recovers again **[6]**. Leng et al. listed some usage areas of shape memory polymers in aerospace industry which are used as deployable structures. Deployable hinges, mirrors, reflectors for antennas and morphing wings are some examples of the studies that are carried out in literature **[7]**.

Shape memory actuation can be applied using different triggering mechanisms. Besides the traditional approaches, the novel techniques play key roles for developing multi functional devices. Thermal triggering is the most common and versatile way of inducing shape memory polymer **[7]**. Electrical actuation has been studied by many researchers using Joule heating principle. An insulated polymer matrix is filled with conductive particles and a certain electrical conductivity is achieved, therefore; it is possible to trigger these materials using electric current **[8]**. Apart from these mechanisms such as light of a particular wavelength, magnetic field, solvents and moisture can be employed as stimulus methods **[7]**.

Both thermoplastics and thermosetting materials can show shape memory properties. In previous studies, polyurethane, polyetherester, polycarbonate based materials and phenoxy resin and also some block copolymers like styrene and poly(1,4-butadiene) were used to obtain shape memory actuation **[4, 9]**. Shape memory thermoplastics are preferred because of their high potential of biocompatibility and biodegradability. Moreover, it is possible to alter shape memory characteristics by changing the ratio of soft and hard domains especially for phase segregated block copolymers **[4]**. Apart from the thermoplastics, thermosetting polymers also gain importance in shape memory concept owing to their superior thermomechanical properties along with unique shape memory characteristics. Styrene based polymers and epoxy resins are the most common thermoset materials that researchers are focused on **[10-12]**. Epoxy resins are chemically stable and resistant to environmental degradation which makes them a possible candidate to be used in high technology aerospace applications **[11]**. Thermal transition temperature which has an important role in shape memory characteristics can be changed according to specific needs by using different types of monomers or fillers. These properties make epoxy based polymers an appropriate research material in shape memory studies **[10]**.

Altering shape memory characteristics using additional monomers is a useful way for epoxy thermosets. With the presence of monomers, the thermal transition temperature of the epoxy polymers can be changed. Neopentyl glycol diglycidyl ether is widely used together with diglycidyl ether of bisphenol A epoxy resin for this purpose **[13]**.

Electrical shape memory actuation is one of the most popular triggering types because of its versatility. Carbon based nano-fillers can increase the conductivity of neat polymer to a great extent and make them possible to be triggered with electrical current. Carbon nanotubes have some benefits like having high modulus, strength and electrical conductivity which are also a result of their high aspect ratio. On the other hand carbon black can be preferred because of its lower cost compared with nanotubes. Although to a lesser extent, they also have decreasing effect on percolation threshold like carbon nanotubes **[14, 15]**.

The main objective of this dissertation was to produce shape memory polymers using thermoset based epoxy resin. Epoxy resin was modified using two different monomers having aliphatic and aromatic structures, and the effects of monomers on mechanical, thermal and shape memory properties were observed. Epoxy based composites were prepared using carbon nanotubes and carbon black particles. In another aspect, both fillers were used together in order to observe a certain synergic effect and an

improvement in characterized properties of polymer. Finally, the best monomer and filler concentrations were selected, and final desired composites were prepared by combining benefits of both additives in one composite.

The first aspect was about of the curing study of the neat polymer and using monomers for modifying the epoxy matrix. Initially the amount of curing was studied to obtain complete curing and the most crosslinked polymer. DSC analysis was done and percentage of curing was calculated with respect to the curing curves. Diglycidyl ether of bisphenol A based resin was cured with an isophorone diamine based cyclo aliphatic curing agent. When desired curing conditions were selected for highest curing percentage, the polymer matrix was modified using aliphatic epoxide, neopentyl glycol diglycidyl ether (NGDE) of three different fractions; 5 %, 10 % and 15 % by weight. Also an aromatic modifier resorcinol diglycidyl ether (RDE) was used in same fractions with NGDE. Modifiers were used in order to obtain lower glass transition temperature and advanced shape memory properties. In this part effects of aliphatic and aromatic monomers were observed and compared. Polymer samples were characterized in terms of mechanical, thermal and shape memory characteristics using tensile and impact tests, DSC analysis and bending test, respectively.

Afterwards, composites of neat epoxy were prepared using carbon nanotubes in concentrations of 0.25 %, 0.5 %, 1 % and 2 % by weight. In addition to it, carbon black containing composites were prepared in four different fractions of 0.5 %, 1 %, 3 % and 5 % by weight. The effects of particulate and nanotube fillers were compared. According to the percolation threshold values of both fillers, appropriate fractions were selected for the preparation of hybrid composites; carbon black amount was kept constant at 1 % while carbon nanotube amount was varied as 0.25, 0.5 and 1 %. The synergistic effect emerging from the combination of particulate and nanotube fillers was investigated. In addition to the mechanical, thermal and shape memory characterizations, electrical conductivities of the composites were also measured.

The final aspect was the combination of the first two parts of the study by modifying the epoxy based composites of carbon black, carbon nanotubes and hybrid formulations with 15 wt. % NGDE and RDE monomers. In this part, the purpose was to combine the superior shape memory properties, which were achieved by monomers, and high electrical conductivity with high elastic modulus, which were the contributions of carbon based fillers. Mechanical, thermal, electrical and shape memory properties were analyzed. Finally, electrical actuation for shape memory effect was investigated for the formulation having the highest electrical conductivity.

CHAPTER 2

BACKGROUND

2.1 Smart Materials

Smart materials have variety of promising abilities like changing shape, resistivity, colour or refractive index, which make them a rising research subject in the field of material sciences. They can distinguish certain physical changes in the environment and react as response to them. With the utilization of these materials, producing high technology devices is possible. Smart materials can be divided mainly in two groups; sensors and actuators. Sensors can be optical fibers or piezoelectric polymers, whereas piezoelectric ceramics, magnetostrictive materials, electrorheological fluids and shape memory materials are studied under the actuators group. Actuators can be programmed for responding to thermal, magnetic or electrical changes in the environment. Being very outstanding among actuators, shape memory materials can remember their shape under the application of external changes **[16]**.

2.2 Shape Memory Materials

Ability to change shape is one of the most promising properties of smart materials. These kinds of materials have a large potential of usage in different application areas. Shape memory materials which can be accounted as the most fundamental group among shape changing materials, can be fixed into a certain shape under the application of an external stimulus, and can recover their original shape when the same stimulus is exerted on the material. Shape memory polymers have received considerable amount of attention owing to their preferable properties such as, low density, low production cost, and easy processing. Tuning properties of polymers being much easier than alloys, is also a definite advantage of shape memory polymers over shape memory alloys. Polymers have broad range of application temperatures and they are easily deformed at temperature values higher than their glass transition temperature. Additionally, they can be potentially biocompatible and biodegradable which make them promising materials in biomedical industry **[8-14]**.

2.2.1 History and Application Areas for Shape Memory Polymers

First research on shape memory polymer is known to be done in 1941, in which L.B. Vernon found that methacrylic acid ester had shape changing properties upon increase of temperature **[17]**. This subject did not gain much interest until 1960 when the heat shrink tubing was discovered. Tubes made of covalently crosslinked polyethylene had the ability

of shrinking with application of heat. Heat shrinking tubes were used for insulating electricity cables, which is still used for the same purpose today. Number of studies published related with shape memory polymers started to increase after 1980s **[3, 18]**.

Deployable aerospace application is one of the most potential application areas in the industry for shape memory polymers. Hinges for aerospace crafts which are able to recover their original shape in 100 seconds, mirrors which can be deformed for ease of packaging, and reflectors used for antennas can be triggered with power supply to get their original shape when they are going to be used. Morphing structures and folding wings can be beneficial for the efficiency of missions of aircrafts and lead to certain advantages like improvement in speed and energy saving. Examples of shape memory antenna reflector and morphing wing are shown in Figure 2.1 **[7]**.

Figure 2.1 Shape memory applications a) antenna reflector, b) morphing wing **[7]**

Second main application field is biomedicine, in which biodegradable shape memory polymers can be used for the curing treatments of several diseases. Enlargeable vascular stents can be injected to a human's blood and when it reaches the desired location, it can be enlarged by the help of optical or laser heating applied on that location. Same kind of materials can be used for the blood clot removal applications. Shape memory sutures can be shrinked and get tighten with the application of heat after being loosely applied on the wound. Degradation with time can be possible if biodegradable polymers are used in this process. Figure 2.2 shows shape memory material design for clot removal and suture application. Finally, in orthodontic applications shape memory concept can lead to improvements. In a study, stretched orthodontic wires were attached to the misaligned teeth. Shape recovery procedure was applied on the wires by applying heat and misaligned teeth became perfectly aligned in 1 hour **[4-7]**.

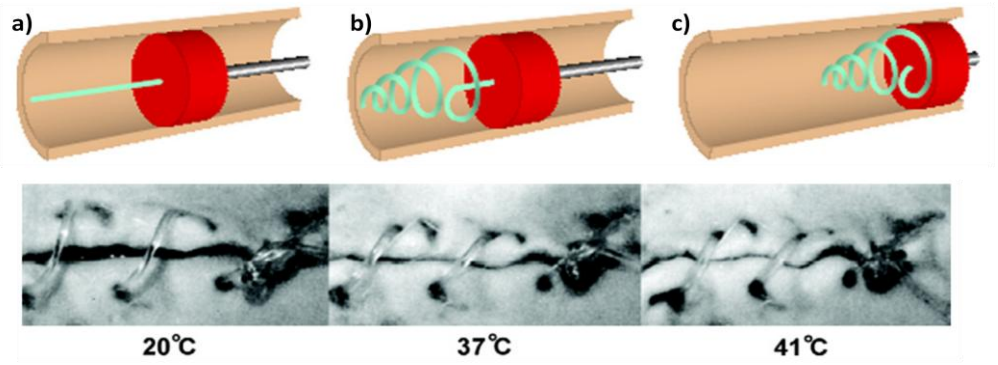

Figure 2.2 Shape memory materials used for clot removal and suture application **[7]**

Some researchers found beneficial effects of shape memory concept in textile industry. Hu et al. found out that shape memory fibres used in production of fabrics can make clothes recover their original flat shape when they are heated above their glass transition temperature. In another application, when the wearer of a cloth changes, the cloth can easily get the shape of the new wearer without the necessity of tension. Later on the cloth can recover its original shape with heat application **[7]**.

2.2.2 The Mechanism of Shape Memory

The mechanism for the shape change lies beneath the two phase structure of the shape memory polymers. The fixing phase, which is also called as hard segment, is responsible for the recovery of the permanent shape. On the other hand, the reversible phase which is called as soft segment accounts for the fixing of the temporary shape. Chemical and physical crosslinks and chain entanglements construct the hard phase of the polymer. Covalent bonds constitute the chemical crosslinks while the physical crosslinks occur in polymers having both crystalline and amorphous domains. The domain which has the highest thermal transition is dominant and acts as the hard segment in physically crosslinked polymers. The soft phase which is governed by the segment which has the second highest thermal transition generates the switching mechanism between two domains and builds up reversible crosslinks during the fixation of temporary shape. The melting temperature of the soft segment crystals and glass transition act as reversible phase **[4-14]**. Figure 2.3 illustrates shape memory mechanism; hard segment is shown as net points, whereas soft segment is shown as blue lines.

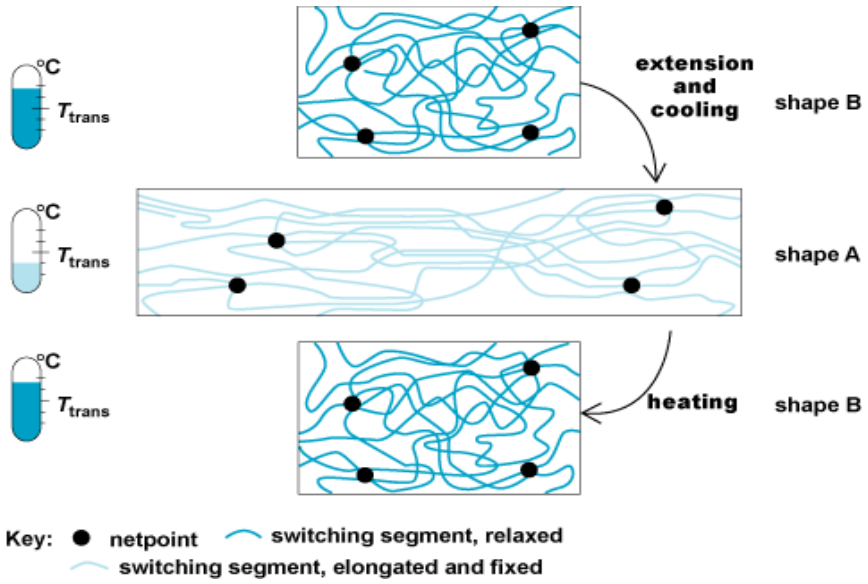

Figure 2.3 Shape memory mechanism **[19]**

Determination of shape memory properties are achieved by cyclic thermomechanical tests. Thermomechanical cycle is composed of 4 different steps. In the 1st step the sample is deformed into a different shape at a temperature value higher than glass transition temperature. 2nd step is the fixation of the deformed shape which can be achieved by decreasing the temperature below transition temperature without removing the applied force until sample reaches the room temperature. The force is removed without changing the temperature at the 3rd step, and it can be seen that strain does not change since the deformed shape has been fixed in the prior stage. In the final stage the polymer sample is heated again above its transition temperature and the deformed shape recovers to the original shape of the polymer. Figure 2.4 shows the steps of thermomechanical cycle of shape memory actuation in all stages starting from deformation and ending with the recovery **[11]**.

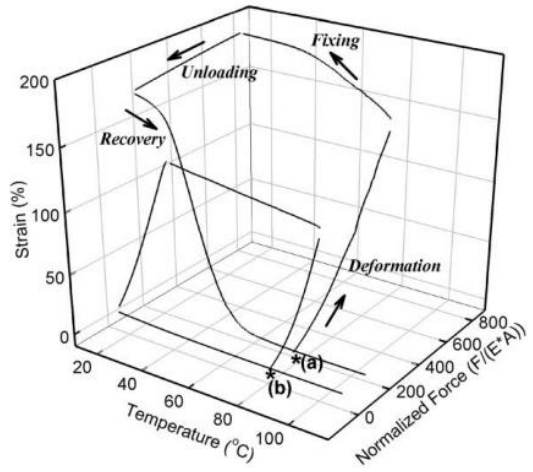

Figure 2.4 Thermo-mechanical cycle of shape memory procedure for a) a shape memory polymer and b) natural rubber **[3]**

Shape recovery effect can be actuated in different ways. Even though the traditional and common way is the application of heat, there are also other kinds of triggering mechanisms which started to gain the attention of researchers. Heating is not practical for every process, therefore a method called Joule heating, in which the specimen is heated by applying electrical current. Advantage of joule heating is not only the heating is achieved very quickly, but also there is not a necessity for ovens operating at high temperature. When non-conducting polymer matrices are filled with conductive particles such as carbon based fillers, semi conductive polymers are obtained. This kind of composites can be triggered by electricity **[8, 12]**. Additionally, there are also other triggering types such as solution, infrared radiation, or magnetic field triggering mechanisms **[20, 21]**.

Bending test is a method for the application of the thermomechanical cycle and it is also useful for quantifying shape memory properties easily. Three different shape memory properties are investigated in order to analyze the performance of recovery. Shape recovery ratio (R_r) shows how the material remembers and recovers its permanent shape after being fixed into a deformed shape. It reflects the potential of material to remember its original shape. Shape fixity property is related with the capability of soft domain to stay stable at a certain deformed shape. It is calculated as the ratio of deformation angle after being fixed to the deformation angle during the application of load. The third shape memory property is the shape recovery time which is the time required for the polymer to recover its original shape; it gives information about the response speed of the smart material **[4]**. In Figure 2.5 bending test and the parameters are shown. Θ_f shows fixed angle and Θ_r stands for recovered angle.

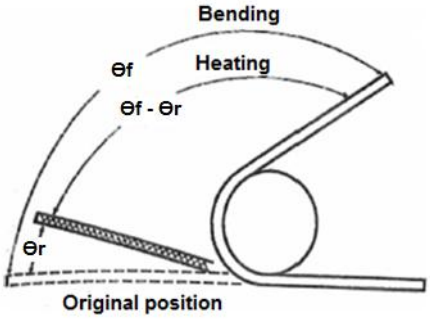

Figure 2.5 Schematic representation of the bending test

2.2.3 Epoxy Resin as a Shape Memory Polymer

Wide range of polymer types can show shape memory properties. Polyethylene **[22]**, polystyrene **[12]**, polyurethane **[14]**, polymethacrylate **[23]** and epoxy resin **[10]** are some of the polymers that have shape memory capability. Epoxy resin has superior properties when compared with other types of shape memory polymers. Epoxy polymer has better mechanical properties, especially high tensile strength and modulus of epoxy make it a durable polymer. Moreover, it is possible to tune properties of epoxy polymers by changing the amount of curing agent used, or by mixing additional monomers with the resin **[10]**.

Epoxy resin is made by the reaction of bisphenol A and epichlorohydrin. The formation reaction of epoxy resin is shown in Figure 2.6. The commonly used type of epoxy is called diglycidyl ether of bisphenol A (DGEBA). The curing reaction of epoxy resin takes place at the each side of DGEBA; oxirane rings can react with different molecules for the formation of polymer. Curing is an autocatalytic reaction; it initiates fast and then slows down around the gelation point. At gelation point, crosslink density increases rapidly, thus, the T_g of polymer increases. During this reaction, the polymer switches from rubbery phase to brittle glassy phase. In the final stage of the vitrification, curing reaction slows down and stops **[24]**.

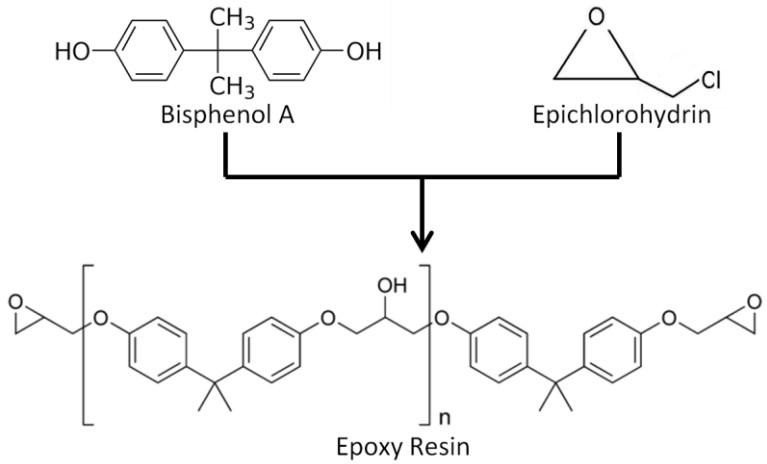

Figure 2.6 Formation reaction of epoxy resin

2.2.4 Diamine Curing Agents

Amines, imidiazoles, polymercaptan, anhydrides and dicyandiamide type of curing agents are commonly used. Diamine curing agents are compounds that contain two amine groups in one molecule. In the curing reaction, hydrogen elements of diamine molecule react with the oxirane ring of epoxy resin to form a thermoset network. Primary amines initially react with the oxirane ring of an epoxy molecule, then the secondary amine reacts with the oxirane ring of another epoxy **[25]**. Figure 2.7 shows the stoichiometry of the reaction of diamine and epoxy groups.

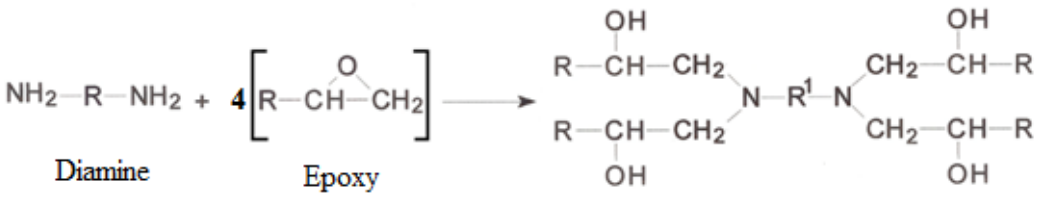

Figure 2.7 Curing reaction of epoxy resin with diamine curing agent

Aliphatic, cyclo-aliphatic and aromatic curing agents can be used for curing reaction of epoxy resin. Aliphatic curing agents can be cured at ambient temperature which is practical for coating applications. Cycloaliphatic amines and aromatic amines need much higher temperatures for curing and the resulting polymer has better mechanical characteristics and high glass transition temperature compared to the one that is cured with aliphatic curing agent **[25]**.

2.2.5 Monomer Usage for Modification of Epoxy Matrix

Monomers are generally used for diluting epoxy matrix in order to tune mechanical and thermal properties of the polymer. Monomer addition causes increase in toughness and lower glass transition temperature. Moreover, since monomers are smaller molecules compared to epoxy resin, lower viscosity values are attained during mixing. Low viscosity enables better mixing and stable structure of the prepolymer. Monomers also contribute to shape memory properties in a positive manner. Leng and co-workers **[10]** found that addition of a linear monomer caused a decrease in glass transition temperature and therefore decreased the time required for full shape recovery. The difference between rubbery and glassy modulus has enlarged, which led to increase in shape fixity property. The research groups of Luo **[8]** and Xie **[13]** also found similar results related with monomer usage in epoxy polymer.

2.2.6 Conductive Polymer Composites

Polymers are highly insulating materials. They show a resistive manner to flow of electrical current. Conductive polymer composites obtained by incorporation of conductive fillers, have gained attention since the processing and fabrication of polymers is much easier than metals. Conductive polymers can be used in variety of applications such as energy storing devices, electromagnetic shielding, aerospace applications, biomedical devices, over-current protection devices, photo thermal and optical recording, etc **[26]**.

The electrical resistivity is a material property and it can be calculated by multiplying the resistance with the cross sectional area and dividing to the length of the specimen. The formula for volume resistivity can be seen below **[15]**. ρ is electrical resistivity, R, l and A are resistance, length and area of the specimen respectively.

$$\rho = R \times \frac{A}{l} \tag{2.1}$$

Materials can be categorized under 5 groups according to their electrical resistivity properties. First group is the insulators, which has the volume resistivity between 10^{12} and 10^{22} Ω.cm. Most polymers are classified in this group. Semi-insulators are the ones having volume resistivity of 10^{7} and 10^{12} Ω.cm. The next category is the semi-conductors and they have volume resistivity between 10^{-3} and 10^{7} Ω.cm. Conductors have the volume resistivity in the range of 10^{-6} and 10^{-3} Ω.cm. Finally materials having zero Ω.cm resistivity are considered as superconductive materials **[27]**.

For a polymer composite, the value of volume resistivity is not directly proportional with the filler amount in the polymer matrix. Volume resistivity decreases slowly as filler amount increases, and a sharp decrease is observed at a certain filler content, which is

called as percolation threshold **[26]**. Percolation threshold is the critical concentration at which the conductive particles get in touch to each other and form conductive networks. Below this value the conductivity is dominated by the insulating polymer matrix, when the concentration is increased above this value, the polymer switches to the semi-conductive and conductive regions **[28, 29]**. Percolation region can be seen in Figure 2.8.

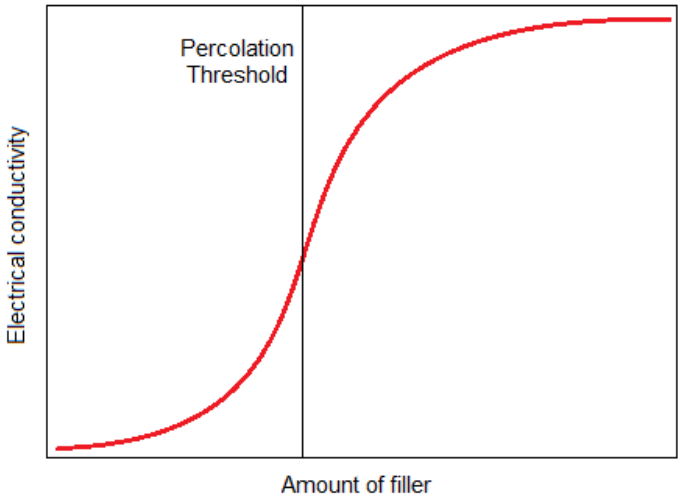

Figure 2.8 Indication of percolation threshold in a conductivity vs. filler amount plot

2.2.7 Shape Memory Polymer Composites

Heating shape memory polymers to high temperature values using external heaters is not always convenient for practical usage. In order to suggest an easy solution to this problem, heating of shape memory polymers by means of electrical current has been investigated. Heating by voltage application is called Joule heating and it is found to be fast and practical method **[30]**.

Many studies showed that, polymers filled with conductive filler particles can be used in shape memory actuation, carried out by electrical triggering. Composites containing carbon nanotubes **[14]**, carbon black **[15]**, carbon nanofibers **[8]**, thermoexpanded graphite **[31]**, magnetite **[32]**, etc., were employed as shape memory actuators. The polymer needs to have a certain electrical conductivity in order to give the way for heating the sample to its shape recovery temperature by applying constant voltage. The polymer can be heated up very easily if the resistivity is low enough, however the desired conductivity may not be achieved for poor dispersion of conductive particles. Some conductive fillers such as carbon nanotubes are affected by van der Waals forces which lead carbon nanotube particles to have a tendency of agglomerating. It is important to minimize the agglomerates and homogenize the distribution of particles by adapting the mixing process of CNT's with the polymer matrix. Some ways of enhancing the dispersion of CNT's can be solvent aided mixing, melt mixing with extruder or electrospinning **[8, 33]**.

2.2.8 Conductive Fillers

2.2.8.1 Carbon Nanotubes as Conductive Fillers

Some conductive particles that can be used for enhancing the conductivity of polymers are carbon nanotubes (CNT), carbon black (CB), graphite, carbon fibers, metal powders like nickel. Among these types, carbon nanotubes set forward superior mechanical properties besides enhanced conductivity. In this respect the key role belongs to the aspect ratio which is described as the ratio of length to the diameter. As a fibrous filler, CNTs have higher aspect ratio, typically 10000 or higher, when compared with particulate fillers such as CB. CNTs can be described under two categories; single walled carbon nanotubes (SWNT) and multi walled carbon nanotubes (MWNT). The difference between them is that, SWNT are composed of one rolled graphene sheet, whereas MWNT is made up of more than one concentric rolled graphene sheets. Figure 2.9 shows both the structures of SWNT and MWNT **[34]**.

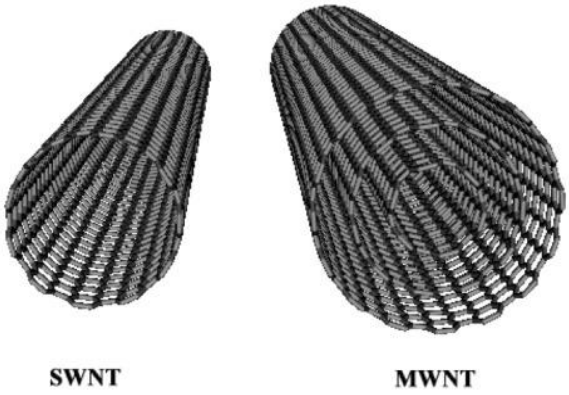

Figure 2.9 SWNT and MWNT structures **[35]**

2.2.8.2 Carbon Black as Conductive Fillers

Unlike carbon nanotubes, carbon black is particulate filler and therefore, has lower aspect ratio. Particle diameter of carbon black generally varies between 10 to 400 nm. Carbon black is a low cost conductive filler, which is approximately $1/1000^{th}$ the cost of carbon nanotubes **[36]**. Its low cost lead it to be preferable for applications, however the low aspect ratio which is around unity causes lower performance in conductivity when compared to carbon nanotube filled polymers **[36]**. Figure 2.10 shows carbon black particles as aggregates and SEM image.

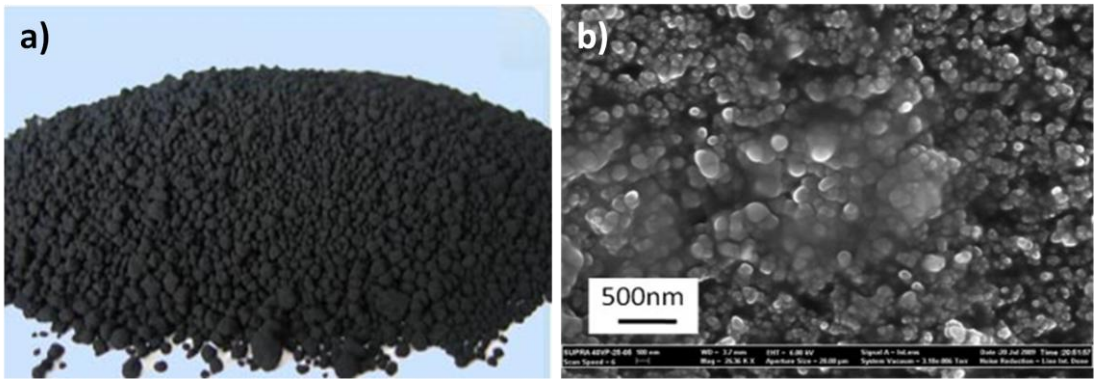

Figure 2.10 a) Carbon black aggregates b) SEM image of carbon black **[37]**

2.2.8.3 Hybrid Filler Usage

Combining two filler types having different aspect ratios is suggested to cause a low percolation threshold value and therefore improves conductivity performance of resulting polymer. The theory lies behind the synergistic effect between the two fillers. The second filler fills the non-conducting regions in the matrix which the first filler could not fill; therefore it helps increasing the conductivity by functioning as bridges between the particles of the first filler and forms a network. Dang and co-workers **[38]** also claim that usage of two fillers in different shape and aspect ratios would have contributions on the positive temperature coefficient (PTC) effect, which is the decrease in electrical resistivity as the temperature increases. Presence of both fillers causes to weaken the negative temperature coefficient (NTC) effect for the PTC applications **[38]**.

In Figure 2.11, the proposed synergy mechanism of hybrid fillers such as carbon black and carbon nanotube in epoxy polymer by Sumfleth et al. **[39]** is shown. According to this mechanism, for the case 1, additional carbon black platelets may help dead branches of existing carbon nanotube networks to join and create new networks for electron transport. In this case, the electrical resistivity is expected to decrease in a significant amount. In the 2nd case, carbon black particles may substitute with some of the existing carbon nanotube chains, so the resistivity may increase **[39]**.

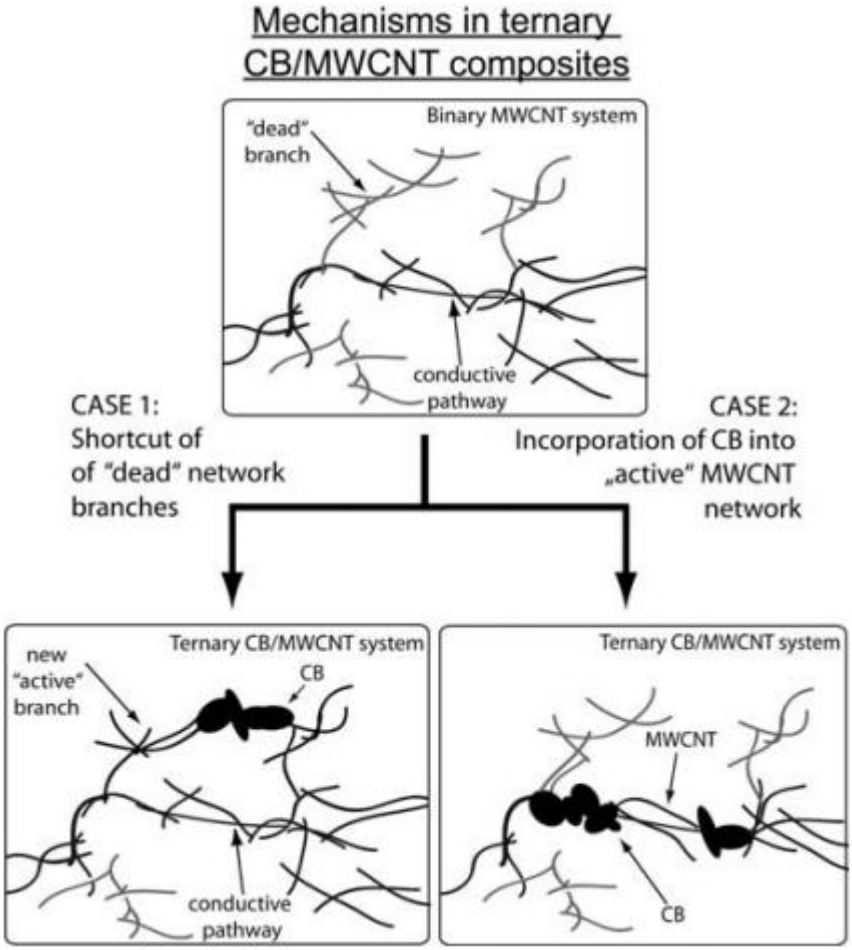

Figure 2.11 Conductive network formation of carbon black and nanotube particles in epoxy matrix **[39]**

There are not many examples of studies related with hybrid filler usage in shape memory applications in literature. Yu et al. **[12]** introduced carbon black and carbon nanotubes into the styrene resin and concluded that the electrical conductivity was enhanced with the existence of both fillers. Moreover, the sample containing both fillers and the sample filled with carbon nanotube as a chained structure showed faster heating in electro-induced shape recovery, therefore faster recovery is achieved **[12]**.

2.2.9 Methods for Preparation of Epoxy Based Shape Memory Polymer

Epoxy polymers are obtained by the reaction of two components, which are the epoxy resin and curing agent. These components are mixed in a certain ratio depending on the reaction stoichiometry. In order to obtain epoxy composites with the incorporation of fillers, ultrasonication method in different kinds of solvents can be utilized. Finally for the

shaping, epoxy polymer blends are molded and demolded after the curing reaction is completed.

2.2.9.1 Solvent Aided Ultrasonication Method for Producing Composites

Mixing nano sized fillers in the epoxy matrix with high dispersion and homogeneity is a very challenging process. For instance, carbon nanotubes in an epoxy mixture are under the effect of van der Waals forces, and therefore they tend to stay close and form aggregates **[33]**. High viscosity of epoxy resin also constitutes a disadvantage for the dispersion of nano sized carbon particles. In order to make this process easier and more effective, some researchers dissolved nano particles in a solvent and apply ultrasonication for improved dispersion **[40]**.

Lau et al. **[40]** and Yesil **[41]** applied solvent aided ultrasonication in their studies. This method involves dissolving nanoparticles in a solvent such as ethanol, acetone or N-dimethylformamide, and applying ultrasonication for certain time. When the particles are well dissolved in the solvent, the epoxy resin is added to the slurry and ultrasonication is applied for further time to assure the dispersion of nano fillers in the epoxy matrix. The solvent decreases the viscosity of epoxy resin, which helps better mixing of nano particles. In the final step, solvent should be evaporated completely by heating the mixture for long time and mixing at the same time **[40, 41]**.

2.2.9.2 Mechanical Mixing

Mechanical mixers are used in epoxy polymer formation procedure in the step of mixing epoxy resin and the hardener. Complete mixing of two components can be achieved by the application of shear forces created by the mixer. The shear force created by mechanical stirrer helps fracturing of the filler agglomerations and thereby a better dispersion is obtained as it can be seen in the Figure 2.12 **[42]**.

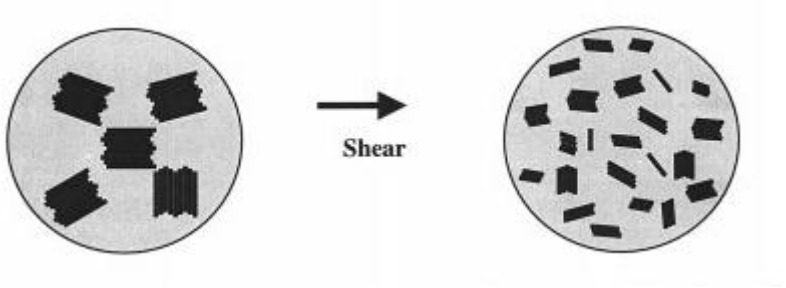

Figure 2.12 Influence of shear force on the agglomerate size **[42]**

The time of the mixing and the speed depends on the curing characteristics and the viscosity of the polymer. The mixing time should not exceed gelation time of the epoxy polymer. At the gelation time the reactants starts to react in a irreversible way and to form a three dimensional network. The viscosity of the blend starts to increase suddenly and the blend gets hot. After this point molding of epoxy blend is impossible, therefore time of mixing should be decided according to the gelation time **[43]**.

For high viscosity resins, lower mixing rate should be used for preventing air bubble formation of the matrix **[44]**. High mixing rate can cause high amount of bubbles which lower the mechanical properties. In Figure 2.13 mechanical mixer and some impeller types are shown.

Figure 2.13 Mechanical mixer and some types of impellers **[45]**

2.2.9.3 Molding of Epoxy Polymer

Epoxy blends are molded as soon as it is ensured that the components are well mixed. Molds are made of different kinds of materials, for instance aluminum and teflon ones are frequently used for polymer molding. Teflon is non-adhesive and easier to demold. On the other hand for aluminium molds, lubricants should be applied before pouring the polymer blend to the molds.

2.2.10 Characterization Methods for Shape Memory Polymers

The shape memory characteristics strongly depend on the material's thermal, electrical and mechanical properties. Morphological characterization gives idea about the netpoints, phases and also determining the orientation of fillers used. Thermal transition gain importance since it is the point at which shape recovery procedure could be activated. Electrical resistivity is a necessary point to focus on especially for the electrical shape memory activation researches. To conclude, all of these characteristics mentioned above have crucial roles in investigation of shape memory phenomena and should be identified in order to understand the behavior of these smart polymers properly **[18]**. Methods used for property characterization are explained in detail in this part of the dissertation.

2.2.10.1 Mechanical Characterization

Under the title of mechanical characterization, tensile and impact properties of the polymer can be investigated. Properties such as tensile strength, Young's modulus, elongation at break and impact strength are calculated according to the data obtained from tensile and impact tests.

2.2.10.1.1 Tensile Test

Investigation of stress-strain behaviors is done by applying a uniaxial tensile test on the sample. The mechanical properties of polymers are highly sensitive to the strain rate of uniaxial loading and temperature. Therefore it is important to conduct tensile experiments under constant strain rate and temperature **[16]**. ASTM D638-10 (Standard Test Method for Tensile Properties of Plastics) is a general standard for tensile testing. In Figure 2.14 uniaxial tensile loading is represented.

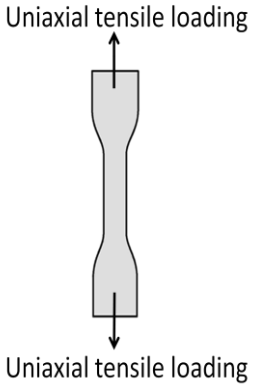

Figure 2.14 Representation of uniaxial tensile loading

In Figure 2.15 typical stress strain relationships for different polymers can be seen. A belongs to a brittle polymer which fractures suddenly without any plastic deformation. B is a plastic polymer showing a yield after elastic deformation and continues with plastic deformation. Necking occurs at yielding point. C is an elastomeric polymer having large strain at low stress values **[16]**.

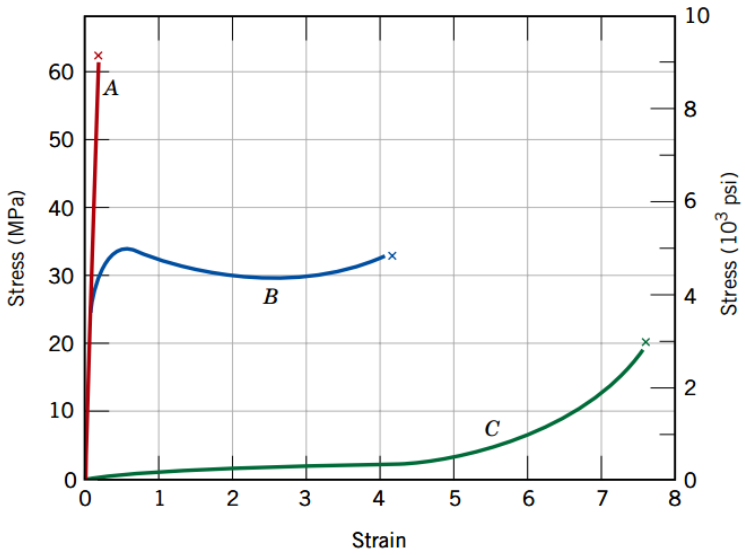

Figure 2.15 Typical stress strain behaviors of polymers **[16]**

According to Figure 2.16, tensile strength (τ) of the material is measured as the maximum stress mostly at the fracture point. Young's modulus (E) is the ratio of change in stress to the change in strain measured at the elastic region. This is why Young's modulus is also called as elastic modulus. Young's modulus gives idea about stiffness of the material, in other words endurance of the material to elastic deformation. Elongation at break ($\%\epsilon_{break}$) is the percentage of elongation at the point which the fracture occurs. It gives the information about the ductility and brittle characteristics of the material. For instance, materials having elongation at break value lower than 5 % are brittle materials.

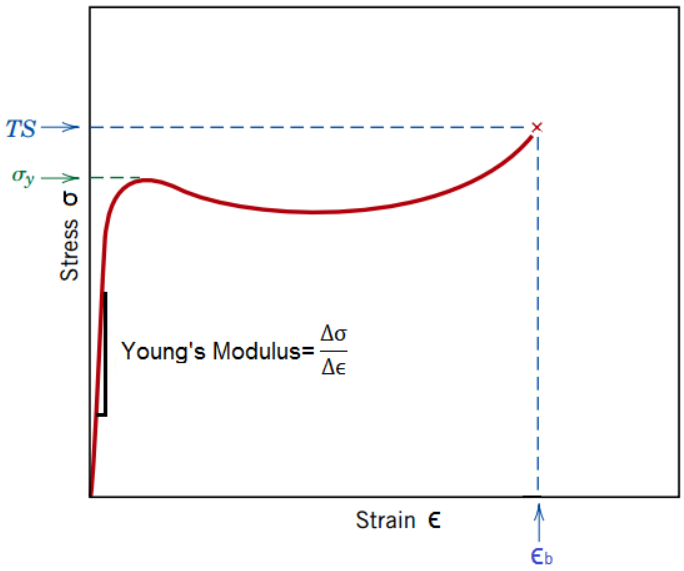

Figure 2.16 Stress-strain curve showing yielding and fracture points

Three tensile properties are calculated by the following formulas **[16]**. F and A_o are force and cross sectional area of the specimen, $\Delta\sigma$ and $\Delta\epsilon$ stands for change in stress and change in strain. ϵ_b and ϵ_o are strain at break and initial strain.

Tensile strength, $$\tau = \frac{F}{A_o} \quad (2.2)$$

Young's modulus, $$E = \frac{\Delta\sigma}{\Delta\epsilon} \quad (2.3)$$

Elongation at break, $$\%\epsilon_{break} = \frac{\epsilon_b - \epsilon_o}{\epsilon_o} \quad (2.4)$$

2.2.10.1.2 Impact Test

Impact test measures the amount of energy absorbed by the specimen as a pendulum falling from a constant height crashes at the specimen with high velocity. Impact strength is the endurance to breakage and it is related with the toughness of the material. Unlike tensile test, impact testing gives information about fracture behaviors of the material. ISO 179-1 Non-Instrumented Impact Test, is the standard that is used in this thesis. A typical impact test instrument is shown in Figure 2.17 **[46]**.

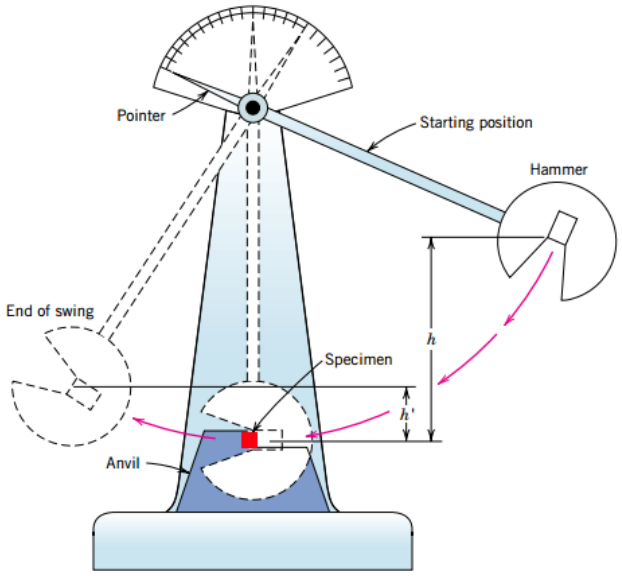

Figure 2.17 Representation of impact testing instrument **[16]**

There are different test types according to the position of the specimen placed on the instrument. Charpy and Izod tests are two different modes for impact testing. In both of the techniques samples with same dimensions can be used. Discrepancy between two methods is related with the way the sample is supported. In both modes, the amount of energy is absorbed by using the maximum height that the pendulum reaches after it crashed the specimen. Figure 2.18 shows Charpy and Izod type specimen positions **[16]**.

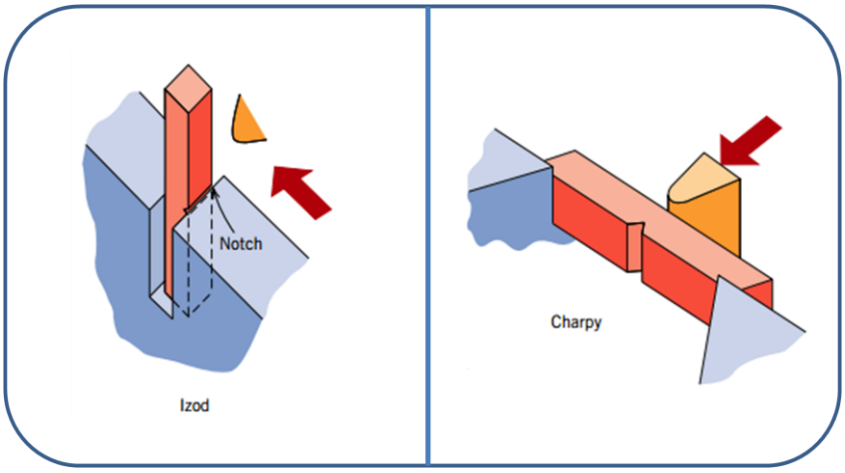

Figure 2.18 Specimen positions for Izod and Charpy impact tests **[16]**

2.2.10.2 Thermal Characterization

2.2.10.2.1 Differential Scanning Calorimetry Test

Differential scanning calorimetry is used to measure the heat flow from or into a specimen under heating at constant pressure. Thermal transitions and curing kinetics can be easily quantified using this method. First order transitions occur as peaks whereas second order transitions are observed as discrete changes in heat. Figure 2.19 shows a typical DSC plot for a thermosetting polymer in which both glass transition and percentage curing can be seen **[47]**.

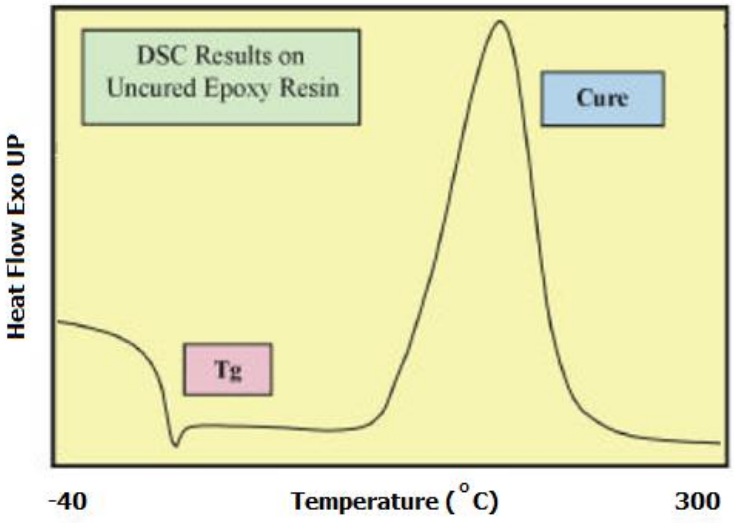

Figure 2.19 DSC plot for an uncured thermoset epoxy resin

Glass transition temperature is one of the most important parameters that have direct effect on shape memory application temperature. The change from glassy structure to rubbery state for the fixation of new temporary shape occurs at glass transition. Tuning T_g by changing the material composition is very essential regarding the application area and the range of application temperature. Thus investigation of T_g plays an important role in shape memory studies **[13]**.

Before glass transition the polymer is in glassy state, it starts to switch from glassy to rubbery state after glass transition. The polymer is softened like a rubber at this state. T_g is an endothermic transition. The glass transition temperature can be determined as the onset, endset or the inflection point of the second order transition. In this dissertation, inflection point was considered in the measurement of T_g values **[47]**.

When the uncured resin in Figure 2.19 is further heated above T_g, an exothermic peak appears which represents the heat of curing. For the polymers which are not fully cured, this peak can be observed. If the reaction between epoxy resin and the hardener is completed, only glass transition is observed in the DSC thermogram. In Figure 2.20 it is

represented that as the curing amount of the polymer increases, chains become more reacted and crosslink density increase. In the final case all the chains are attached to each other by forming networks, so that no more heat can be absorbed for the totally cured polymer **[48]**.

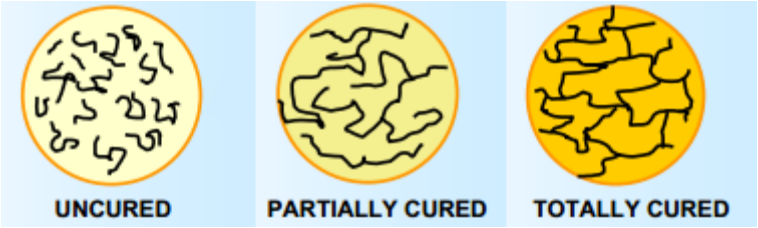

Figure 2.20 Increase in crosslink density with increase in amount of curing **[48]**

There is a relationship between amount of curing and the glass transition temperature. As the amount of curing increases, a polymer having higher T_g can be obtained. Figure 2.21 shows the behavior of curing peak and the glass transition with respect to increasing curing percentage values **[48]**.

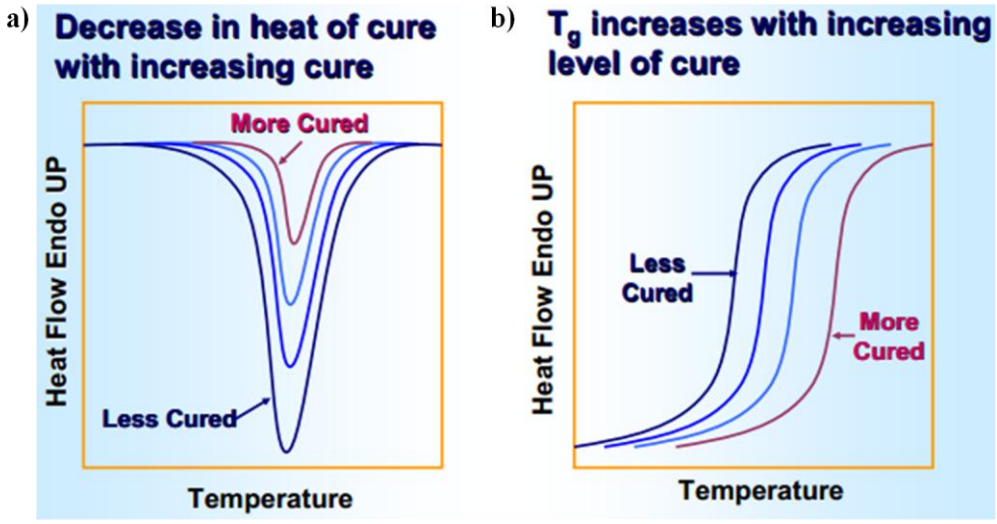

Figure 2.21 The behavior of heat of a)curing and b)T_g with increasing curing percentage **[48]**

Heat of cure measured in the DSC thermogram can be used to calculate the percentage curing value of a partially cured polymer. The following formula, Equation 2.5 is for the calculation of curing percentage. $\Delta H_{uncured}$ is the heat of cure of the physical blend which was mixed recently and did not cure. ΔH_{cured} is the heat of cure of the specimen for which

the percentage cure is to be calculated. For instance if ΔH_{cured} is measured as zero, the percentage cure is calculated as 100 %.

$$\%Cure = \frac{\Delta H_{uncured} - \Delta H_{cured}}{\Delta H_{uncured}} \times 100 \quad (2.5)$$

The amount of curing specifies various properties of polymer such as, mechanical strength, solvent resistance, impact resistance, brittleness and long term stability. Polymers having low curing percentage have lower glass transition temperature values and lower stability when compared to highly cured products. On the other hand when the polymer reaches extremely high curing percentage, it becomes over cured which leads to more brittle matrix and therefore, has weaker mechanical properties **[49]**.

2.2.10.3 Shape Memory Property Characterization (Bending Method)

Bending test is the most basic method carried out for characterization of shape memory properties. The principle of the bending test is based on four steps. Initially, temperature of the specimen is increased above transition temperature by any stimulus (heat, electricity, etc.) and a certain deformation is applied on the specimen externally (F_{ext}) as shown in Figure 2.22. In the second step application of stimulus is stopped and when the temperature of the specimen reaches back to room temperature, the strain is noted as L_i. When the sample is cooled down, additional physical crosslinks are formed by the solidification of switching domains. In the third step the external force is stopped being applied. At this point, stress is revealed a little depending on the shape fixity property of the material. New strain is noted as L_f **[18, 11]**. Shape fixity is the ratio of these two strain values as shown in Equation 2.6.

$$R_f = \frac{L_i}{L_f} \quad (2.6)$$

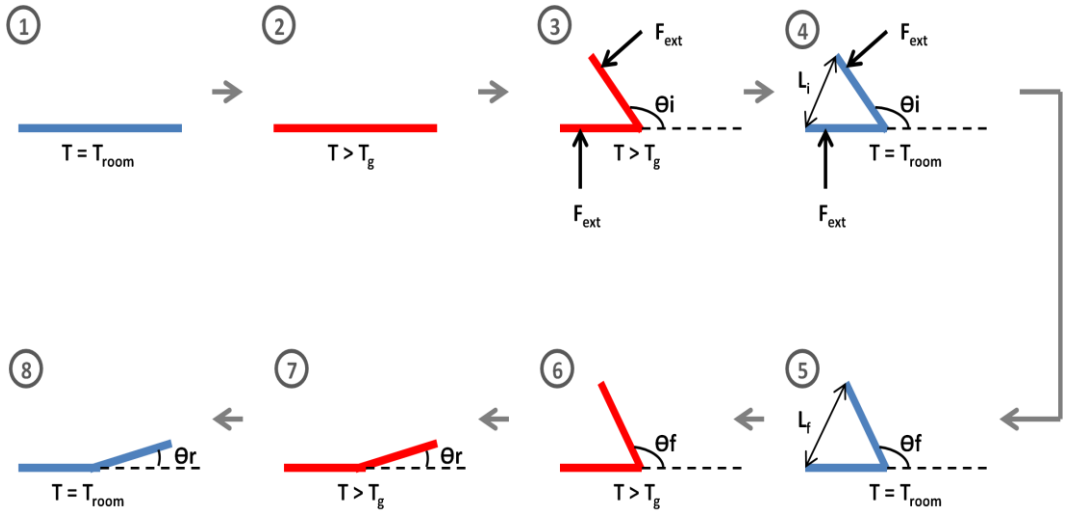

Figure 2.22 Schematic illustration of a bending test

The deformation angle is recorded as θ_f. In the final step, the sample is reheated to a value above its glass transition. At this step, the additional physical crosslinks are melted and the sample goes back to its original shape which is governed by the main chemical crosslinks. After this step, the sample may not recover its original shape fully, depending upon the stability of hard segment and it reflects the amount of recovery. The final angle of the sample is noted as θ_r and the shape recovery ratio can be calculated by the following Equation 2.7.

$$R_r = \frac{\theta_f - \theta_r}{\theta_f} \tag{2.7}$$

Electro-active triggering method is used to avoid external heating and actuate polymers by heating with direct current. Conductivity property of the polymer is essential for this kind of triggering method. Bending method is used also in electrical triggering. Specimens are heated with the application of electricity and bended at certain angle. After bending, applied power is switched off, so that the new shape is fixed. After the polymer is fully cooled, power supply is switched on and recovery of the polymer could be observed. Fillers like carbon black, carbon nanotube, short carbon fibers could be used in the processing of the polymer. In the recent shape memory researches electro-active triggering studies are common, however it is a challenging process to produce a polymer having good conductivity, decent mechanical and shape memory properties at the same time **[30]**.

2.2.10.4 Two Point Probe Electrical Resistivity Measuring Method

Electrical resistivity concept is described as the resistance to current flow through the unit volume of a material. It is dependent on the type of the material, and the amount of irregularities in the material constitutes the electrical resistivity. In order to determine the electrical resistivity, electrical resistance should be measured initially. According to Ohm's rule, electrical resistance can be calculated using the following formula **[27]**:

$$R\ (\Omega) = \frac{V}{I} \tag{2.8}$$

where V is the applied voltage and I is the current passes through the specimen under constant V voltage.

Measuring electrical resistivity can be executed using two point probe method for which the demonstration of the method can be seen in Figure 2.23. In this procedure the total resistance between two electrodes can be measured. Two probes are attached at each ends of the specimen. Constant voltage is applied using a DC source and amount of current passes through the specimen is noted. Resistance of the specimen is calculated according to Equation 2.8. The electrical resistivity value is calculated using the following formula, Equation 2.9 in which S stands for cross sectional surface area perpendicular to the current flow and l represents the length of the specimen between the probes.

$$\rho\ (\Omega.cm) = R \times \frac{S(cm^2)}{l(cm)} \tag{2.9}$$

Figure 2.23 represents two point probe method in which l, h and w are length, height and width of the sample.

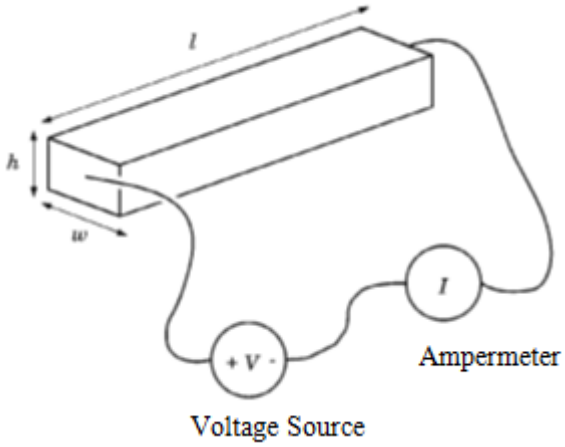

Figure 2.23 Demonstration of the two-point probe method **[44]**

The resistance that is measured by the two point probe method is total resistance which includes probe resistance, contact resistance, spreading resistance and the actual material resistance **[27]**. It is not possible to distinguish them in two point probe method, nevertheless contact resistance can be reduced to negligible small values owing to silver paste application. Silver paste is a two component conductive ink, one of which is the resin and the other component is curing agent. Two components are mixed in same amounts and applied on each ends of the specimen and left for curing. When the probes are attached to those silver parts, by means of the high conductivity of silver paste, contact resistance is lowered to negligible amounts **[50]**.

2.2.10.5 Scanning Electron Microscopy Method

Investigation of detailed morphological characteristics is mandatory for a shape memory research. Morphology gives idea about the netpoints formed in the matrix which play critical roles in this study. Scanning electron microscopy (SEM) is one of the nondestructive microscopy techniques that can be used in determination of shape memory morphology **[18]**.

In scanning electron microscopy method, an electron beam is focused on the surface of the specimen and it generates an enlarged image of the polymer surface. It determines the topography, the chemical composition and the dispersion of the materials that are used in the production of the specimen by sending an electron beam through the sample surface. The electrons that are scattered back are gathered by electron detector and the detector creates a highly magnified image **[18]**. Electrically insulating samples should be surface coated by some metals or alloys to achieve conductivity. The schematic drawing of a SEM instrument is presented in Figure 2.24.

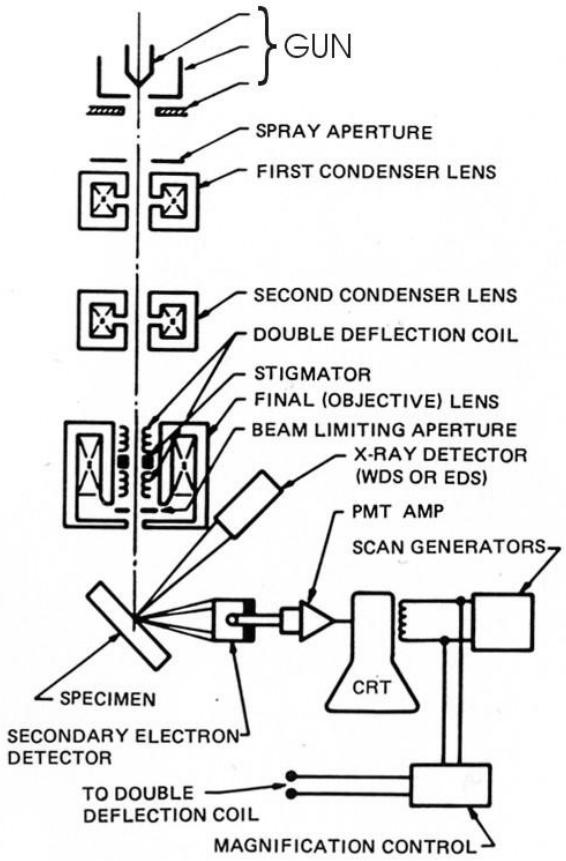

Figure 2.24 Schematic representation of SEM instrument **[51]**

2.3 Previous Studies

Lan et al. **[15]** studied thermoset styrene based shape memory polymer as a matrix and used carbon black as filler. They aimed to produce shape memory polymer composite that can be triggered by electricity. As a result of thermal, electrical and shape memory characterizations, they observed that increasing amount of carbon black inside the matrix led up to decrease in the glass transition temperature. They remarked that this behavior is due to a certain chemical interaction between the filler and the polymer matrix. They found that the percolation threshold of the samples was 3 % as a result of the electrical resistivity test and minimum resistivity was achieved for the sample containing 10 wt. % carbon black around 10^1 Ω.cm. Finally, they achieved successful shape recovery cycle for 10 % carbon black filled composites under the application of 30 V. The sample recovered in 100 s in consequence of bending test **[15]**.

Yoo et al. **[33]** investigated the shape recovery properties of polyurethane filled with multi-walled carbon nanotubes (MWNT). In order to disperse nanotubes effectively, they applied in-situ polymerization procedure and they proved the enhanced dispersion of nanotubes by SEM test. Mechanical tests implied that MWNT filling enhanced tensile strength and modulus, and did not cause decrease in elongation at break values. Composites containing 3 wt. % MWNT were subjected to electro-active shape recovery

tests. Under the application of constant 50 V, the samples recovered their actual shape in 40 s **[33]**.

Xie et al. **[13]** studied with a thermoset polymer which is produced by the reaction of diglycidyl ether of bisphenol A (DGEBA) epoxy monomer and the hardener poly(propylene glycol)bis(2-aminopropyl)ether. In addition to these, neopentyl glycol diglycidyl ether (NGDE), which is an aliphatic epoxide, was used as additive and decylamine was used in order to reduce the crosslink density. The aim of their study is to tailor the transition temperature by producing composites using different amounts of additives in order to obtain the best shape recovery property. As the result of characterization tests, glass transition temperature was found to decrease with the addition of NGDE in the matrix. They explained that this effect is due to the substitution of aromatic DGEBA with aliphatic epoxide chains of NGDE, which causes an increase in chain flexibility. As a result of shape recovery tests, addition of NGDE enhanced shape fixity and shape recovery properties. Finally, they observed that, complete recovery was achieved in 6 s when the composites are immersed in 70˚C water bath **[13]**.

Liu et al. **[52]** studied shape memory resin with diglycidyl ether of bisphenol A (DGEBA) epoxy monomer and an aromatic curing agent, 4,4'-diaminodiphenyl methane. They investigated the effect of curing percentage on thermal, mechanical and shape memory properties of the polymer. DSC results revealed that increasing curing percentage caused higher glass transition temperature values because of higher crosslinking density. They focused on 60 % cured epoxy polymer. Shape recovery properties were identified by fold-deploy shape memory test, which is the same method as bending test. Tests showed that, the samples had shape retention ratio higher than 99.5 %. In addition, the repetition of shape recovery cycles had little effect on the shape memory properties **[52]**.

Yu et al. **[12]** investigated the effect of addition of carbon nanotubes which would serve as a long distance conductive channel into the styrene based shape memory polymer/carbon black composites. Effect of hybrid filler usage has studied in this research. Additionally, samples were subjected to electrical field before curing styrene resin. SEM images showed that electrical field caused carbon nanotubes to align and generate chains inside the matrix. Electrical resistivity values for hybrid composites were lower than samples filled with only carbon black. Chaining carbon nanotubes had much significant effect on lowering resistivity compared to randomly distributed carbon nanotube containing composites. Sample containing 1 % carbon nanotubes and 15 % carbon black were subjected to shape recovery tests. These tests were applied by first prebending the sample at 80˚C and fixing its shape by cooling, then 25 V DC was applied. Full shape recovery was achieved for the composite containing chained carbon nanotubes **[12]**.

2.4 Motivation of the Thesis

Ability to give response to a certain stimulus is an attractive property for any kind of application area. To develop such kind of a material with superior properties is not straightforward. The polymer should have hard and flexible segments together which provide the shape memory mechanism to work properly. Thermal transition temperature is important since it identifies the application temperature of shape memory procedure. Moreover, to achieve electrical triggering mechanism, conductive particles should be added to the matrix. It is also a complicated process to disperse conductive nanoparticles in the polymer.

The motivation of this thesis lies beneath all these challenging objectives. Achieving the shape memory ability, comparing effects of linear monomers, comparing effects of particulate and nanotube fillers, using both fillers together in different amounts to achieve synergistic effect, selection of the overwhelming monomer concentration, filler concentration and using them together to produce the desired shape memory polymer are all together sounds exciting and form the structure of the thesis.

This study will be the first to investigate the shape memory properties of a polymer containing both a linear monomer and hybrid fillers. Besides, resorcinol diglycidyl ether as an epoxy diluent had not been used in any shape memory research before.

CHAPTER 3

EXPERIMENTAL

3.1 Materials

3.1.1 Epoxy Resin

The diglycidyl ether of bisphenol A (DGEBA) type epoxy resin (EPIKOTE 828) was used as polymer matrix and was ordered from Momentive. It is a medium viscosity liquid epoxy resin produced from bisphenol A and epichlorohydrin. Chemical structure and properties of epoxy resin are shown in Figure 3.1 and Table 3.1, respectively.

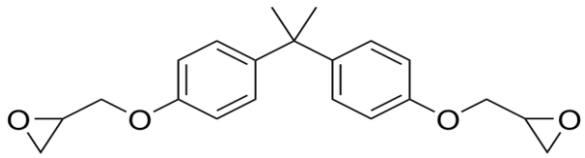

Figure 3.1 Chemical structure of epoxy resin EPIKOTE 828

Table 3.1 Properties of epoxy resin [53]

Property	Test Method	Unit	Value
Epoxy group content	SMS 2026	mmol/kg	5260-5420
Viscosity at 25°C	ASTM D445	Pa.s	12-14
Density at 25°C	SMS 1347	kg/L	1.16
Flash Point (PMCC)	ASTM D93	°C	>150
Molecular weight		g/mol	340.41

3.1.2 Curing Agent

The curing agent used which is a low viscosity cycloaliphatic isophorone diamine was used as hardener (EPIKURE F205), and was purchased from Momentive. Chemical structure and some properties of the curing agent are listed in Figure 3.2 and Table 3.2, respectively.

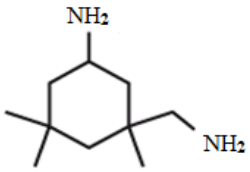

Figure 3.2 Chemical structure of curing agent, EPIKURE F205

Table 3.2 Properties of curing agent [54]

Property	Test Method	Unit	Value
Basic nitrogen content	ASTM D2896	% (m/m)	6.0-8.0
Viscosity at 25°C	ASTM D445	Pa.s	0.5-0.7
Density at 25°C	ASTM D792	kg/L	1.04
Flash Point (PMCC)	ASTM D93	°C	100-106
Recommended proportion with EPIKOTE 828		%	58

3.1.3 Monomer

Two types of monomers were used in order to modify the epoxy resin. The first one was neopentyl glycol diglycidyl ether (NGDE) based linear monomer which was obtained from Sigma Aldrich. Its chemical structure and properties are shown in Figure 3.3 and Table 3.3, respectively.

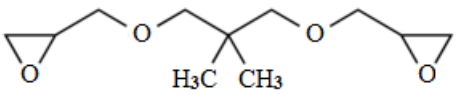

Figure 3.3 Chemical structure of NGDE

Table 3.3 Properties of NGDE [55]

Property	Unit	Value
Viscosity at 25°C	Pa.s	0.01-0.03
Density at 25°C	kg/L	1.04
Boiling Point (PMCC)	°C	103-107
Molecular weight	g/mol	216.27

The second monomer was resorcinol diglycidyl ether (RDE) which was purchased from Sigma Aldrich. It has an aromatic group in its structure unlike NGDE. Chemical structure and some properties of RDE are shown below in Figure 3.4 and Table 3.4, respectively.

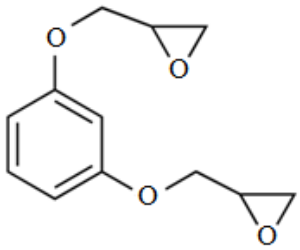

Figure 3.4 Chemical structure of RDE

Table 3.4 Properties of RDE [56]

Property	Unit	Value
Viscosity at 25°C	Pa.s	0.3-0.5
Density at 25°C	kg/L	1.21
Boiling Point (PMCC)	°C	172
Molecular weight	g/mol	222.24

3.1.4 Conductive Filler

Two different types of conductive fillers were used. The first one was multi-walled carbon nanotubes (MWNT, Nanocyl 7000) which was ordered from Nanocyl. The second conductive filler was carbon black (CB) having a trade name of PRINTEX XE 2-B which was supplied by Orion Carbons. Some properties of carbon nanotubes and carbon black are listed in Tables 3.5 and 3.6.

Table 3.5 Properties of carbon nanotubes

Property	Unit	Value
Average diameter	nm	10
Length	μm	0.1-10

Table 3.6 Properties of carbon black

Property	Unit	Value
Particle size	nm	32
Density	kg/L	2.04-2.11
Iodine adsorption	mg/g	1140

3.1.5 Solvent

Acetone was used as solvent in the application of solvent assisted mixing method for preparing nanocomposites. The solvent used was extra pure acetone obtained from Sigma Aldrich and having the product number of 24201. Its chemical structure and physical properties are given in Figure 3.5 and Table 3.7, respectively.

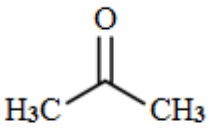

Figure 3.5 Chemical structure of acetone

Table 3.7 Properties of acetone [57]

Property	Unit	Value
Vapor pressure	mmHg	184
Boiling point	°C	56
Melting point	°C	-94

3.2 Preparation of Epoxy Polymer

In the preparation of epoxy specimens, different procedures were followed for each production stage. There were four production stages, namely; preparation of neat epoxy matrix, preparation of monomer added epoxy matrix, preparation of composites containing conductive fillers, and preparation of final composites containing both conductive fillers and monomer.

3.2.1 Preparation of Neat Epoxy Matrix

The first procedure was for the preparation of neat epoxy polymers. Epoxy resin and curing agent were degassed in a vacuum oven at 55°C and -0.8 bar for 3 hours in order to avoid air bubbles. Secondly, they were kept at room temperature for 30 minutes for cooling. The hardener was added with a ratio of 100:58 parts (epoxy/hardener) by weight and they were mixed with the mechanical mixer at 40 rpm for 25 minutes in a 250 ml beaker. The mixture was poured on aluminum molds in dimensions of 80x10x4 mm^3 for impact specimens and teflon molds in dimensions of 70x5x1 mm^3 for shape memory specimens. The molded polymer was cured at room temperature for 1 hour, at 90°C for 17 hours and postcured at 130°C for 3 hours. The flowchart for neat sample preparation can be seen in Figure 3.6.

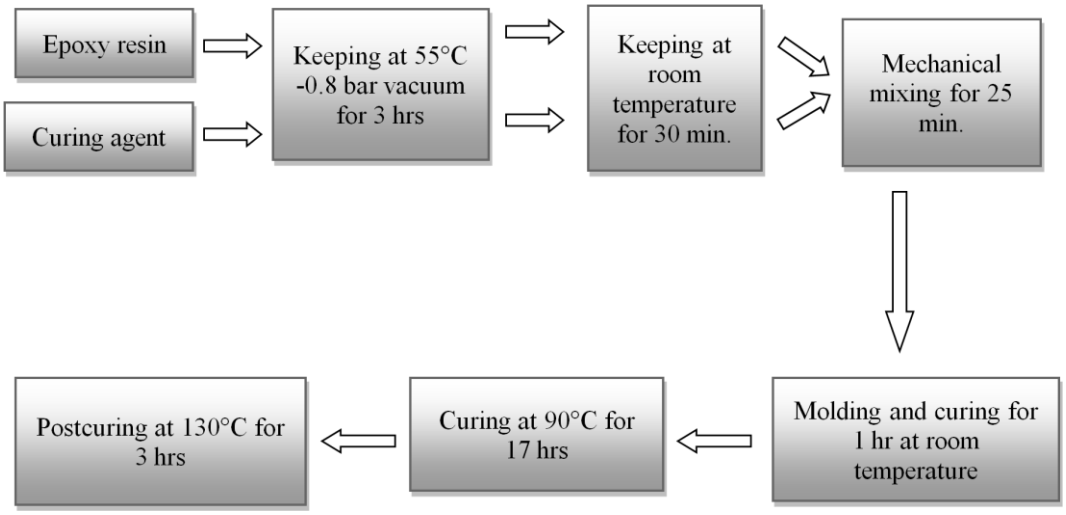

Figure 3.6. Flowchart of neat specimen preparation (according to the first procedure)

The second procedure was for the monomer containing samples. The epoxy resin and the hardener were kept inside vacuum oven for 3 hours at 55°C -0.8 bar as mentioned in the first procedure. After being kept at room temperature for 30 minutes, the monomer was mixed with epoxy resin at 40 rpm for 15 minutes. The monomer added in the polymer was 5, 10 and 15 wt. % of the total polymer content. Then this mixture was degassed in oven at 55°C and -0.8 bar for 45 minutes and cooled for 30 minutes. After, the epoxy-monomer mixture and the hardener were mixed for 25 minutes at 40 rpm, and finally the same curing cycle with the first procedure was applied. The flowchart of the second procedure is seen in Figure 3.7.

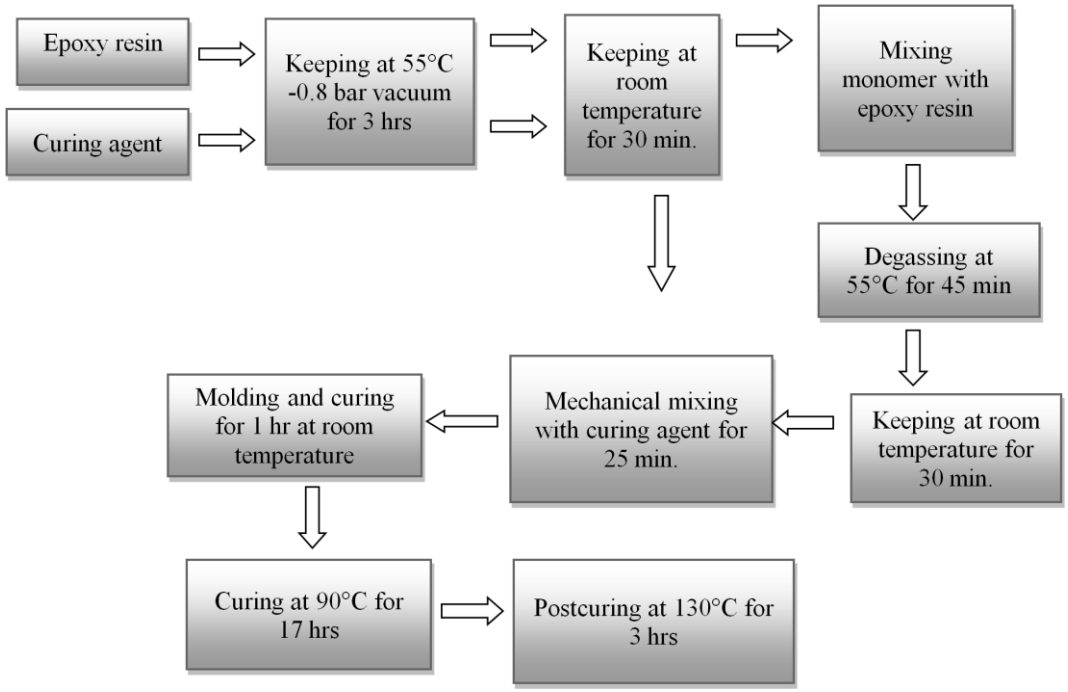

Figure 3.7. Flowchart of preparation of specimens containing monomer (according to the second procedure)

The third procedure was applied for the composite materials. Carbon black and carbon nanotubes were used as conductive fillers, moreover; they were also used together as hybrid fillers. The same procedure was followed for each of them. The composites were prepared having 0.5, 1, 3 and 5 wt. % carbon black and 0.25, 0.5, 1 and 2 wt. % carbon nanotubes. For all of the hybrid composites, 1 wt. % carbon black was used; the amount of carbon nanotubes was varied as, 0.25, 0.5 and 1 wt. %. The flowchart of the composite preparation is seen in Figure 3.8.

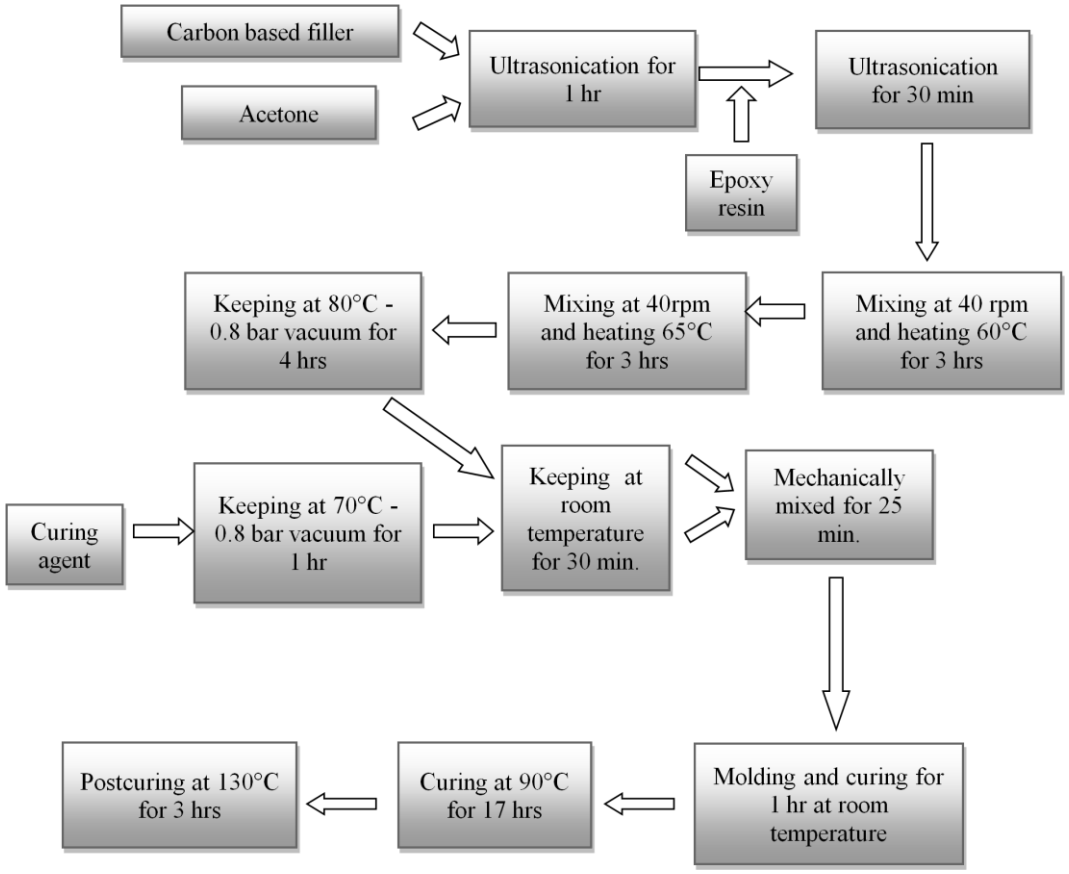

Figure 3.8. Flowchart of composite preparation (according to the third procedure)

The procedure was different than the previous ones in terms of using a solvent assisted sonication method. The carbon fillers were mixed in 250 ml beaker with acetone, which was three times the weight of epoxy used. Ultrasonic treatment was applied to this mixture for 1 hour. Then, the epoxy resin was introduced to this slurry and ultrasonic treatment was applied 30 more minutes. The mixture was started to be heated in water bath at 60°C, and it was mixed with mechanical stirrer at 40 rpm at the same time. After 3 hours, the temperature was raised to 65°C and mixing was carried on for 3 more hours. The solvent was completely evaporated during 6 hours of total heating. The epoxy resin was kept at 80°C and -0.8 bar vacuum for 4 hours in order to remove the remaining solvent and air bubbles inside the resin. Then, curing agent was kept at 70°C and -0.8 bar vacuum for 1 hour. After keeping them at room temperature for 30 minutes, they were mixed with mechanical stirrer at 40 rpm for 25 minutes. Finally the molding and curing part were applied which were the same with the first two procedures. The flowchart of the procedure is seen in Figure 3.8.

The final procedure was for the composites which contained monomer and carbon based fillers at the same time. This procedure was quite same with the third procedure except in the step of epoxy addition to the carbon based filler and acetone mixture, monomer was also added to the epoxy. The flowchart of the procedure is seen in Figure 3.9.

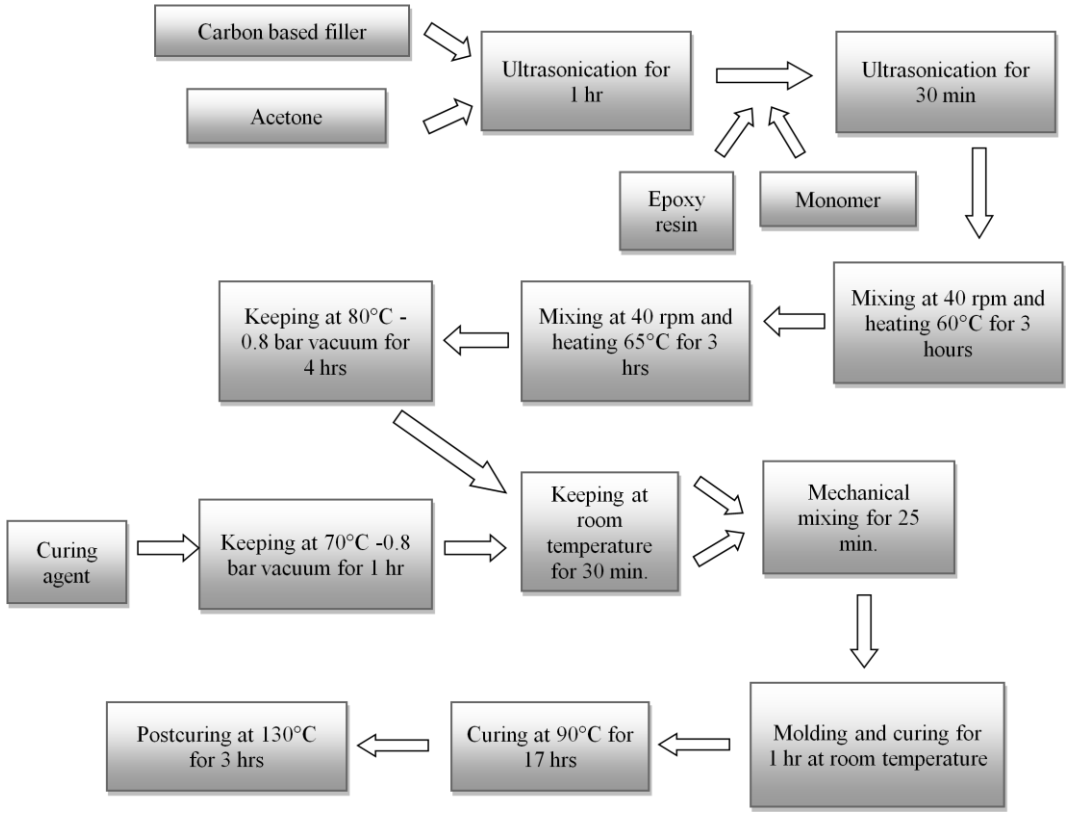

Figure 3.9. Flowchart of composite preparation (according to the fourth procedure)

The compositions of the samples which were produced and characterized in this thesis are shown in Table 3.8.

Table 3.8 The compositions of the formulations

Sample Code	Epoxy (%)	NGDE(%)	RDE(%)	CB(%)	CNT(%)
Neat Epoxy	100	0	0	0	0
E-5N	95	5	0	0	0
E-10N	90	10	0	0	0
E-15N	85	15	0	0	0
E-5R	95	0	5	0	0
E-10R	90	0	10	0	0
E-15R	85	0	15	0	0
E-0.5CB	99.5	0	0	0.5	0
E-1CB	99	0	0	1	0
E-3CB	97	0	0	3	0
E-5CB	95	0	0	5	0
E-0.25CNT	99.75	0	0	0	0.25
E-0.5CNT	99.5	0	0	0	0.5
E-1CNT	99	0	0	0	1
E-2CNT	98	0	0	0	2
E-1CB-0.25CNT	98.75	0	0	1	0.25
E-1CB-0.5CNT	98.5	0	0	1	0.5
E-1CB-1CNT	98	0	0	1	1
E-15N-1CB	84	15	0	1	0
E-15N-0.5CNT	84.5	15	0	0	0.5
E-15N-1CB-0.5CNT	83.5	15	0	1	0.5
E-15R-1CB	84	0	15	1	0
E-15R-0.5CNT	84.5	0	15	0	0.5
E-15R-1CB-0.5CNT	83.5	0	15	1	0.5

3.3 Characterization Methods

Neat epoxy samples, the samples containing monomer and the composite specimens were subjected to several characterization tests for the determination of their mechanical, thermal, electrical, shape memory properties and morphology. For the measurement of mechanical properties, tensile and impact tests were performed. In order to investigate thermal properties, Differential Scanning Calorimetry (DSC) test was applied to the samples. Additionally, electrical resistivity measurements and Scanning Electron Microscopy (SEM) were carried out for investigation of electrical properties and morphology. Finally, bending tests with both thermal and electrical actuation in order to determine thermal and electrical shape memory properties, were applied on the samples.

3.3.1 Mechanical Characterization

3.3.1.1 Tension Test

The tensile properties were measured using a Shimadzu Autograph AG-100 KNIS MS universal tensile testing instrument, photograph of which can be seen in Figure 3.10. Tensile specimens were prepared according to ASTM D638-10 (Standard Test Method for Tensile Properties of Plastics). The specimen dimension obeys Type IV. Some important dimensions of tensile samples are given in Figure 3.11 and Table 3.9.

Figure 3.10 The universal tensile testing instrument

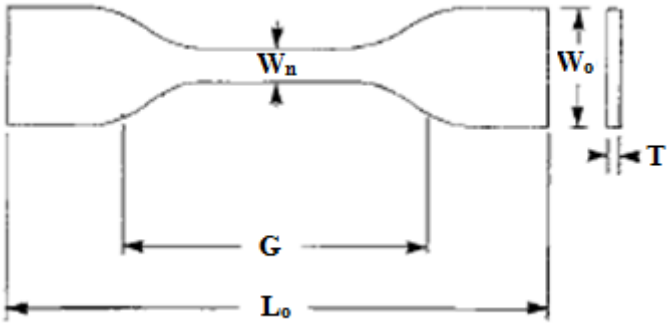

Figure 3.11 Tensile test specimen

Table 3.9 Dimensions of tensile specimen G L_o W_o T

Property	**Unit**	**Value**
Overall Length L_o	mm	115
Thickness T	mm	4
Width of narrow section W_n	mm	6
Width of wide section W_o	mm	19
Gauge length G	mm	65

The crosshead speed of the testing machine was adjusted as 4 mm/min. Using the data obtained from the tensile test, properties like tensile strength, elongation at break and Young's modulus were calculated. For each formulation five different specimens were tested and the average of these specimens was calculated. Standard deviations from mean values were calculated and mentioned in the results and discussion section.

3.3.1.2 Impact Test

Impact test was used in order to measure the impact strength of the both neat and composite specimens using a Ceast Resil Impactor 6967 impact testing instrument, the photograph of which is shown in Figure 3.12. Tests were done using 7.5 J hammer at room temperature. Five different samples were used for each formulation for accuracy. Test samples were not notched. Average of the five values and the standard deviation were calculated. The impact specimens were prepared according to the ISO 179-1 (Determination of charpy impact properties). The dimensions of the impact samples are represented in Table 3.10.

Figure 3.12 The impact testing instrument

Table 3.10 Dimensions of impact specimen

Property	Unit	Value
Length	mm	80
Thickness	mm	4
Width	mm	10

3.3.2 Thermal Characterization

3.3.2.1 Differential Scanning Calorimetry Analysis (DSC)

Thermal characterizations of the samples were carried out using a Shimadzu DSC-60 instrument. Initially, to meet the purpose of producing fully crosslinked epoxy resin, curing percentage was estimated for samples which were produced with the application of different curing cycles made up by changing curing temperature and time. Curing percentage was calculated by measuring the area under the curing curve after the DSC analysis. The curing cycle of the sample having the highest calculated curing percentage was selected and used for the production of epoxy polymers.

DSC was used also for the determination of glass transition temperature. Starting from room temperature the samples were heated to 250°C by applying heating rate of 10°C/min. The amount of heat absorbed by the specimen was measured. Using this data, glass transition temperature (T_g) was determined from the average of three different measurements. The visual of the DSC instrument is shown in Figure 3.13.

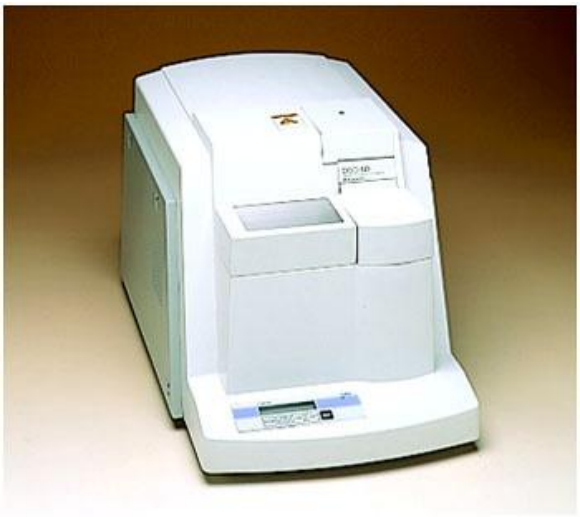

Figure 3.13 DSC instrument

3.3.3 Characterization of Shape Memory Behaviors

3.3.3.1 Thermal Actuation

Shape memory tests with thermal actuation were applied using bending test. The test was carried out in an oven at 90°C for the neat epoxy and samples containing monomers in 5, 10 and 15 wt. %. When the desired concentration of monomer was selected, bending tests were carried out at different temperatures such as 100, 110, 120, 130°C, for that specific monomer concentration. The purpose was to select the optimum temperature for the selected concentration of linear monomer. Optimum temperature was found as 110°C as according to the results of bending tests, therefore the bending tests for the composite samples were applied at 110°C.

The produced shape memory samples had dimensions of 70x5x1 mm^3. The experiment had four different steps. In the first step, the sample was placed in the oven and kept inside for 5 minutes for complete heating. Temperature of the oven was 90°C for the first experiments of samples containing monomer only and 110°C for composites with carbon fillers. The sample was bent in a small beaker having constant diameter of 3 cm in order to keep the applied strain constant. The distance between the ends of the sample when it was inside the beaker was measured which is also shown as L_{iload} in Figure 3.14.

Figure 3.14 Schematic representation of L_{iload}

When the sample reaches room temperature, it was taken out of the beaker. The distance between the ends of the sample is L_i. The shape fixity property R_f was calculated using the following formula **[58]**.

$$R_f = \frac{L_i}{L_{iload}} \times 100 \tag{3.1}$$

The angle of the sample was measured after it is taken out of the beaker and the measured angle is θ_f. The sample was placed in the oven at 110°C and kept inside until the shape recovery finished. The recovered sample was taken out of the oven and recovery angle was measured which is shown in Figure 3.15 as θ_r. The shape recovery was calculated using the following formula.

$$R_r = \frac{\theta_f - \theta_r}{\theta_f} \tag{3.2}$$

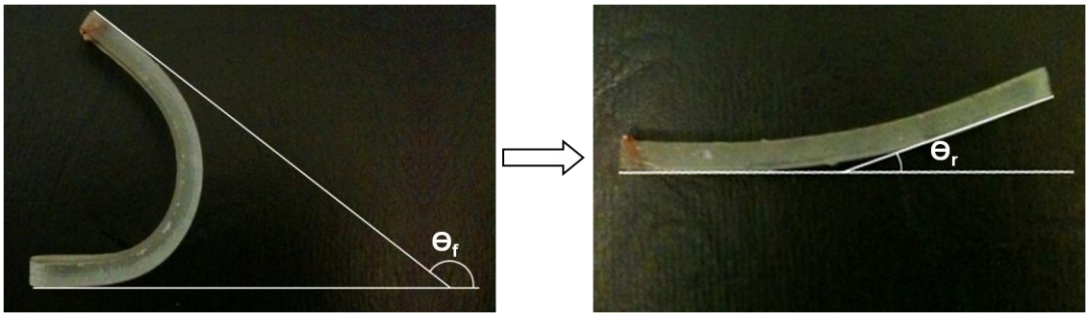

Figure 3.15 Fixed and recovered shape of the specimens

The third shape memory property determined was shape recovery time which is the total duration of recovery procedure starting from the moment of putting the fixed sample in the oven till the sample finishes recovering and it is indicated by t_{rec}. For the accuracy of the test, average of five different samples for each formulation and the standard deviation of these values were calculated.

3.3.3.2 Electrical Actuation

Electrical actuation tests of shape recovery were carried out using Entek TPW100 temperature control and adjustable power supply. N-shaped samples, dimensions of which is shown in Figure 3.17-b, were used for analyzing electrical actuation in shape recovery. The formulation which has the highest electrical conductivity, E-2CNT was subjected to electrical actuation test. The measurement was done for three samples.

The sample was placed on the probes inside the chamber of 25°C constant temperature. Constant voltage of 90 V was applied on the sample; meanwhile the temperature profile of the sample was measured by a thermocouple. When the sample got heated to 50°C, it was bended and the voltage source was closed. The bending force was kept being applied by the help of a thick metal plate until the new shape was fixed. In this condition, the bending angle was measured and recorded as θ_i. As soon as the sample cooled down to 25°C, the metal plate was removed, thus the stress was no longer implemented. In this case the bending angle was recorded as θ_f. 100 V was applied again to achieve the shape recovery. At the same time, recovery time was measured as the time passed starting from the recovery initiation till the end of recovery. It is indicated by t_{rec}. When the angle of the sample no longer changed, it meant that recovery was finished and the final measured angle of the sample was recorded as θ_r. Fixed and recovered shapes of E-2CNT sample can be seen in Figure 3.16. Shape fixity and shape recovery values were calculated using the following formulas.

$$R_f = \frac{\theta_i}{\theta_f} \tag{3.3}$$

$$R_r = \frac{\theta_f - \theta_r}{\theta_f} \tag{3.4}$$

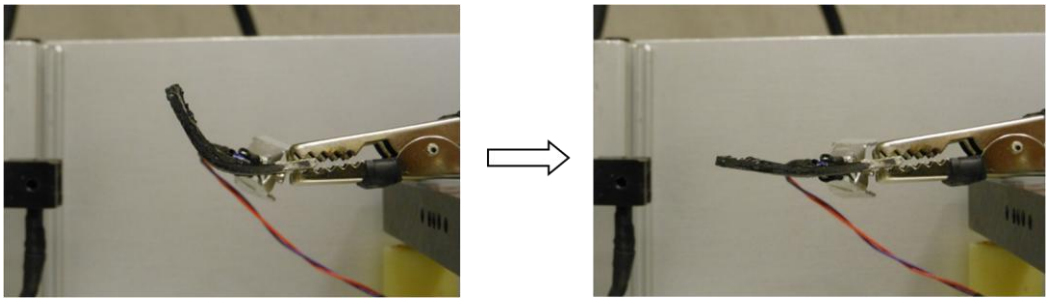

Figure 3.16 Fixed and recovered shapes of electrically actuated samples (EP-2CNT)

3.3.4 Electrical Characterization

The resistivity values of the epoxy polymer composites containing carbon black, carbon nanotube and hybrid fillers, were calculated according to two point probe method using a Keithley 2400 voltage source (Figure 3.17-a). The measurement was done at room temperature. In order to minimize the contact resistance, silver paste (ELECOLIT 325, Eurobond), was used. Two components of the silver paste were mixed in same amounts in weight and applied on the tips of n-shaped samples, the dimensions of which are represented in Figure 3.17-b. Silver paste was cured at 150°C for 5 minutes. Two probes were contacted on the silver pastes at both ends. With the application of constant DC voltage of 20 V, the current passing through the specimen and the resistivity value were calculated by the software. The measurement was done using 5 different specimens and each specimen was subjected to this test three times to reach the highest accuracy.

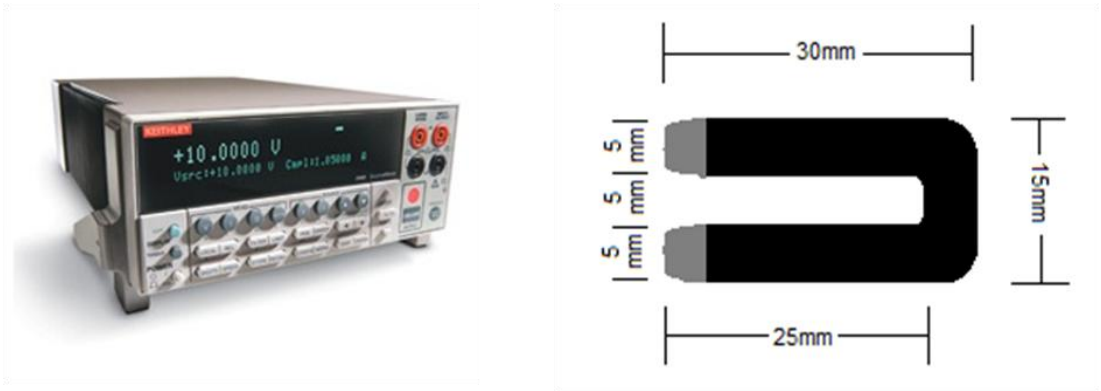

Figure 3.17 a) Constant voltage source b) N-shaped sample

3.3.5 Morphological Characterization

Scanning electron microscopy (SEM) QUANTA 400F was used for the morphology studies. Tensile fractured surfaces were examined using magnification values between x2000 and x20000. Palladium-gold coating was applied on the surfaces of the specimens

before the application of SEM test in order to provide conductivity on the surface. Effect of linear monomer, carbon nanotubes, carbon black and hybrid filler on the morphology of the samples was investigated.

3.3.6 Performance Tests of Shape Memory Polymers

Shape memory polymers were subjected to 10 cycles of shape memory tests with the purpose of investigating the durability of the shape memory properties like recovery, fixity and recovery time against successive shape memory cycles. Rectangular shape memory samples were used which has the dimensions of 70x5x1 mm^3. Each cycle of this performance test was composed of the thermal actuation procedure described in section 3.3.5.1. Polymer samples was heated up to 110°C in an oven, bent into u-shape in a beaker and left in the beaker for cool down afterwards. Shape fixity value was measured according to the thermal actuation procedure described previously. The bent sample was placed inside 110°C oven and the recovery duration was examined. Shape recovery and recovery time values were determined according to the thermal actuation procedure in section 3.3.5.1. Cycles was carried out 30 minutes after each other.

CHAPTER 4

RESULTS AND DISCUSSION

4.1 Calculation of Percentage Curing of Neat Epoxy Matrix

In order to obtain a polymer which has excellent mechanical, thermal properties and chemical resistance, it is considerably important to obtain a complete curing reaction between the resin and the curing agent. The percentage curing of the neat polymer was calculated to check curing parameters, the DSC plots and % curing calculation are shown in Appendix A. In Figure A.1, the differential scanning calorimetry plot for the uncured resin-hardener mixture is seen. A large peak was observed which indicates the heat of curing for the uncured sample. In Figure A.2 the DSC plot belongs to the cured sample with the curing parameters explained in the experimental methods section of this thesis **[49]**.

According to the formula, Equation 2.5 the curing percentage was calculated as 95.05 %, which is very close to 100 %, therefore it can be claimed that the polymer produced is nearly fully cured and has better mechanical properties and chemical resistance than the ones having lower curing percentage.

4.2 Effect of Monomer Addition to the Epoxy Matrix

Two different kinds of monomers were introduced to the polymer matrix and the effect of them on the mechanical, thermal, shape memory, electrical and morphological characteristics of the polymers were investigated. Neopentyl glycol diglycidyl ether (NGDE) is composed of aliphatic groups, whereas resorcinol diglycidyl ether (RDE) consists of aromatic groups. The chemical structures of the monomers are different from each other, therefore; they show different effects on characterization results when they are added to the polymer matrix. These effects will be discussed in this section.

4.2.1 Tensile and Impact Tests of the Samples

Tensile strength values are determined and represented in Figure 4.1. Detailed measurement results can be seen in Appendix B, Table B.1. It is seen that addition of NGDE and RDE show different effects in tensile strength characteristics. Strength values vary between 58 and 67 MPa. The tensile strength of neat epoxy is found to be 63 MPa which is higher than the most values represented in literature **[10, 44]**. A slight decrease in tensile strength is observed as the concentration of NGDE increases in the polymer matrix. The aliphatic nature of NGDE increases the distance between the chemical

crosslink points which causes the crosslink density to decrease. In an epoxy network the ability to carry a load is dependent to the crosslink points, therefore; tensile strength is expected to decrease with increasing NGDE content **[10, 59]**. On the other hand, addition of RDE does not result in a significant effect. This can be explained by its aromatic nature; RDE does not decrease the crosslink density as much as NGDE does.

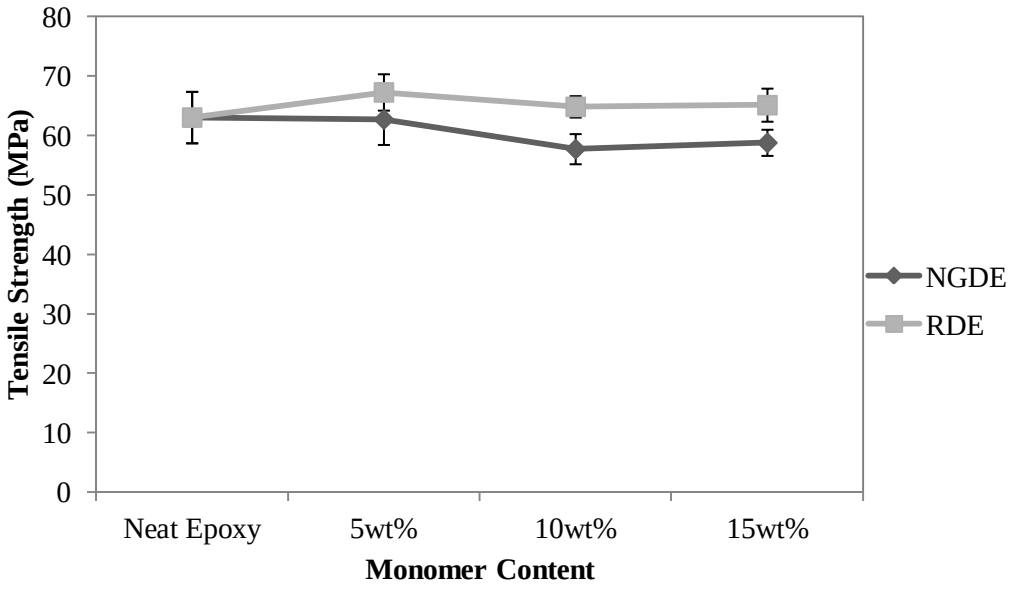

Figure 4.1 Tensile strength values of neat epoxy and samples containing NGDE and RDE

Young's Modulus property is also affected from the monomer addition. In the previous studies Young's Modulus values generally show a decreasing trend as monomer concentration increases due to the fact that monomer has lower modulus compared to the matrix, therefore; according to the modified rule of mixtures, modulus values are expected to decrease **[59]**. As shown in the Figure 4.2, Young's Modulus values did not show a significant change but a slight increase which may be due to the possible reactions occurred among the functional groups of epoxy resin, monomer and curing agent. Detailed measurement results can be seen in Appendix B, Table B.1.

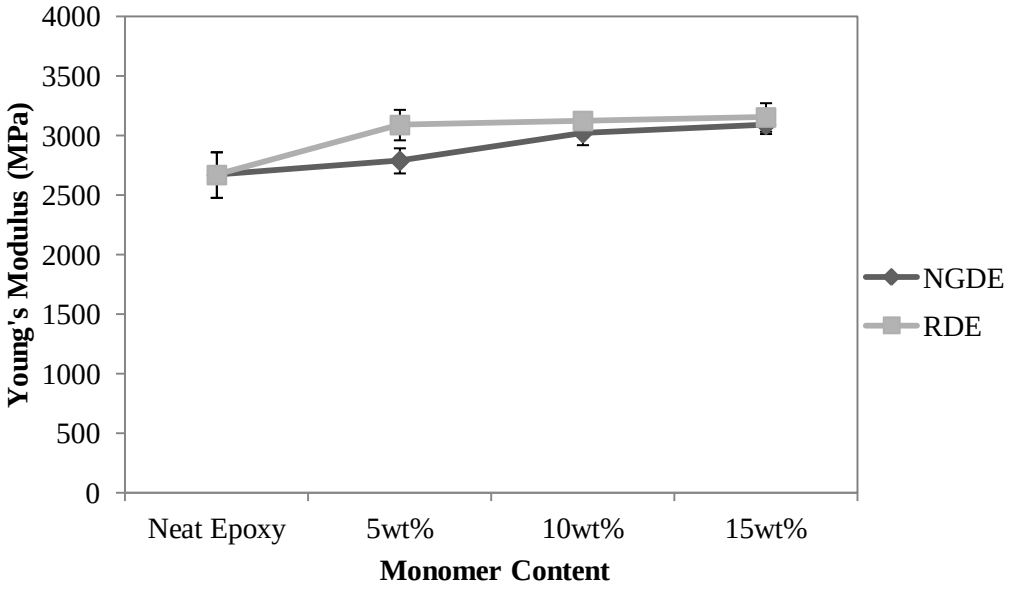

Figure 4.2 Young's Modulus values of neat epoxy and samples containing NGDE and RDE

Elongation at break values for polymer samples containing different amounts of monomers are represented in Figure 4.3. Table B.1 in Appendix B represents detailed results. Increasing amount of NGDE in polymer matrix resulted in a decrease in elongation at break. This is an unexpected result since linear NGDE chains decrease the crosslink density, increase flexibility and therefore increase in elongation at break values was expected. Increase in elongation at break values can be attributed to the potential reactions between epoxy resin, curing agent and monomer. In literature, some researchers also found increase in elongation at break when they introduce a monomer in polymer matrix **[10]**. Chen and co-workers worked with epoxy and a linear chain monomer. They found that, failure strain first increased, but then decreased sharply as the amount of monomer increased **[59]**.

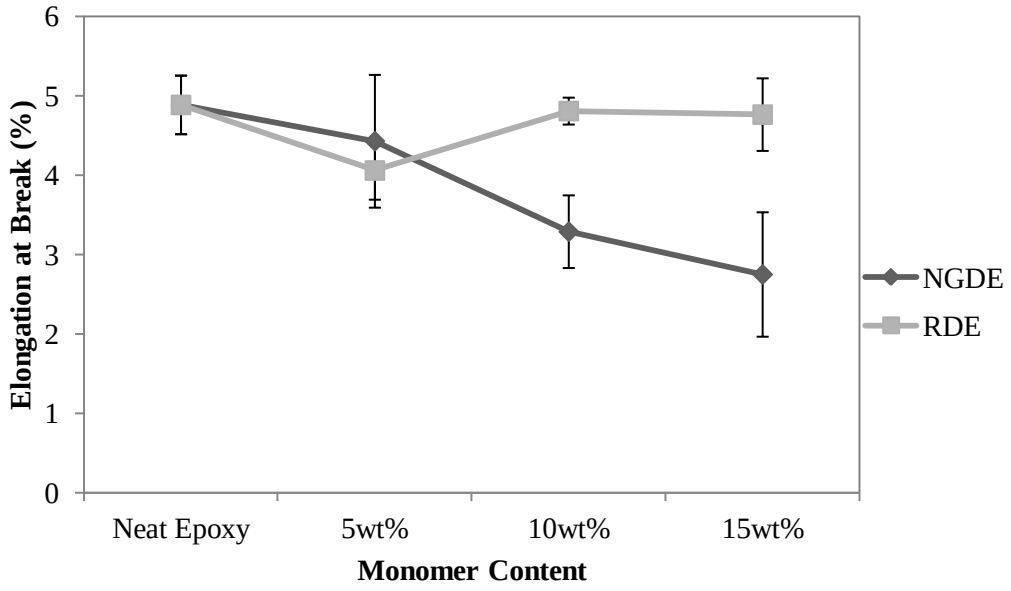

Figure 4.3 Elongation at break values of neat epoxy and samples containing NGDE and RDE

Impact strength of the epoxy polymers can be improved by introducing flexible chain modifiers into the system. With the addition of NGDE, the mobility of the chain segments were increased, the resulting polymer is less brittle and therefore, the impact strength was increased for these specimens (Figure 4.4). There is only a slight decrease of impact strength at 10 wt. % NGDE which can be explained by the aggregations which may have occurred as a result of unreacted chains. On the other hand, RDE had low contribution to the flexibility of the chains owing to its aromatic nature, thus, significant changes in impact strength was not observed for the samples containing RDE. Impact energy is strongly related with the amount of soft segment present in the epoxy matrix. Lou and co-workers have also observed higher impact strength with the addition of long chain of modifier to the polymer matrix due to the increased toughness of polymer matrix **[60]**. Tabulated numerical values of impact test result can be seen in Appendix B, Table B.1.

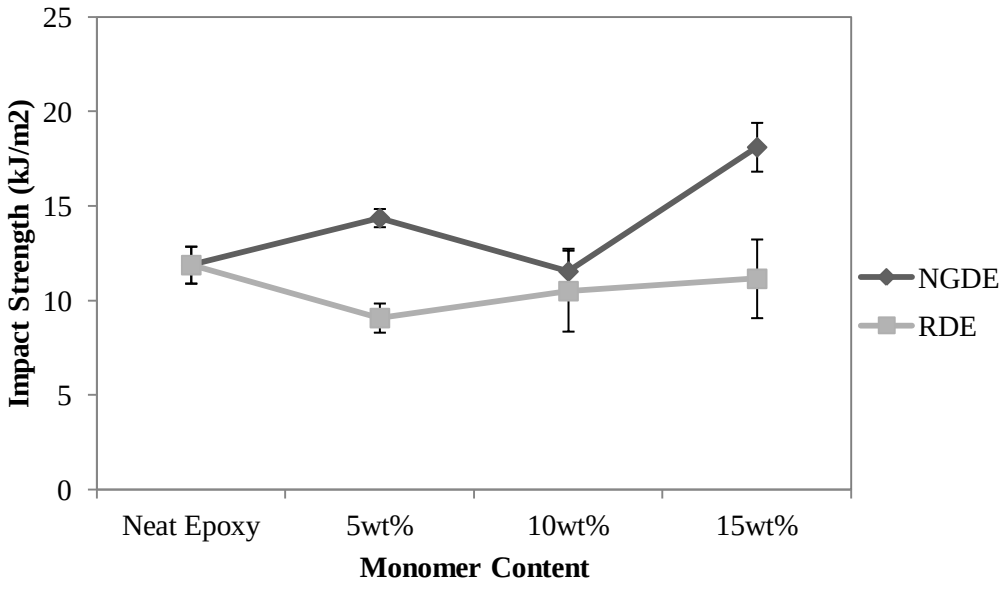

Figure 4.4 Impact strength values of neat epoxy and samples containing NGDE and RDE

4.2.2 Differential Scanning Calorimetry Tests of the Samples

Glass transition temperature (T_g) values for polymer samples containing different amounts of monomers are represented in Figure 4.5 and listed in detail in Table C.1 of Appendix C. For the aliphatic NGDE, a clear decrease in T_g could be observed, on the other hand, this effect could be seen slightly for RDE monomer. Aliphatic chains enlarged the distance between crosslink points, which resulted in a decreasing trend in crosslink density. The segments became more flexible and thereby T_g values were decreased. Similar results were obtained by researchers in the literature **[13, 10]**. Low T_g values could be an advantage for shape memory polymers in industry since they can be triggered using lower temperatures. For the case of aromatic RDE, decrease in T_g was smaller than NGDE which showed that the polymer kept its stiffness and rigid structure even at high concentrations of monomer. The epoxy polymer containing RDE could be used in applications where high temperature is necessary.

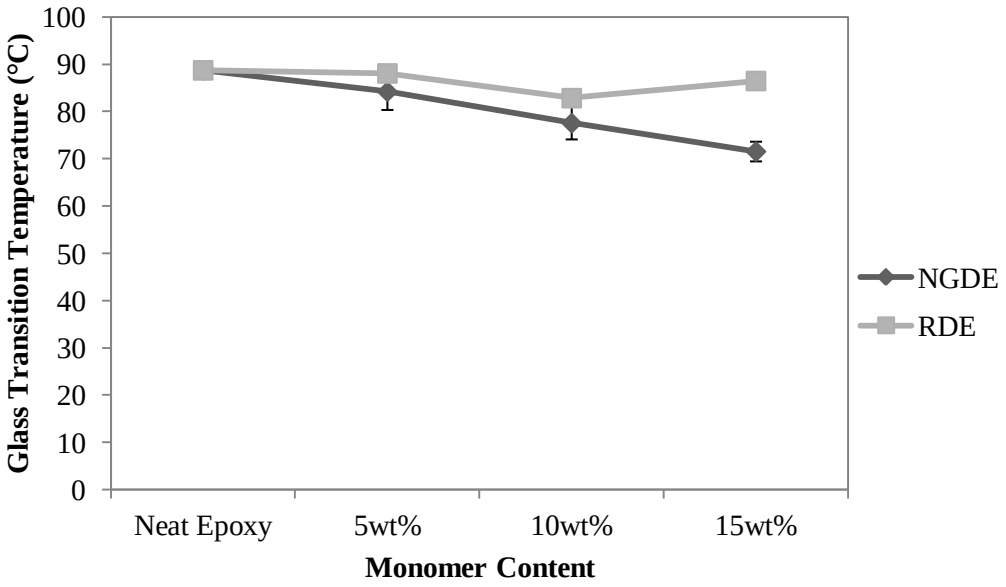

Figure 4.5 Glass transition temperature values of neat epoxy and samples containing NGDE and RDE

4.2.3 Thermal Shape Memory Tests of the Samples

The results for thermal shape memory tests of monomer containing samples which were carried out at 90°C are shown in Figures 4.6-4.8. Detailed results are listed in Table D.1 of Appendix D. In order to obtain shape memory effect, elastic deformability is necessary in a certain extent. Two different monomers added in the epoxy matrix were aimed to improve shape memory performance of brittle epoxy matrix. The results for shape recovery show that the aim was reached successfully. An increasing trend for shape recovery was observed with the addition of monomers. Introducing low molecular weight and long chain monomers into the matrix helped the polymer reach the desired deformability by developing the soft segment as it can be seen in Figure 4.6 **[4]**.

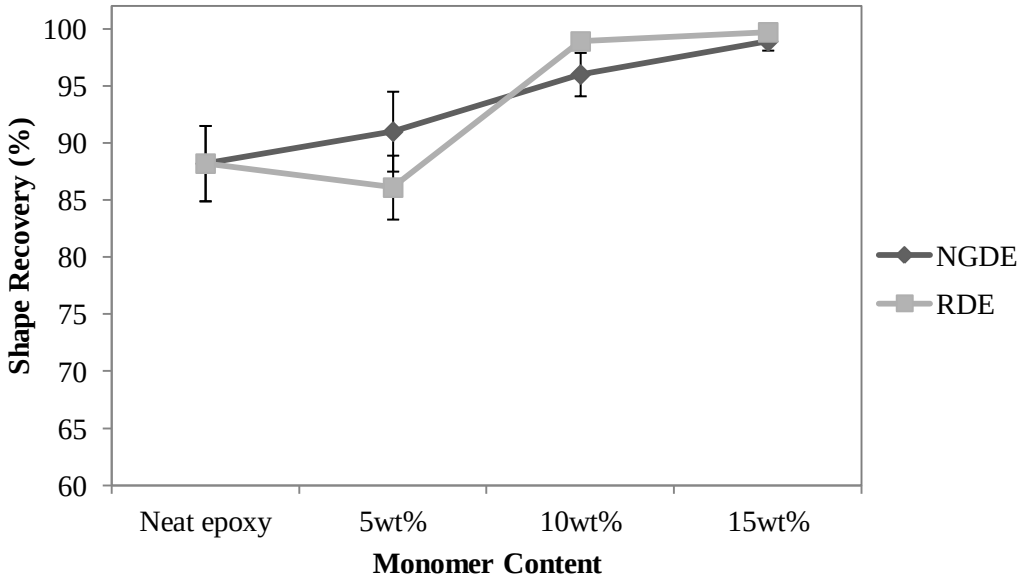

Figure 4.6 Shape recovery values of neat epoxy and samples containing NGDE and RDE

Shape fixity values for epoxy samples containing varying amounts of monomer are represented in Figure 4.7. For all formulations, it can be said that shape fixity is above 95 %. Fixity property did not change significantly as the monomer amount in the matrix increased for both monomer types. Effects of NGDE and RDE amounts on shape fixity property are similar to each other. Addition of linear monomer decreased the crosslink density and enhanced the elastic ratio according to the previous studies **[10]**. It was claimed that large elastic ratio led to high shape fixity when cooling and it could fix large amount of strain with application of smaller stress. With regard to this explanation, it is reasonable to get improvement in fixity property by addition of more monomer into the matrix.

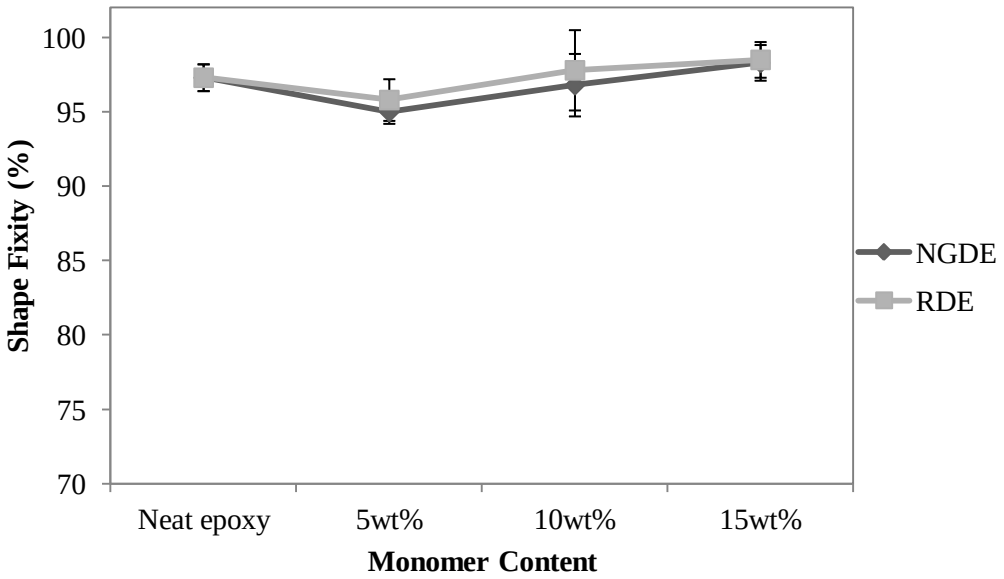

Figure 4.7 Shape fixity values of neat epoxy samples containing NGDE and RDE

As it can be seen in Figure 4.8, recovery time shows a decreasing trend as the monomer amount in the structure is increased. This effect is due to the dominating soft segment, which is a result of low crosslink density. Existence of especially aliphatic monomers in the structure causes decrease in crosslink density **[61]**. With the addition of long chains, the distance between crosslink points becomes longer, and therefore crosslink density decreases. A material having less crosslink density has more dynamic networks and free volume change is less restricted at high temperatures. Moreover, samples having low T_g started recovering earlier and therefore full recovery is achieved in a shorter time. It is possible to indicate that recovery is much faster for monomer added samples because of these reasons.

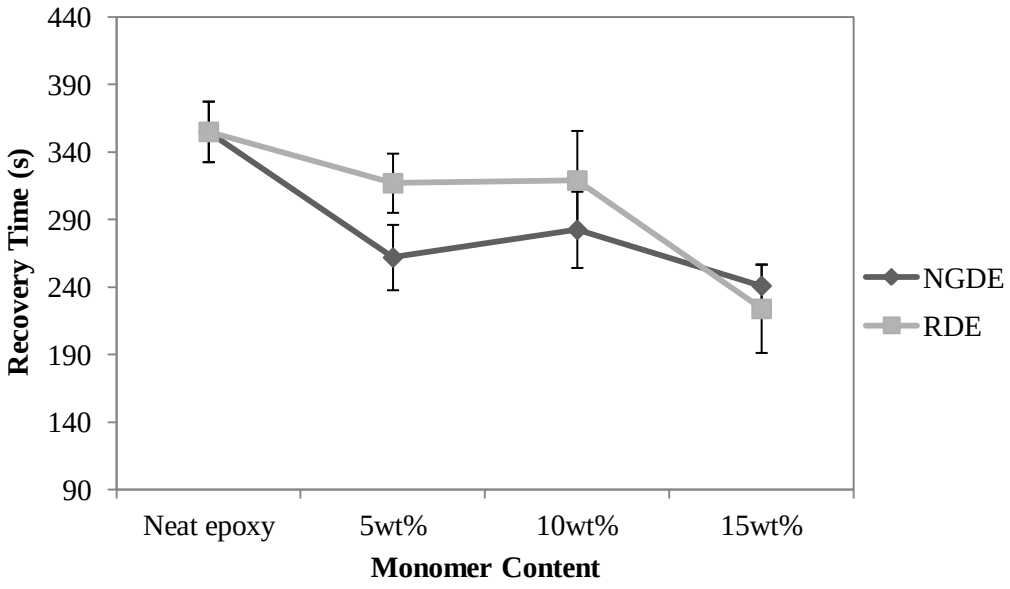

Figure 4.8 Recovery time values of neat epoxy samples containing NGDE and RDE

4.2.4 Scanning Electron Microscopy Tests of the Samples

Scanning electron microscopy photographs of neat and monomer containing samples are represented in this section. Figure 4.9 shows the images for increasing amount of NGDE monomer. In Figure 4.9a, a smooth brittle structure was observed for neat sample. On the other hand, with increasing amounts of NGDE, the structure became rougher which indicates less brittle matrix when compared to neat epoxy. The image of neat epoxy showed a smooth surface with less amount of deformation. This could be also verified by the impact results, showing low impact strength for neat epoxy sample. There was also no sign of particle or agglomerations indicating no phase separation between NGDE and DGEBA resin. Moreover, the ridges formed in the structure of NGDE samples inhibited crack growth during the fracture. Similar results were also obtained by other research groups; Yao et al. and Yang et al. **[62, 63]**.

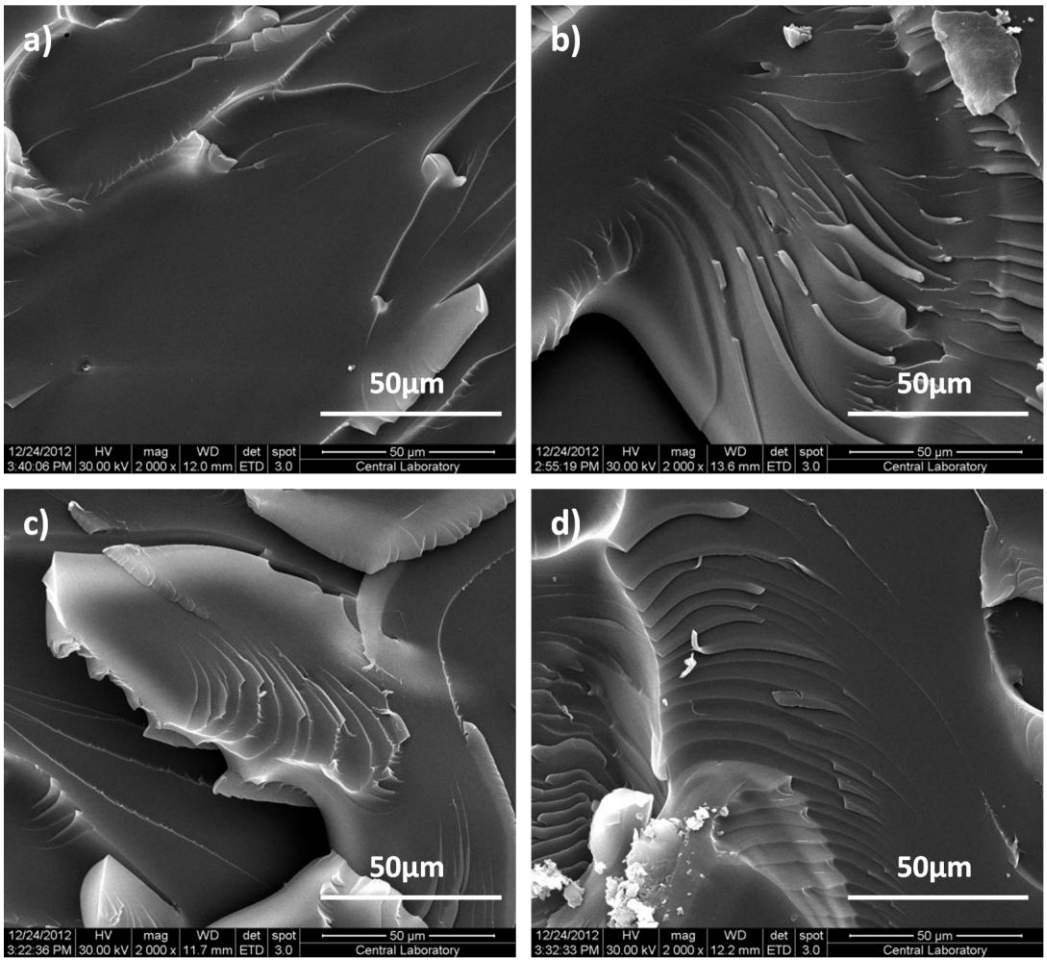

Figure 4.9 SEM images at 2000x magnification for a)Neat epoxy, and NGDE loaded polymers, b)5NGDE, c)10NGDE, d)15NGDE

SEM images for RDE samples can be seen in Figure 4.10. RDE samples exhibited similar behaviors with NGDE samples, however low amount of ridges were observed showing that fracture surface of RDE samples were not as rough as NGDE samples. It can be said that homogeneous dispersion of RDE was achieved and no separation of phases between the epoxy resin and the monomer was observed. In Figure 4.10d, it was seen that there were some parts at which crack initiation started, but they did not continue. This was a visual indication of crack inhibition property provided by monomer usage **[62]**.

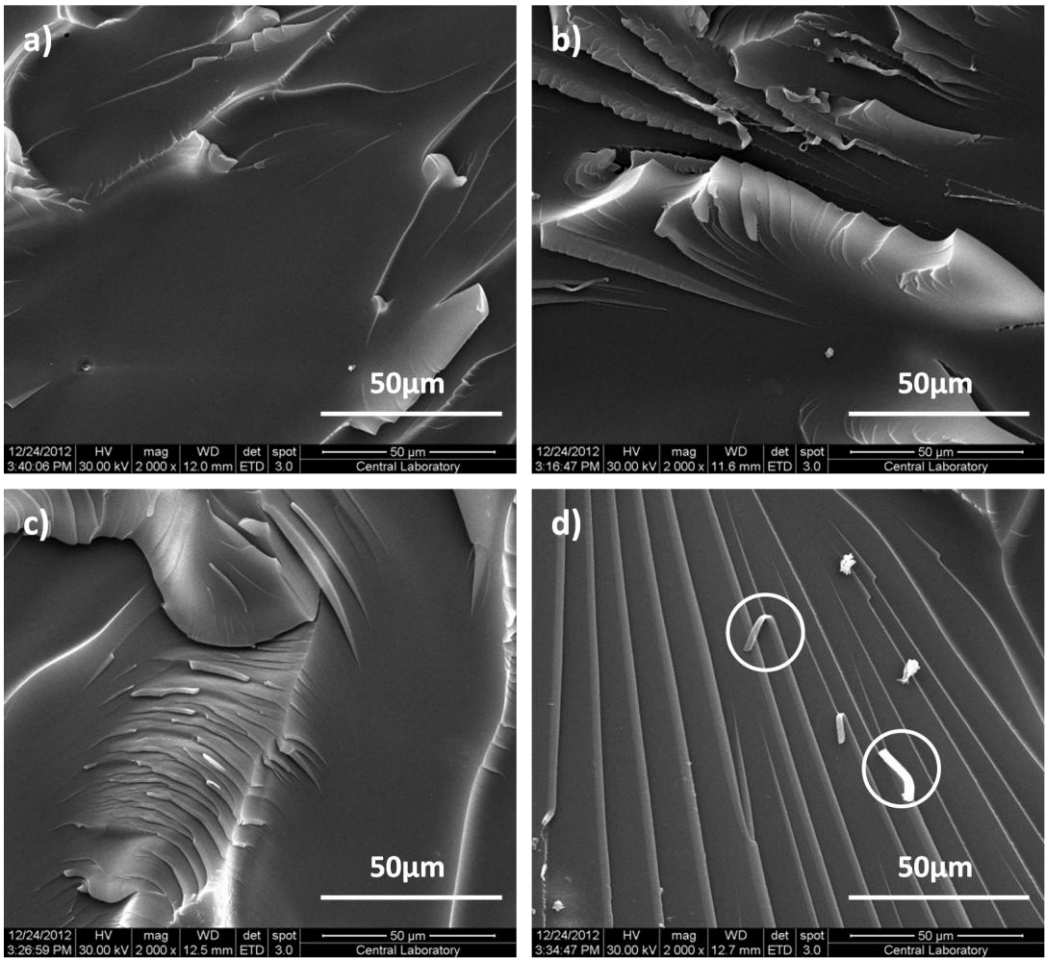

Figure 4.10 SEM images at 2000x magnification for a)Neat epoxy, and RDE loaded polymers, b)5RDE, c)10RDE, d)15RDE

4.2.5 Effect of Temperature on the Shape Memory Properties

As a result of the study carried out using different amounts of monomers, two different formulations were chosen to be used for further studies. E-15R and E-15N samples were found to be more promising in mechanical and shape memory point of view. These samples showed high tensile and impact strength properties and also highest shape recovery and fixity values. Moreover, recovery time was the lowest for these samples among the other ones.

Shape memory tests which were carried out at 90, 100, 110, 120 and 130°C to obtain information about the effect of temperature on shape memory. In the following experiments E-15N and E-15R samples were examined for the investigation of optimum temperature that should be used for the further shape memory tests. Figure 4.11 gives a general idea about the shape recovery percentage, which shows that shape recovery did not change significantly with varying temperature values. In Figure 4.12, shape fixity values also remained constant above 98 %. In other studies it was concluded that, as far as the application temperature is above T_g, large changes in shape recovery and fixity

could not be observed. Besides, the test was applied for samples containing 15 wt. % monomer; which showed superior recovery and fixity even at 90°C. In this case further increase of these properties could not be observed **[10]**. Additionally, this is because these two properties mainly depend on the ratio of hard to soft segment. Application of different temperature did not make any change in hard to soft segment ratio, on the other hand it affected only how fast the temperature of the sample was increased during heating. It can be seen in Figure 4.13 that a significant decrease was observed in shape recovery time which is in accordance with the previous comments. As the application temperature increased, the polymer heated faster and started recovery earlier than other samples and this resulted in much faster recovery when compared with the ones tested at lower application temperature. The tabulated results can be seen in Table D.2 of Appendix D.

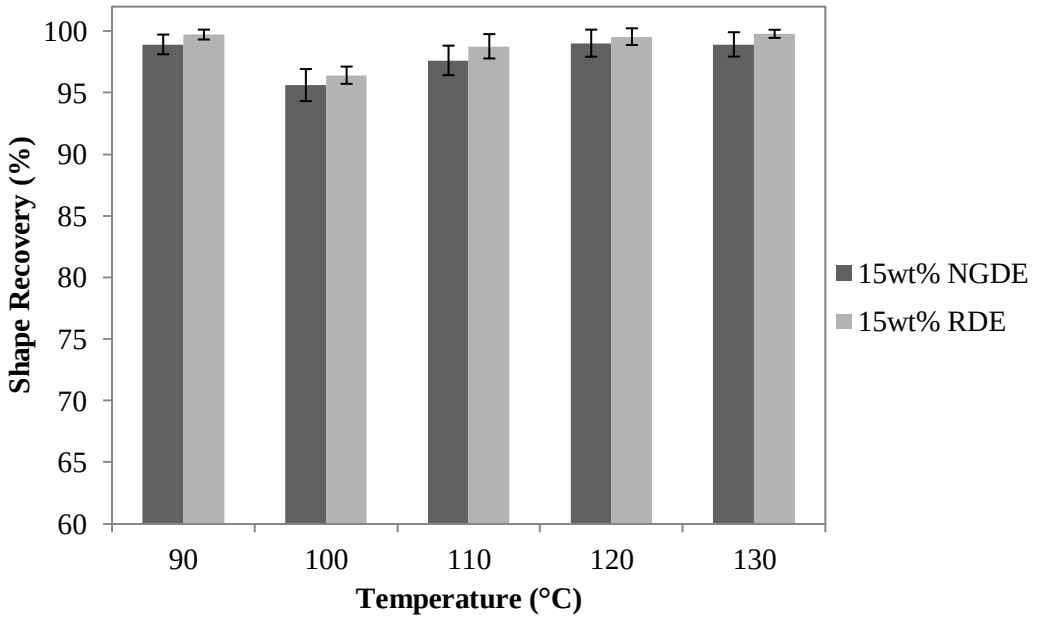

Figure 4.11 Shape recovery values at varying temperatures

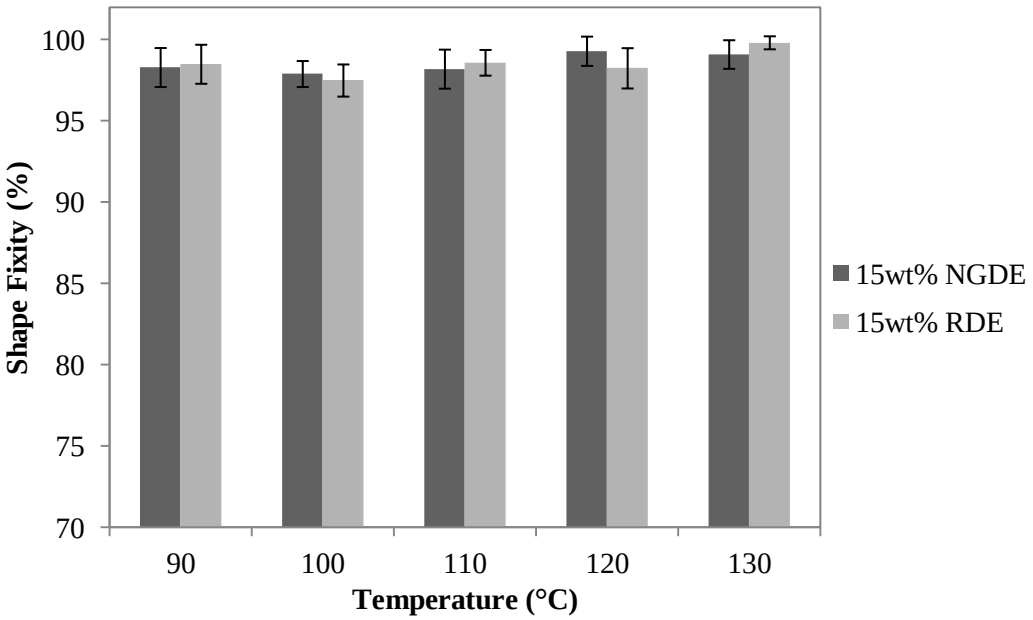

Figure 4.12 Shape fixity values at varying temperatures

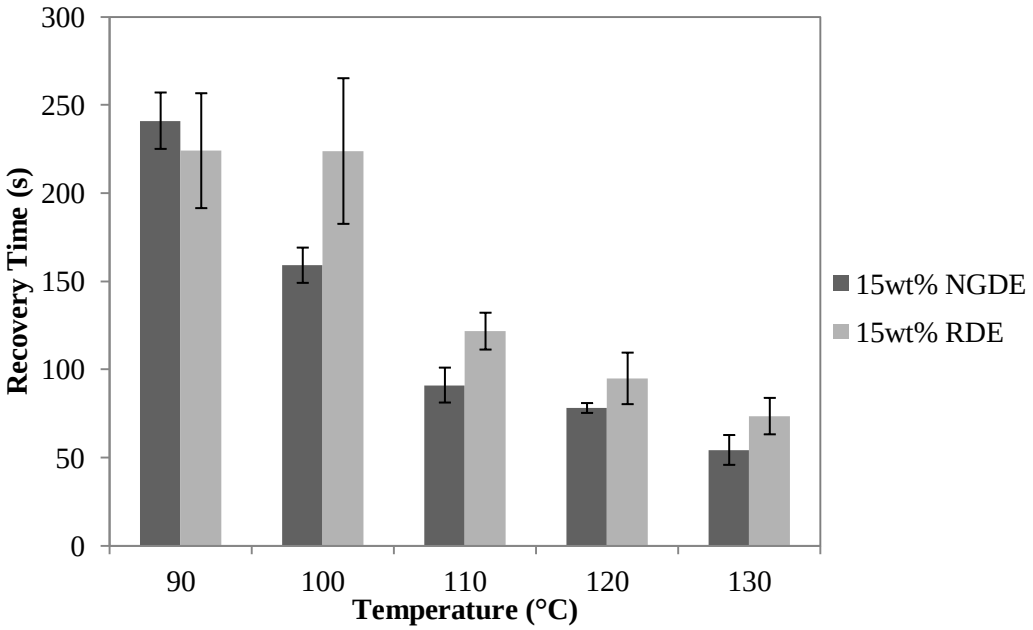

Figure 4.13 Recovery time values at varying temperatures

In the consideration of above analysis, the most optimum application temperature was selected. It seemed logical to work with higher temperatures, so that to obtain the least recovery time; on the other hand, trying to create a more practical method was also a purpose of this thesis, for which very high application temperatures would not help in

creating a convenient method for shape recovery procedure. When these two ideas were considered, application temperature of 110°C was selected and used for further shape memory studies.

4.3 Effect of Addition of Carbon Based Fillers to the Epoxy Matrix

In this section the characterization results of the composites with nano reinforcements are represented. The data for 0.5, 1, 3, 5 % carbon black filled composites, 0.25, 0.5, 1 and 2 % carbon nanotube filled composites and for the hybrid composites which contain fixed amount of carbon black (1 wt. %) and varying amounts of carbon nanotubes as 0.25, 0.5 and 1 %, were illustrated together in the same graph. Tensile and impact tests, DSC test, electrical resistivity test, shape memory tests with thermal and electrical actuation, and SEM analyses were applied in the characterization procedure of the composite samples.

4.3.1 Tensile and Impact Tests of Composites

The tensile properties of the composites are represented in Figure 4.14-4.16. Average results and standard deviation values can be seen in Table B.2 in Appendix B. Tensile results revealed that the highest tensile strength was obtained for the sample containing 0.5 wt. % carbon nanotube. As the fraction of carbon nanotubes increased, dramatic decrease in tensile strength was obtained which can be explained by the stress concentrated areas occurring from the highly agglomerated particles in the matrix **[41]**. Moreover observing the highest tensile strength for the carbon nanotube composite was expected because of its high aspect ratio compared to carbon black particles. Likewise, tensile strength decreased with increasing carbon black content. This can be explained as a consequence of increasing viscosity, which caused difficulties in the mixing procedure of the resin mixture, therefore might produce agglomerates and high amount of air bubbles in the polymer. The stress was focused directly on these inhomogeneous parts which lowered the tensile strength **[46]**.

Figure 4.15 represents the elastic modulus values of the composites. In general, slight increase in modulus is observed for increasing carbon filler amounts in the composites. High aspect ratio of the carbon nanotubes fillers contributed to the hardness of the polymer, thereby high elastic modulus values were obtained for carbon nanotubes filled composites, especially at 0.5 wt. % loading **[41]**. For concentrations higher that 0.5 wt. %, epoxy blend became highly viscous and so the agglomerations prevented further increase of the elastic modulus values of these specimens **[64]**. For hybrid formulations and carbon black composites it can be also said that elastic modulus increased due to the increase of stiffness as more carbon based filler was added to the matrix.

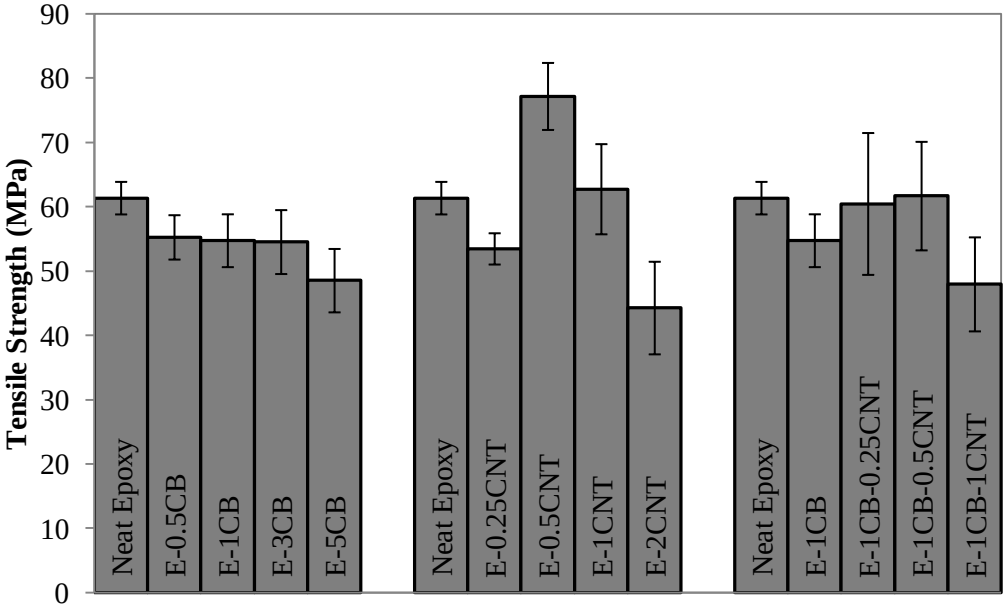

Figure 4.14 Tensile strength values of neat epoxy and its composites

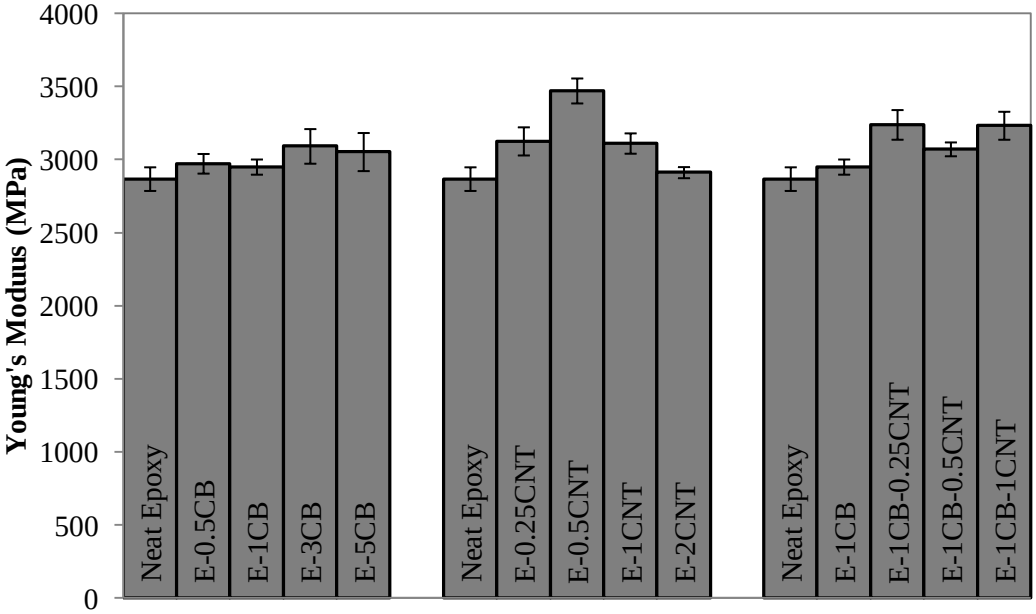

Figure 4.15 Young's Modulus values of neat epoxy and its composites

As can be seen in Figure 4.16, elongation at break values showed a general decreasing trend with the increase of filler loading. This decreasing effect was due to the highly brittle structure of carbon based composites **[65]**. Meincke and co-workers also recorded

that, as carbon black and carbon nanotube contents were increased in the polyamide based matrix, lower values of elongation at break were achieved **[66]**.

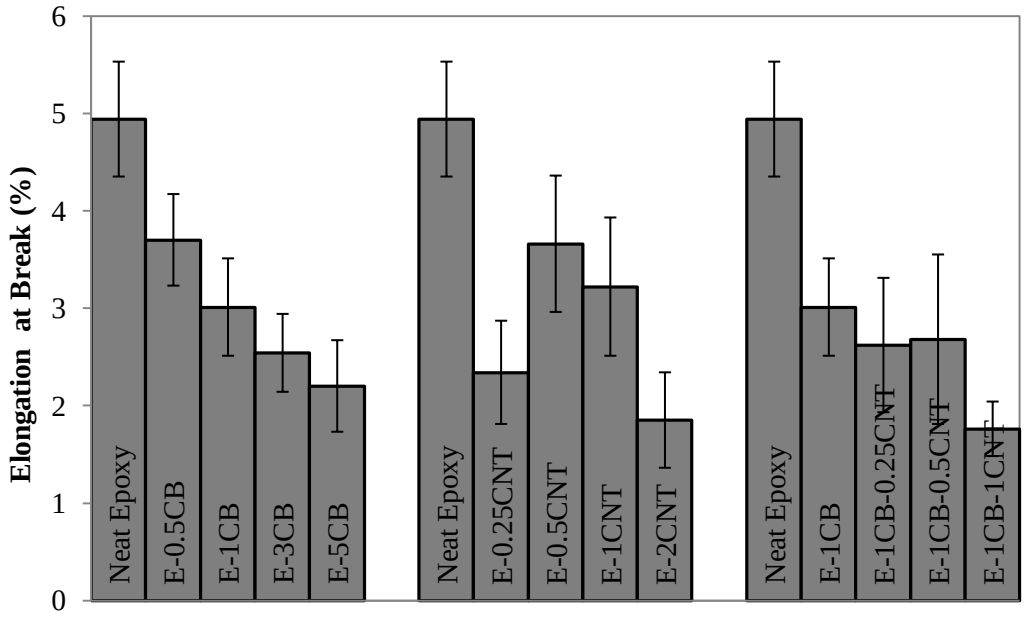

Figure 4.16 Elongation at break values of neat epoxy and its composites

Impact strength values of the composites are shown in Figure 4.17 and data are given in detail in Table B.2 of Appendix B. In literature, it was stated that conductive filler addition to the polymer matrix increased the impact toughness **[67]**. However in this study decrease in the impact strength was observed for binary composites of carbon black and carbon nanotubes. The reason can be explained by the combination of two different effects. The major one was high brittleness of composites which reduced the resistance of material to impact fracture. Secondly, the air bubble formation in highly viscous epoxy matrix reduced the actual cross sectional area of the impact samples which resulted in reduced impact strength values for the binary composites. The situation was a little bit different for hybrid composites. The existence of both type of fillers in the polymer caused a significant increase in the impact strength, which was attributed to the reduced agglomerations of fillers preventing crack propagation in the course of impact fracturing. For instance, in the later parts of this chapter, SEM results of hybrid composites showed that hybrid fillers were dispersed better in the structure when compared to the composites containing single type of filler (Figure 4.34). This phenomenon was dominant until certain amount of carbon nanotubes loading. For E-1CB-1CNT composite, negative effect of voids in the matrix originating from higher viscosity during mixing of polymer resin matrix on impact strength became upfront on the impact strength.

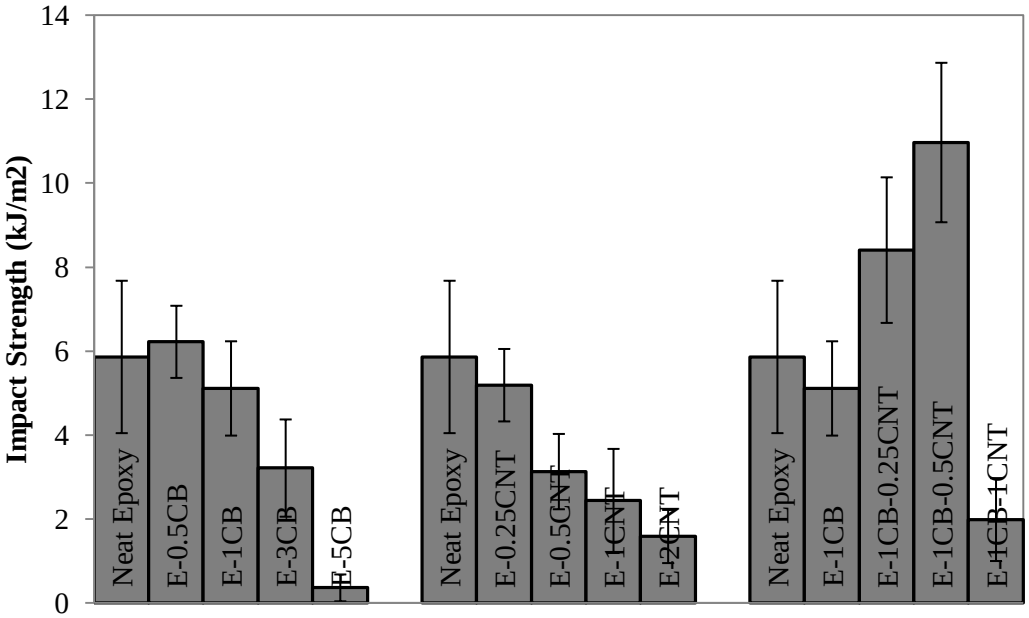

Figure 4.17 Impact strength values of neat epoxy and its composites

4.3.2 Differential Scanning Calorimetry Tests of Composites

Figure 4.18 shows the change in glass transition temperature values with loading of carbon based fillers. Detailed values are listed in Table C.2 of Appendix C. Glass transition was observed to decrease 5°C for 0.25 % CNT containing composite and after that it increased as the carbon nanotubes amount was increased in the matrix. Researchers found an increasing effect of carbon nanotubes on the glass transition temperature values **[68]**. Decreasing effect in this study could be explained by the imperfect dispersion of nanotubes and thereby generation of free voids in the matrix **[69]**. The behaviour of elongation at break for 0.25 wt. % filled carbon nanotube composite could also be explained by the same theory. A decreasing trend in glass transition temperature with respect to the neat epoxy was obtained when carbon black composites are analyzed. The possible reason might be carbon black particles having larger diameter compared with carbon nanotubes preventing polymer chains to be interlocked to each other firmly and thereby decreasing the glass transition temperature **[70]**. Additionally, the agglomerates in the structure behaved like larger particles and thus decreased the glass transition. For hybrid composites, except E-1CB-0.25CNT, lower glass transition values were observed when compared to neat epoxy.

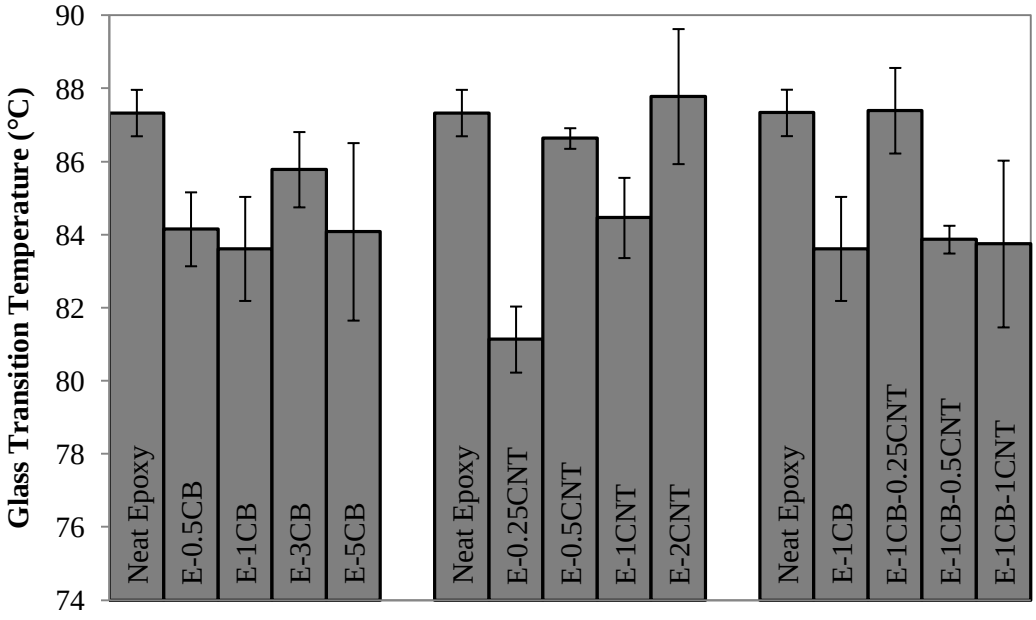

Figure 4.18 Glass Transition Temperature values of neat epoxy and its composites

4.3.3 Thermal Shape Memory Tests of Composites

Figures 4.19-4.21 show changes in typical shape memory properties with respect to filler addition in the matrix. Average values and standard deviations can be seen in Table D.3 of Appendix D. According to Figure 4.19, addition of carbon based filler to the matrix did not cause a significant change on the shape recovery percentage. Shape recovery effect is observed during high amount of change in modulus for epoxy based polymers which is seen during the glass transition. Therefore the effect of carbon particles on this property could not be observed clearly. Mainly the thermal properties of polymer matrix showed effects on shape recovery properties **[71]**.

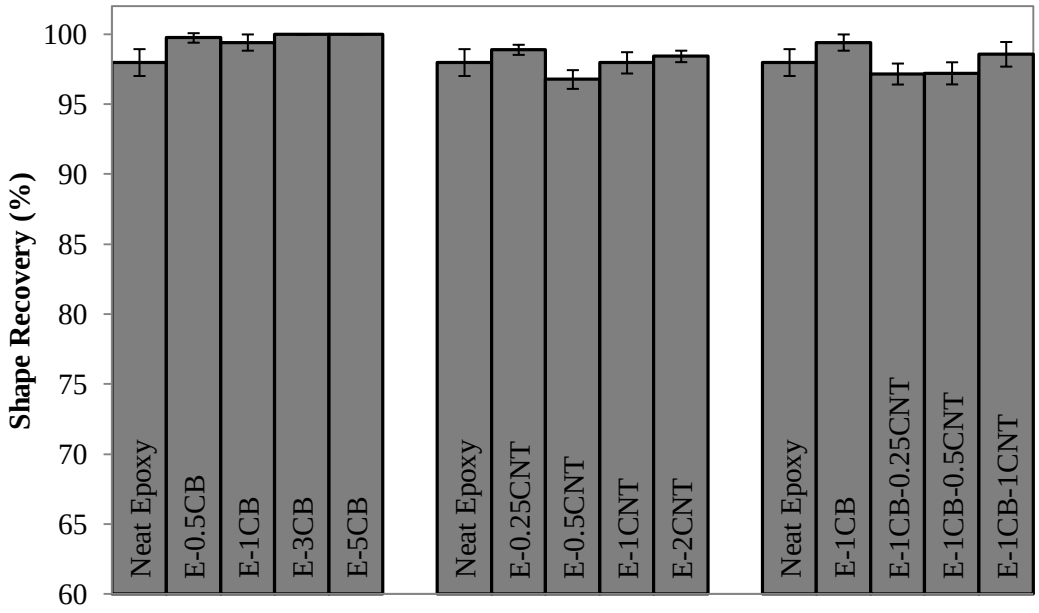

Figure 4.19 Shape recovery values of neat epoxy and its composites

Shape fixity values for all composites can be seen in Figure 4.20. A slight decrease was observed for composites containing carbon black and carbon nanotubes only. Shape fixity property is affected by the soft segment of the polymer. Carbon based materials usually have contribution to the hard segment of the polymer matrix; therefore, the soft domain becomes less dominant. In this case the slight decrease is an expected situation. On the contrary, hybrid composites showed slight increase in shape fixity, which means the hard segment of these samples was not as effective as the composites containing carbon nanotubes only. This reason can also be supported by the decrease in recovery time of hybrid composites in Figure 4.21 **[13]**.

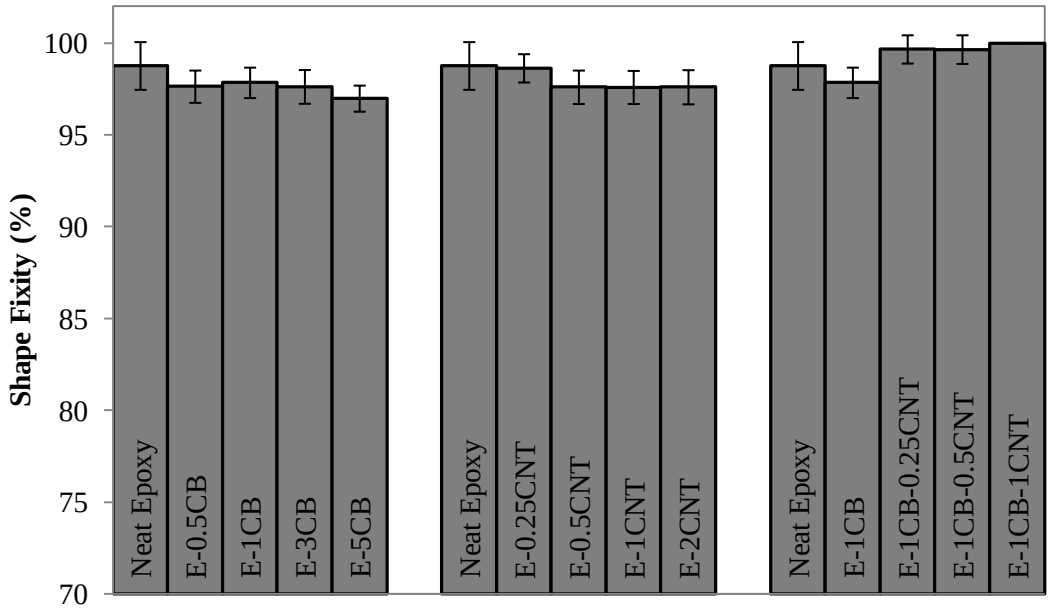

Figure 4.20 Shape fixity values of neat epoxy and its composites

Recovery time of shape memory samples is shown in Figure 4.21. Samples containing higher amounts of carbon nanotubes recovered slower. However a considerable decrease in recovery time for 2 % CNT loading was observed. Carbon based materials supported the hard segment of the matrix and recovery time was related to the stability of the hard segment. Highly developed hard domain of carbon nanotube composites caused decrease in the activity of the soft segment, leading to an increase in shape recovery time. Decrease in E-2CNT could be explained by the inhomogeneity of the structure caused by air bubbles. Carbon nanotubes could not show their actual effect for this formulation. Carbon black composites showed faster recovery due to weaker hard segments in their structure when compared with carbon nanotubes composites. For hybrid composites, similar or slightly higher recovery times were obtained with respect to the neat epoxy. Considering these results, it can be concluded that, by changing the amount of fillers, it is possible to tailor shape memory characteristics according to desired utilization area **[14, 44]**.

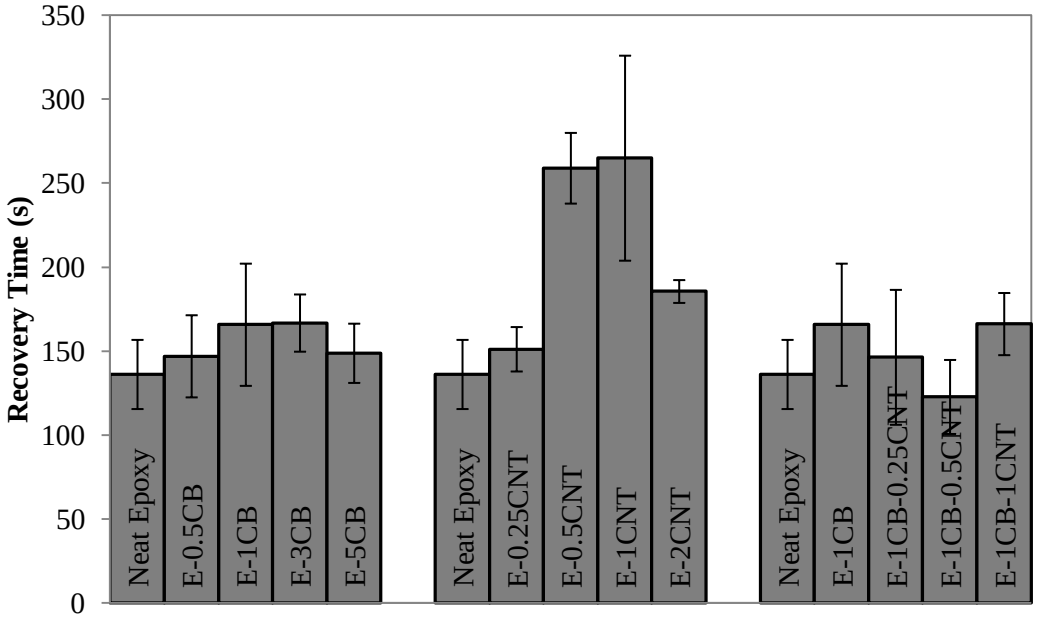

Figure 4.21 Recovery time values of neat epoxy and its composites

4.3.4 Electrical Resistivity Measurements of Composites

Electrical resistivity values measured by two point method were represented in Figure 4.22 on a logarithmic scale, and in Table E.1 in Appendix E. According to the figure, for each filler type, increase in amount of fillers led to a considerable decrease in volume resistivity. This expected behavior originated from the fact that, as the amount of carbon particles in the structure increased, they built conductive bridges by touching each other. This is how conductivity could be achieved by introducing carbon particles to the insulating polymer matrix **[15]**. Percolation threshold for carbon black filled and carbon nanotube filled composites could be observed around 1 % CB loading and 0.25 % CNT loading, respectively. For hybrid composites, percolation threshold is below 1 % CB-0.25 % CNT loading. When carbon black and carbon nanotubes composites are compared, it can be said that lower resistivity values were achieved at lower amounts of carbon nanotubes loading than the carbon black loading. This effect was due to the high aspect ratio of carbon nanotubes which made carbon nanotubes connected to each other more easily than particulate fillers like carbon black. For the hybrid composites, it can be mentioned that the expected synergistic effect could not be observed.

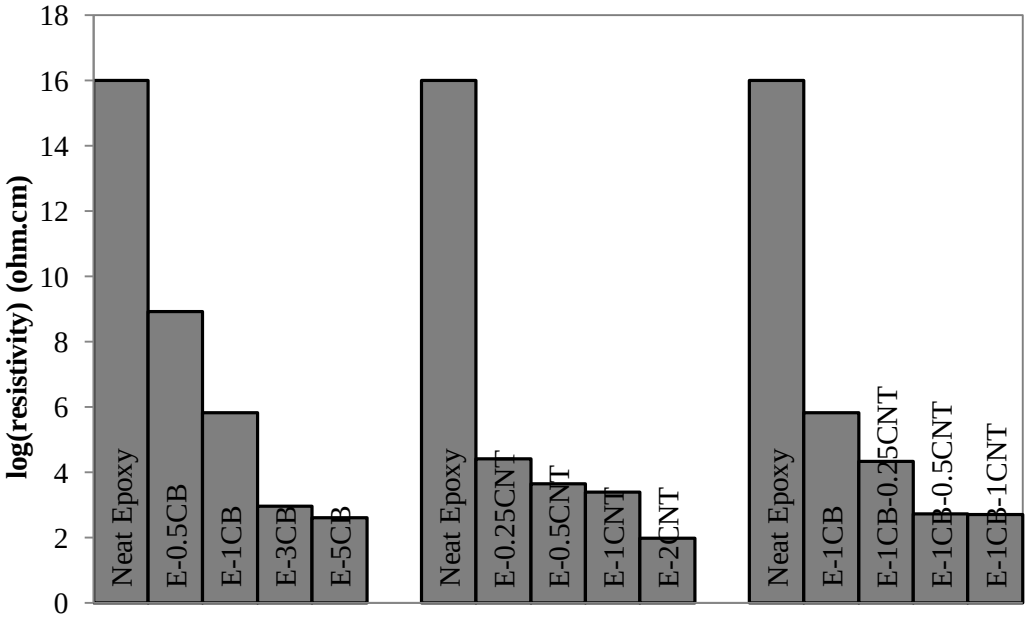

Figure 4.22 log(resistivity) values of neat epoxy and its composites

4.4 Effect of Addition of Filler and Monomer Together to the Epoxy Matrix

In the final part, the nanofillers were introduced to the polymer matrix together with the monomer. In the consequence of composite characterizations, the E-1CB-0.5CNT hybrid composite was selected for further preparations and investigations, since E-1CB-0.5CNT sample was found to show better properties among the other hybrid compositions. In the upcoming results E-1CB, E-0.5CNT and E-1CB-0.5CNT were prepared with both 15 % NGDE and 15 % RDE and characterized according to mechanical, thermal, electrical, shape memory properties and morphology. The effect of addition of 15 % NGDE and 15 % RDE, were investigated for binary and ternary systems of carbon black and carbon nanotubes. Neat polymer containing 15 % NGDE and 15 % RDE were also represented in the same graph for the comparison purposes.

4.4.1 Tensile and Impact Tests of Composites

Figures 4.23-4.25 represent the tensile test results of the final composites. Detailed data are given in Table B.3 of Appendix B. According to tensile strength results, it can be said that addition of each kind of monomer generally decreased the tensile strength values for all composites. Low molecular weight aliphatic NGDE structure increased the length between epoxy crosslink points, thus decreased the crosslink density. Carrying the load is mainly dependent on the crosslink density for epoxy based polymers. Decreasing trend in tensile strength was obtained with monomer addition **[44, 10]**.

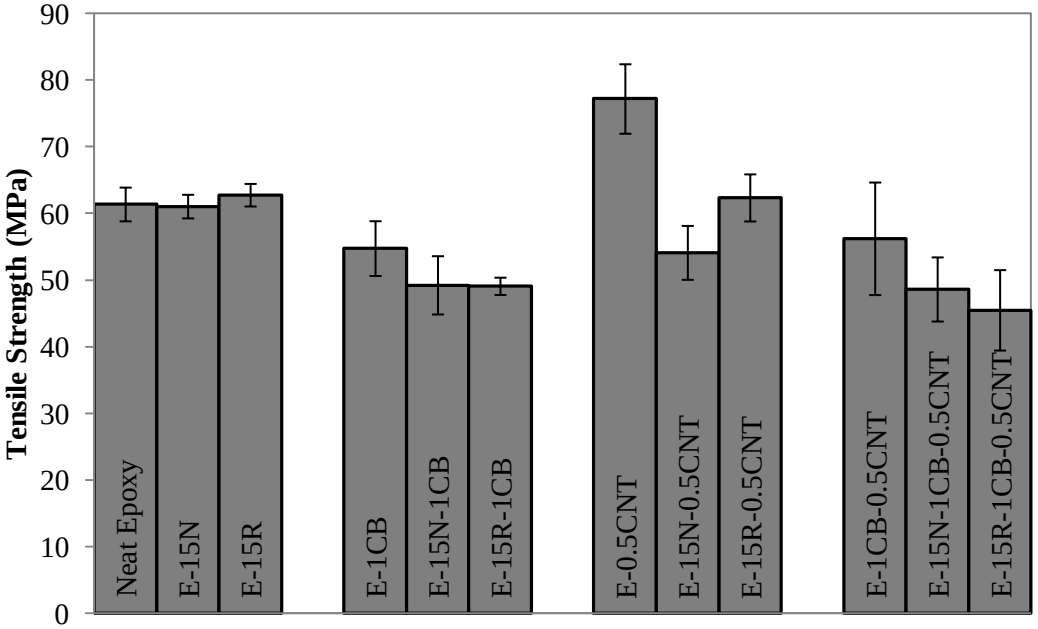

Figure 4.23 Tensile strength values for monomer and carbon filled composites

Young's modulus of the final composites are represented in Figure 4.24. These values decreased with the addition of monomer in the composite structures. According to the modified rule of mixtures for particulate composites, in the case of producing polymer composite with the addition of monomer, the low modulus value of the monomer results in decrease in the overall modulus of the composite **[59]**. Moreover, monomer hybrid composites showed higher modulus values when compared to monomer added carbon black and carbon nanotubes composites in spite of the higher filler amount. With the presence of a monomer in the matrix, further increase of brittleness was prevented with the addition of carbon based materials.

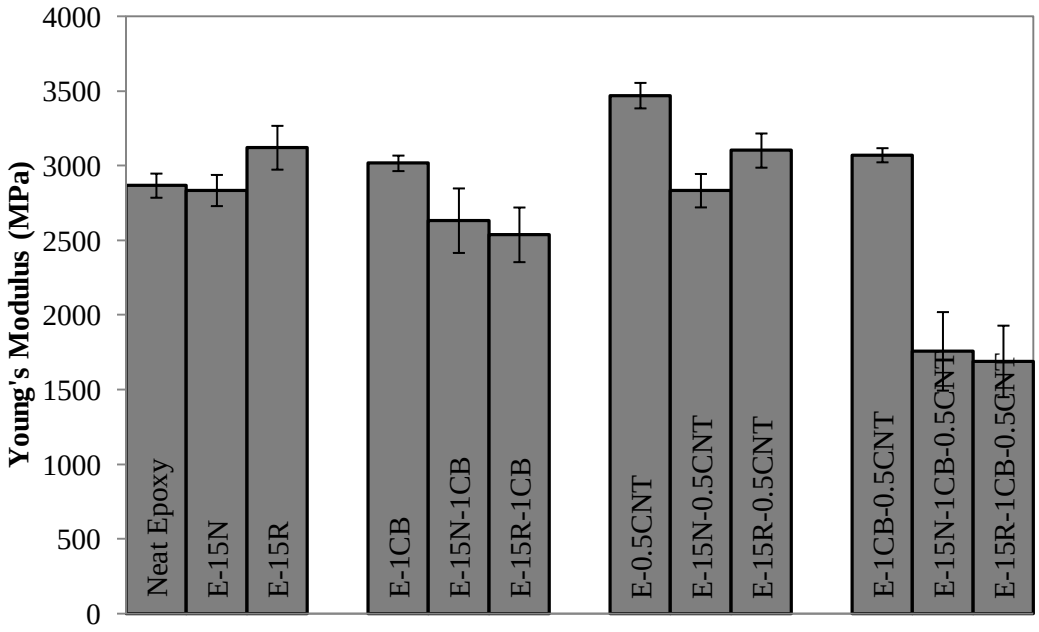

Figure 4.24 Young's modulus values for monomer and carbon filled composites

Percent elongation at break values of composites were affected by the monomer addition to the matrix. Monomer containing composites had higher elongation at break than the ones that did not contain any monomer. This was due to the fact that increasing ductility leads to more elongation during tensile testing. When neat sample was analyzed, a significant drop in elongation was observed with the monomer addition, which was in fact unexpected. This may be attributed to the voids that occur during material preparation with the addition of monomer only. It can be concluded that, presence of carbon particles in the matrix enhanced the interaction among epoxy, monomer and curing agent, and might lower the number of voids so that the resulting composite exhibited an expected behavior.

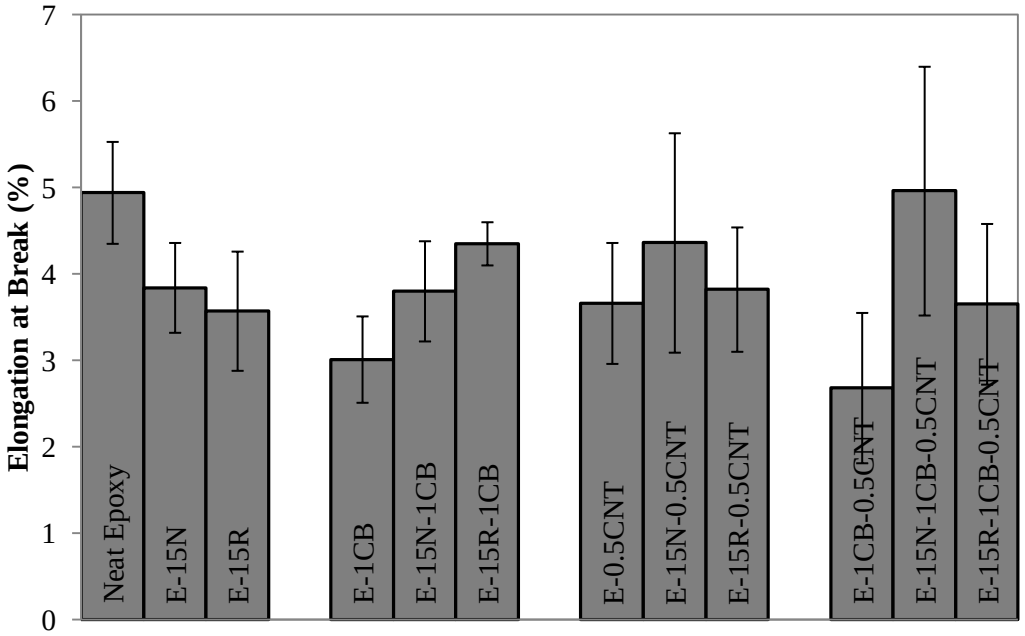

Figure 4.25 Elongation at break values for monomer and carbon filled composites

Figure 4.26 gives information about the impact strength of the final composites. Average values and standard deviation can be seen in Table B.3 of Appendix B. Addition of monomer into carbon filled polymer matrix enhanced the impact strength; especially due to the fact that aliphatic chains of NGDE increased the impact strength to apparently higher values. Impact strength is closely related to the soft segment of the matrix; in this case as the soft segment increased the impact strength was also improved. On the other hand, it was reasonable that, as a result of its aromatic nature, RDE was not as effective as NGDE in increasing impact strength **[63]**. For the hybrid composites, NGDE could not further contribute to the impact strength as much as it did for the composites containing one type of filler, and yet RDE caused a significant decrease. It can be concluded that the hybrid synergy in E-1CB-0.5CNT was not achieved in the E-15N-1CB-0.5CNT and E-15R-1CB-0.5CNT formulations.

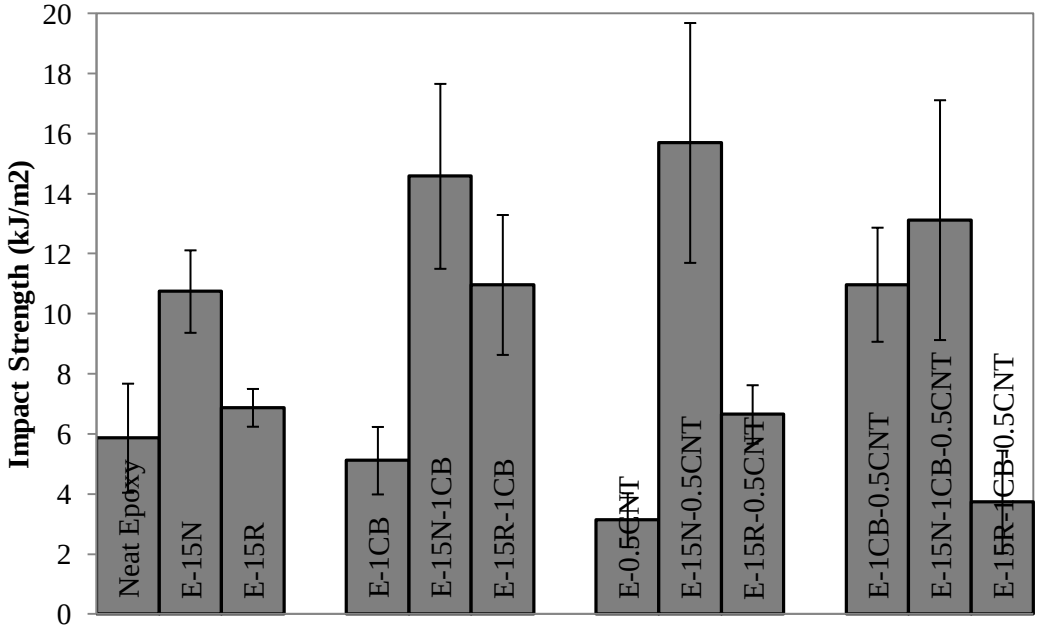

Figure 4.26 Impact values for monomer and carbon filled composites

4.4.2 Differential Scanning Calorimetry Tests of the Samples

DSC results for the final composites are shown in Figure 4.27 and the corresponding data are given in Table C.3 of Appendix C. Addition of both RDE and NGDE chains caused decrease in the glass transition temperature (T_g). Aliphatic NGDE chains did reduce the T_g down to 63°C, on the other hand, RDE could only decrease T_g to 75°C. This behavior was nearly same for neat samples, carbon black, carbon nanotubes and hybrid composites. T_g was mostly affected from the crosslink density of an epoxy network. In previous works T_g also decreased with the addition of monomer in the structure **[10]**. The origin of this effect was that, flexible segment mobility increases much more with the monomer addition, resulting in decrease of T_g. Consequently, it was possible to produce polymer with desired T_g value according to the area of usage, by varying the amount of monomer to be mixed with.

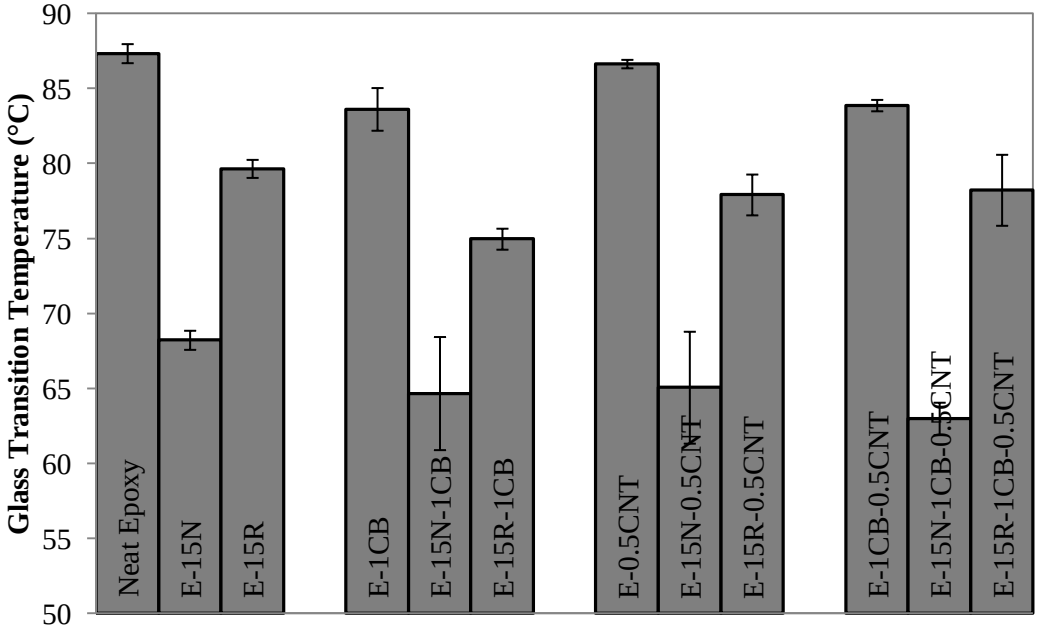

Figure 4.27 Glass transition temperature values for monomer and carbon filled composites

4.4.3 Thermal Shape Memory Tests of the Samples

Shape recovery tests by applying thermal stimulus were done on the final epoxy composites at 110°C. Resulting values are represented in the following three figures (Figure 4.28-4.30), and the detailed results are given in Table D.4 of Appendix D.

Figure 4.28 shows the shape recovery values in percentage. All samples showed recovery higher than 95 %. Even 99 % recovery could be reached for the monomer introduced samples. It can be said that the recovery amount did not change so much with monomer content at 110°C. In a previous study it was concluded that monomers had low influence on shape recovery only for the application temperature values which were much higher than T_g. This explanation was valid also in the present study. The influence of high application temperature on shape recovery dominated the role of monomer addition. At high temperature, the recovery for all samples was between 98 and 100 %, so that the influence of monomer could not be observed **[10]**.

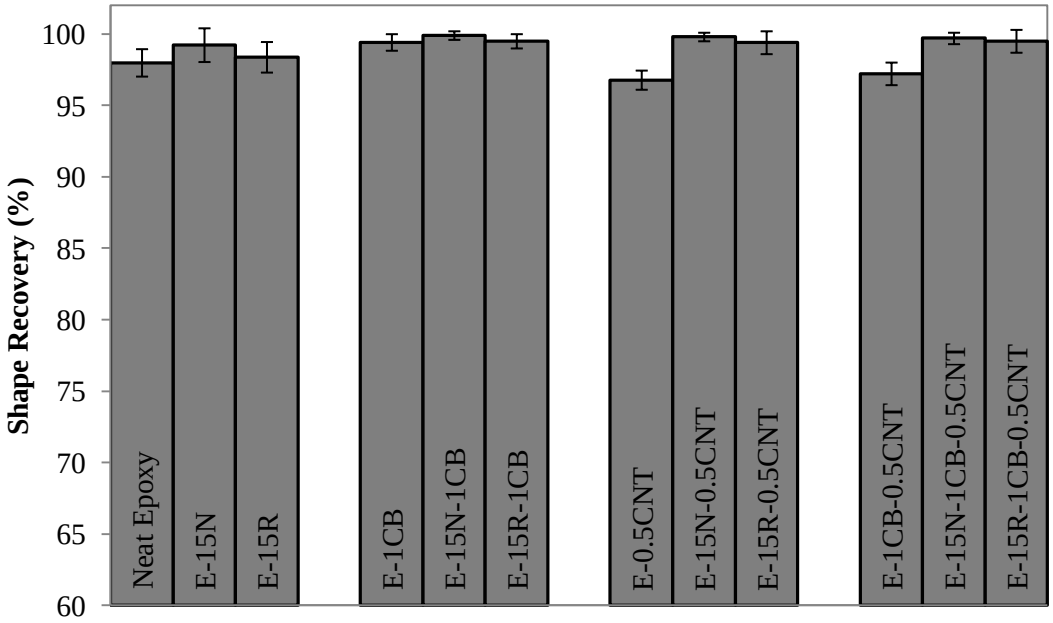

Figure 4.28 Shape recovery values for monomer and carbon filled composites

Shape fixity property of polymer samples are shown in Figure 4.29. It was clearly seen that addition of monomer had influenced the shape fixity of the composites in a positive way. This effect was due to the enhanced elastic ratio. Xie and Rousseau also mentioned in their study that, increasing amounts of NGDE contributed elastic ratio of the samples and the difference between glassy and rubbery modulus got wider, resulting in high ability of fixing large stresses upon small stress application **[13]**. For most of the formulations in this study, fixity values close to 100 % were achieved.

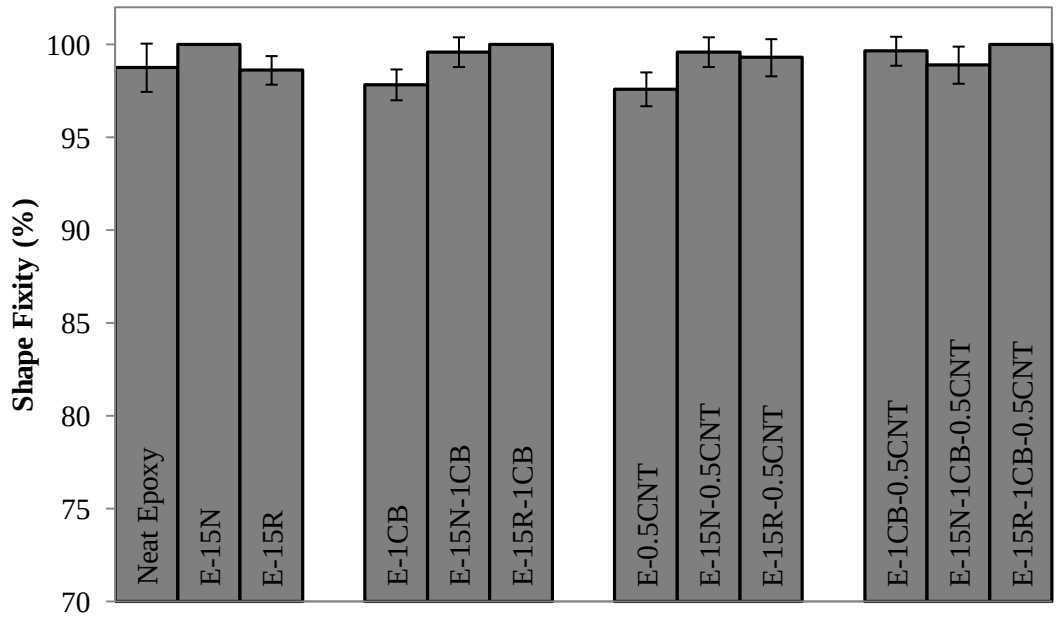

Figure 4.29 Shape fixity values for monomer and carbon filled composites

Recovery time values for shape memory samples are represented in Figure 4.30. With the addition of fillers recovery time became longer, on the other hand, with a certain amount of NGDE inside the matrix, recovery time of the composites decreased below 100 s which was almost as fast as E-15N sample. It can be said that, time for the recovery was strongly dependent on the segment stability of the material. When the hard segment is more dominant, in the case of carbon filled composites, recovery time increased, whereas with monomer addition soft segment was improved and recovery time decreased. Figure 4.27 also supports this idea. As another point of view, the reason for observing low recovery time values for samples having low T_g could be that, during heating of the sample, it started to recover at lower temperature (T_g), in other words the recovery had started earlier for those samples. Thus recovery of those samples finished earlier. This may be one of the contributing factors to decrease of recovery time for samples having enhanced soft segment. This result showed that addition of monomer could compensate the rise in recovery time for carbon reinforced composites **[14]**.

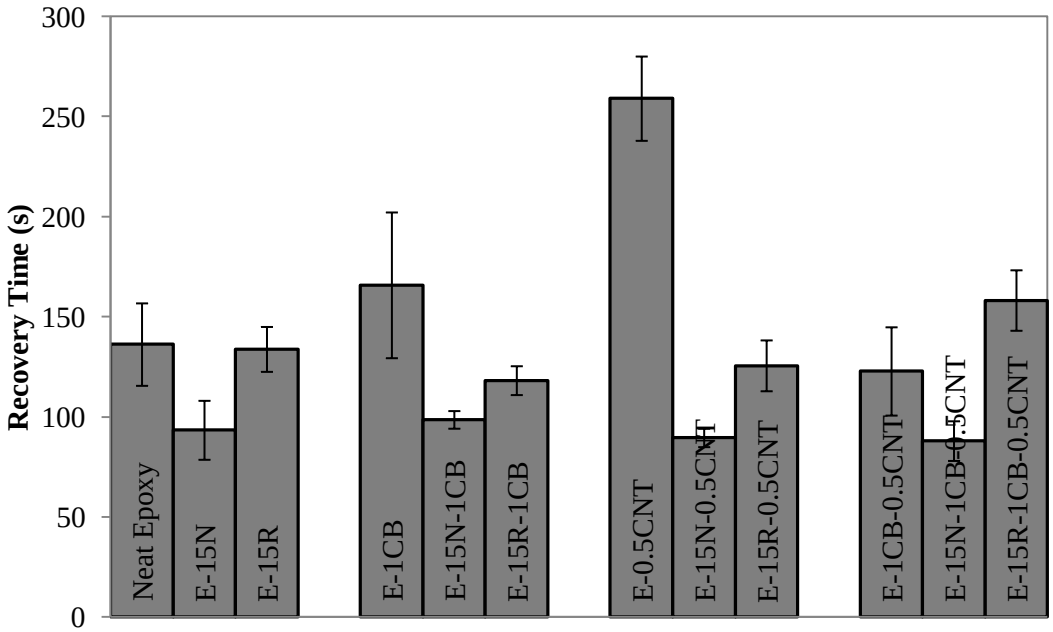

Figure 4.30 Recovery time values for monomer and carbon filled composites

4.4.4 Electrical Shape Memory Tests of the Samples

For the application of electrical triggering, the formulation which showed the lowest volume resistivity was selected for obtaining better performance. The test was applied on three samples of E-2CNT sample and an average of these data was calculated. The fixed and recovered samples of E-2CNT formulation are seen in Figure 4.31.

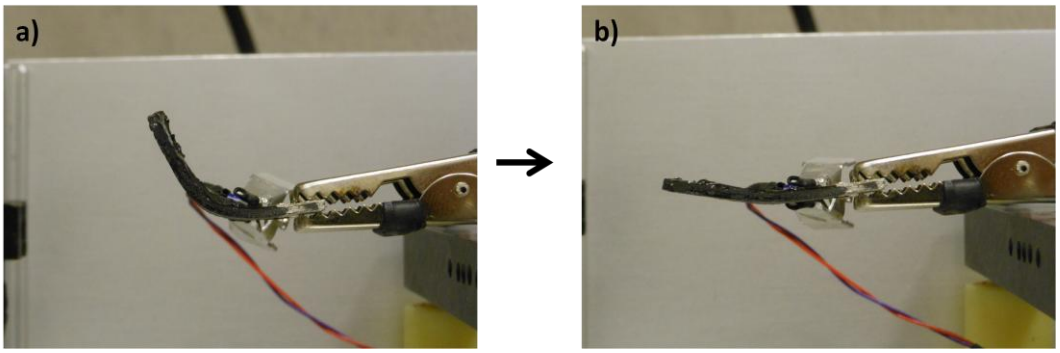

Figure 4.31 a)Fixed shape of E-2CNT sample b)Recovered shape of E-2CNT sample

Shape fixity property at 100 V was high and the time necessary for recovery showed similarity to the value obtained in thermal triggering. Composite had lower shape recovery value when compared with the values in thermal triggering. This was because

conductivity of the sample was not enough and therefore, it was impossible to heat the sample above 50°C by electrical triggering. The material did not absorb enough energy for passing from hard modulus to soft modulus. In the following Table 4.1, the results of the shape recovery test are shown for the electrically triggered E-2CNT sample.

Table 4.1 Shape memory properties of electrically triggered E-2CNT sample

	Voltage (V)	**Current (A) (30°C)**	**Current (A) ($T=T_{rec}$)**	**T_{rec} (°C)**	**Shape Fixity (R_f) (%)**	**Shape Recovery (R_r)(%)**	**Shape Recovery Time (s)**
E-2CNT	100	0.009±0.004	0.010±0.005	48±5	98.3±1.1	79.0±4.9	210±52

4.4.5 Electrical Resistivity Measurements of Composites

Figure 4.32 illustrates information about electrical properties of the final composites and the corresponding data are given in Table E.2 of Appendix E. Volume resistivity values decreased as the amount of filler increased. Addition of monomer had no considerable effect for CNT and hybrid samples, on the contrary a significant decrease in resistivity could be observed for CB composites. For E-1CB composite, it can be said that some carbon particles tended to stay close, form agglomerations and therefore hindered electrical network formations. SEM images showed that with the addition of NGDE and RDE to the carbon black composite, the agglomerations were reduced and carbon black particles dispersed more homogeneously in the structure. As a result, monomers had the advantage of reducing agglomerates and causing generation of more homogenized structure.

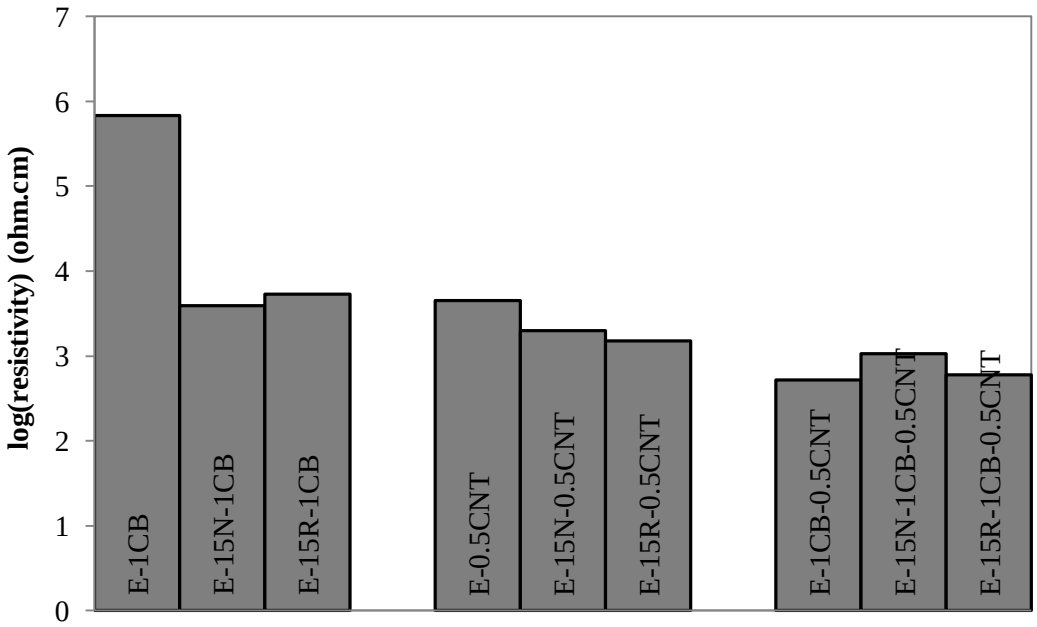

Figure 4.32 log(resistivity) values for monomer and carbon filled composites

4.4.6 SEM Results for Composites Containing Monomer and/or Carbon Based Fillers

Scanning electron microscopy (SEM) analysis was done for the final composites which were mentioned in Section 4.4. By studying the magnified images of the specimens, morphological characteristics were identified. Images were magnified varying between 2000x and 20000x. In Figures 4.33 and 4.34, the SEM images of neat epoxy and the composites of EP-1CB, EP-0.5CNT and EP-1CB-0.5CNT at 2000x and 20000x magnification are represented. Carbon black agglomerates were homogeneously dispersed in the epoxy matrix. The carbon nanotubes tended to stay together and generated agglomerations. The existence of carbon black and carbon nanotubes at the same time reduced the size of the agglomerations. Impact strength enhancement for E-1CB-0.5CNT composite could be explained with this synergy. Similar trends have also been observed by other researchers in literature **[72]**.

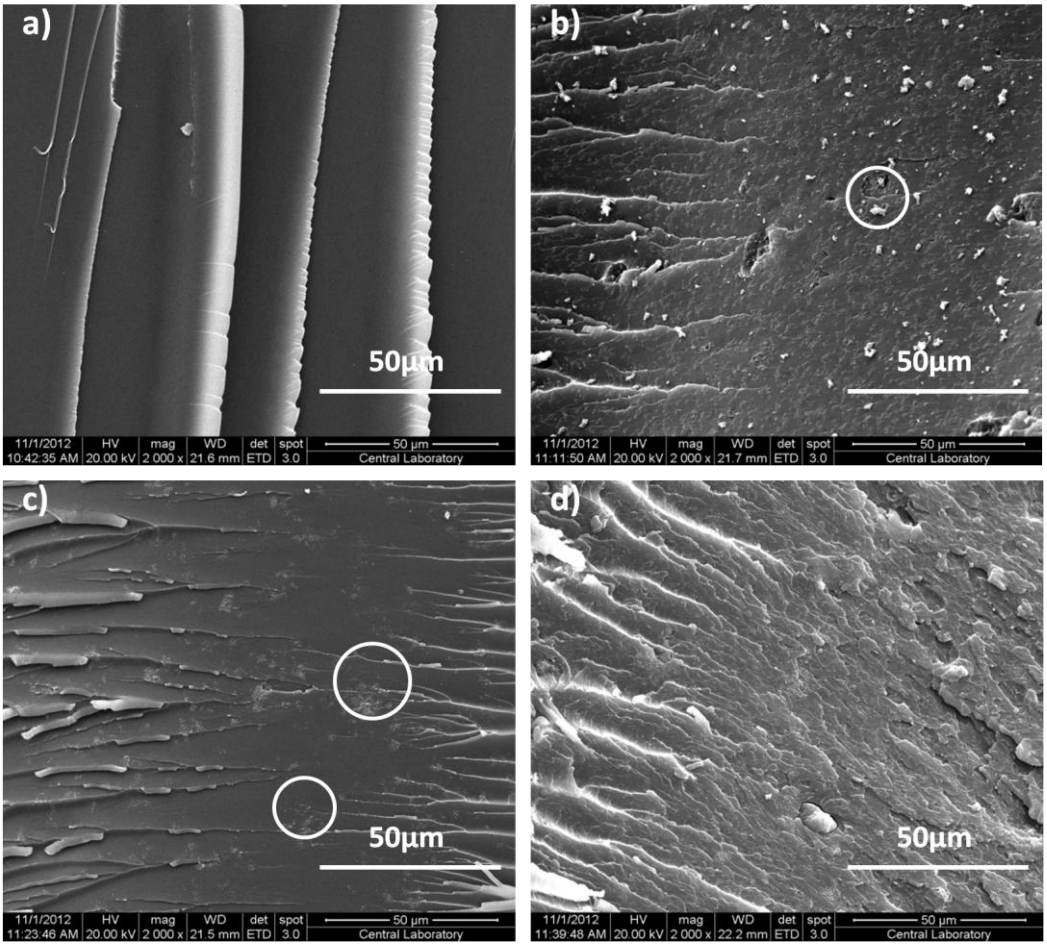

Figure 4.33 SEM images for a) Neat epoxy, b) E-1CB, c) E-0.5CNT and d) E-1CB-0.5CNT at 2000x magnification

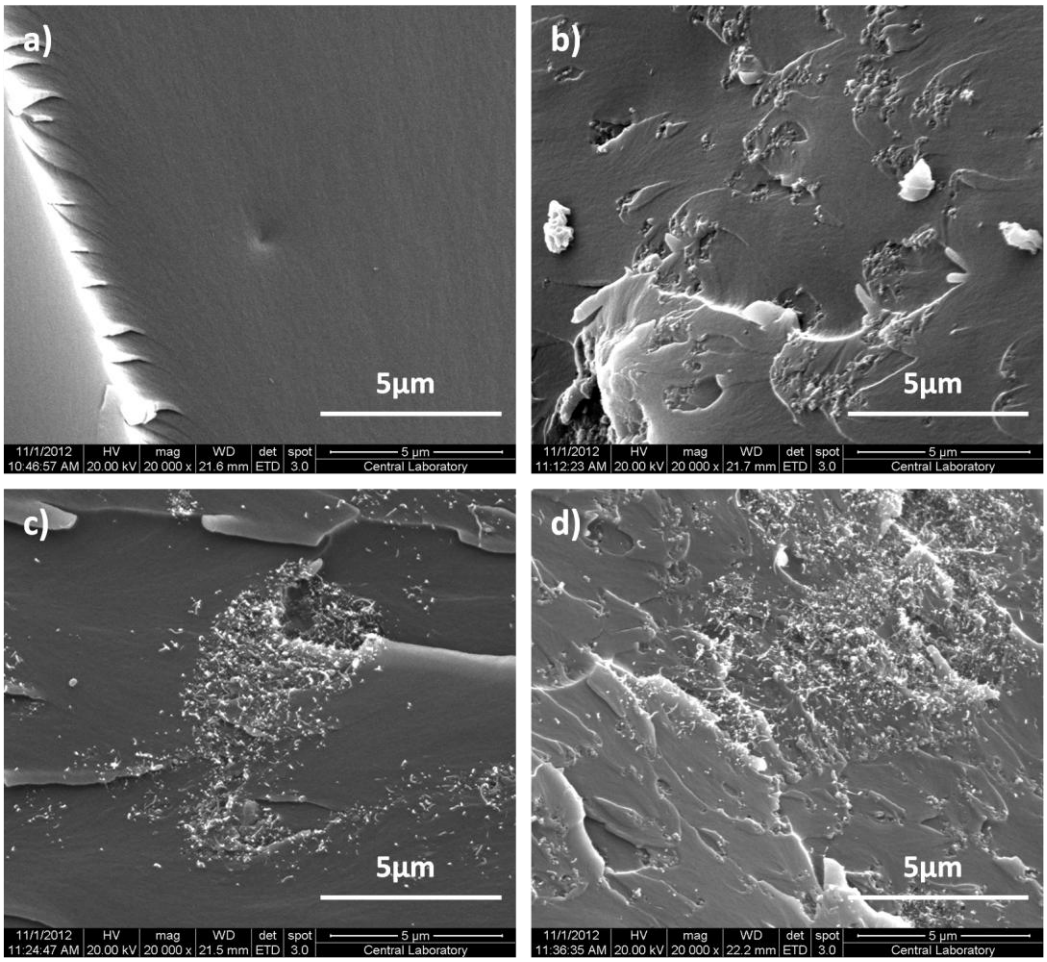

Figure 4.34 SEM images for a) Neat epoxy, b) E-1CB, c) E-0.5CNT and d) E-1CB-0.5CNT at 20000x magnification

Figures 4.35 and 4.36 show the SEM photographs of fracture surfaces of composites containing NGDE monomer. It is clear that the structure was much rougher for these composites when compared to the samples in Figures 4.33 and 4.34. The tough structure of monomer added composites led to an appreciable development in impact fracture strength which was seen in Figure 4.26. With the incorporation of NGDE monomer, carbon nanotube agglomerates had functioned as crack inhibitors as can be seen in Figure 4.35-c. However this kind of behavior could not be observed in Figures 4.35-b and d, which contain carbon black and hybrid fillers in the matrix. Amount of plastic deformations and distorted layers were observed in lower amount on the fracture surfaces of these samples.

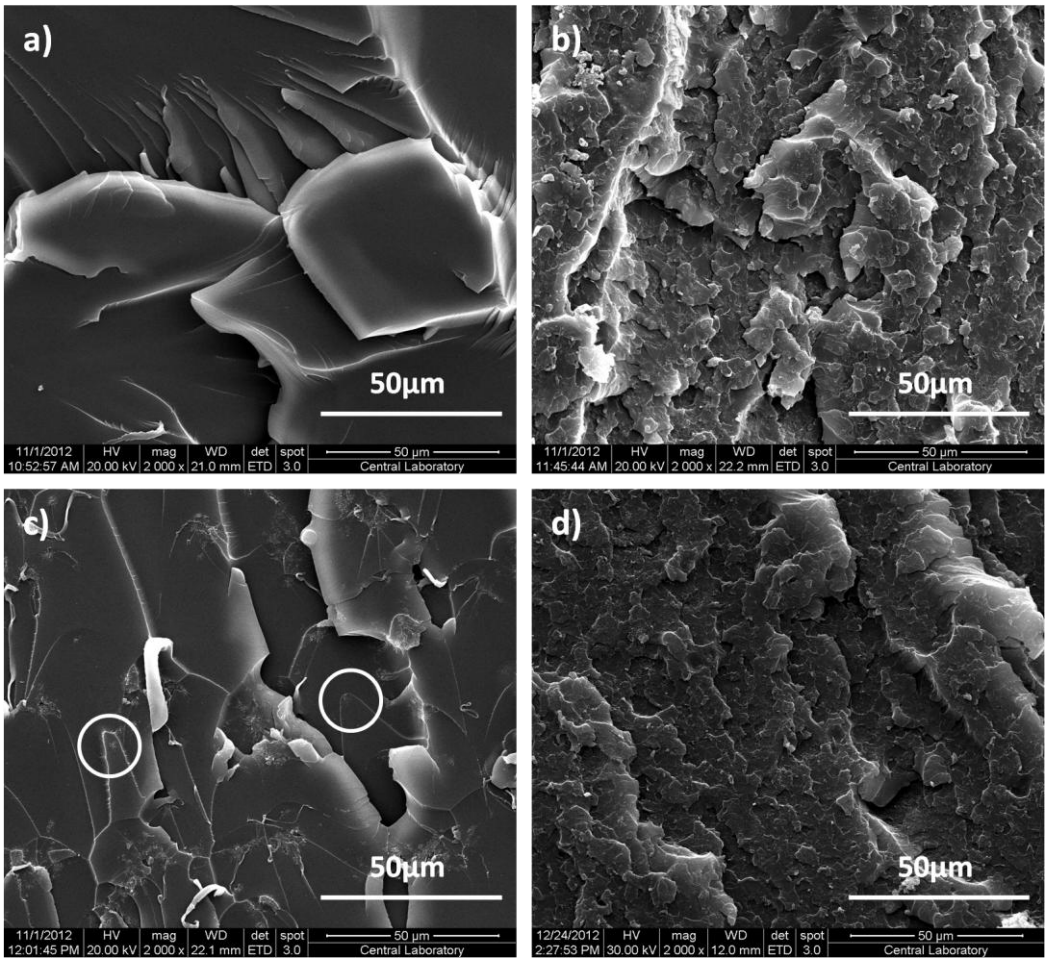

Figure 4.35 SEM images for a) E-15N, b) E-15N-1CB, c) E-15N-0.5CNT and d) E-15N-1CB-0.5CNT at 2000x magnification

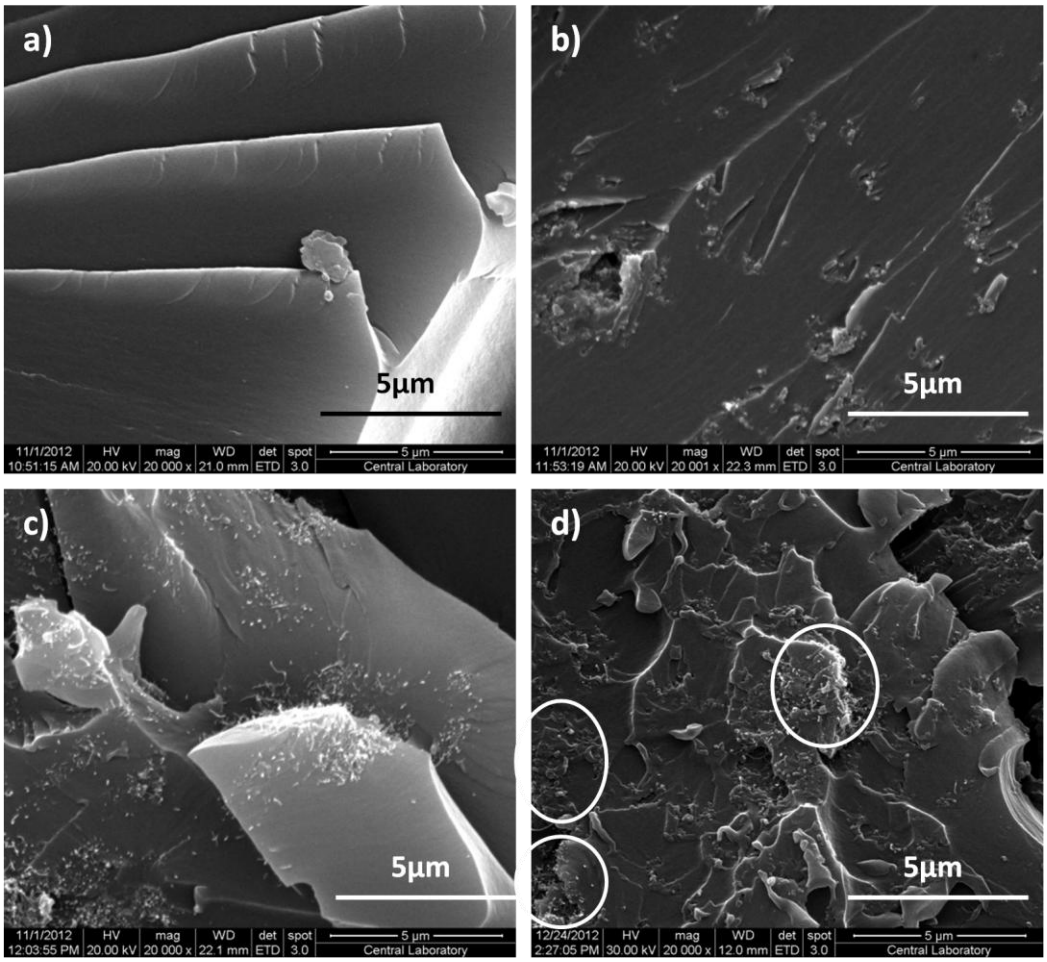

Figure 4.36 SEM images for a) E-15N, b) E-15N-1CB, c) E-15N-0.5CNT and d) E-15N-1CB-0.5CNT at 20000x magnification

Figures 4.37 and 4.38 represent the SEM images of fracture surfaces of RDE reinforced epoxy composites in 2000x and 20000x magnifications, respectively. Fracture surface was slightly smoother than composites filled with NGDE. When both monomers were compared, it can be concluded that the dispersion of carbon based fillers were similar for NGDE and RDE monomer. Carbon nanotubes and carbon black particles did not create a network and make a synergy, contrary to this, they were agglomerated and formed large aggregates among themselves.

When Figures 4.34-d, 4.36-d and 4.38-d are compared, it can be mentioned that hybrid fillers were dispersed better in the neat epoxy matrix (4.34-d), on the other hand, when the matrix was modified with NGDE or RDE, aggregation potential seemed to increase in a great extent (4.36-d and 4.38-d). These images can be a good explanation for the impact test results shown in Figure 4.28. Presence of both filler types in the matrix at the same time provided better dispersion, and therefore an unexpected increase in impact strength was observed. However hybrid composites containing NGDE and RDE, named as E-15N-1CB-0.5CNT and E-15R-1CB-0.5CNT respectively showed decrease in impact

strength, the cause of which might be referred to the carbon nanotubes and carbon black agglomerations formed in the polymer matrix. These agglomerations can be seen in Figures 4.36-d and 4.38-d.

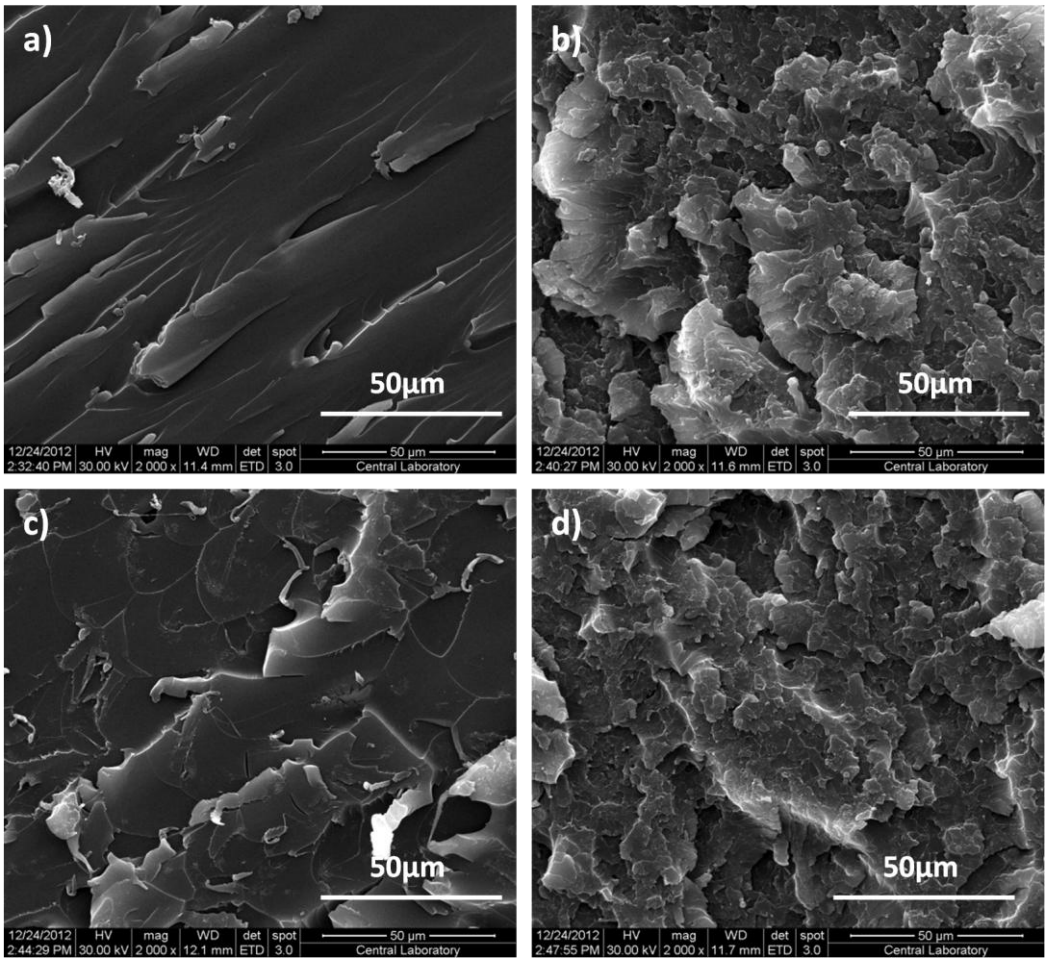

Figure 4.37 SEM images for a) E-15R, b) E-15R-1CB, c) E-15R-0.5CNT and d) E-15R-1CB-0.5CNT at 2000x magnification

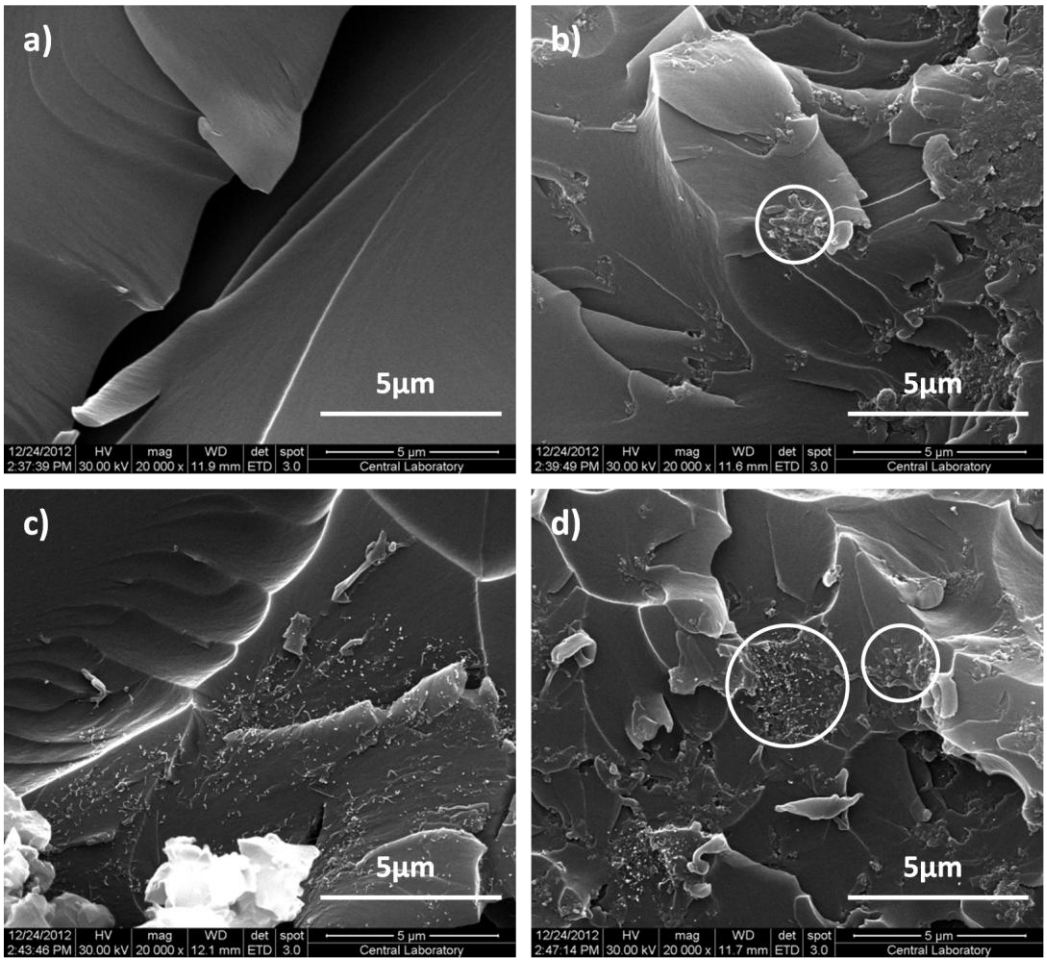

Figure 4.38 SEM images for a) E-15R, b) E-15R-1CB, c) E-15R-0.5CNT and d) E-15R-1CB-0.5CNT at 20000x magnification

4.5 Performance Tests for Shape Memory Polymers

Performance tests of shape memory polymers were applied as consecutive shape memory cycles using thermal actuation. The results of cyclic tests are shown in the following three figures (Figure 4.39-4.41). Detailed results of the performance tests are given in Table D.5 of Appendix D. It can be concluded from Figure 4.39 that number of cycles does not have much effect on shape recovery ratio. Figure 4.40 represents change in shape fixity values for polymer samples with respect to the number of shape memory cycles. It is seen that shape fixity was decreased by 3-4 % after the second cycle for the neat epoxy and E-15N samples. However, addition of carbon based filler into the matrix prevented this behavior and there was not a significant change in shape fixity for the samples containing carbon fillers.

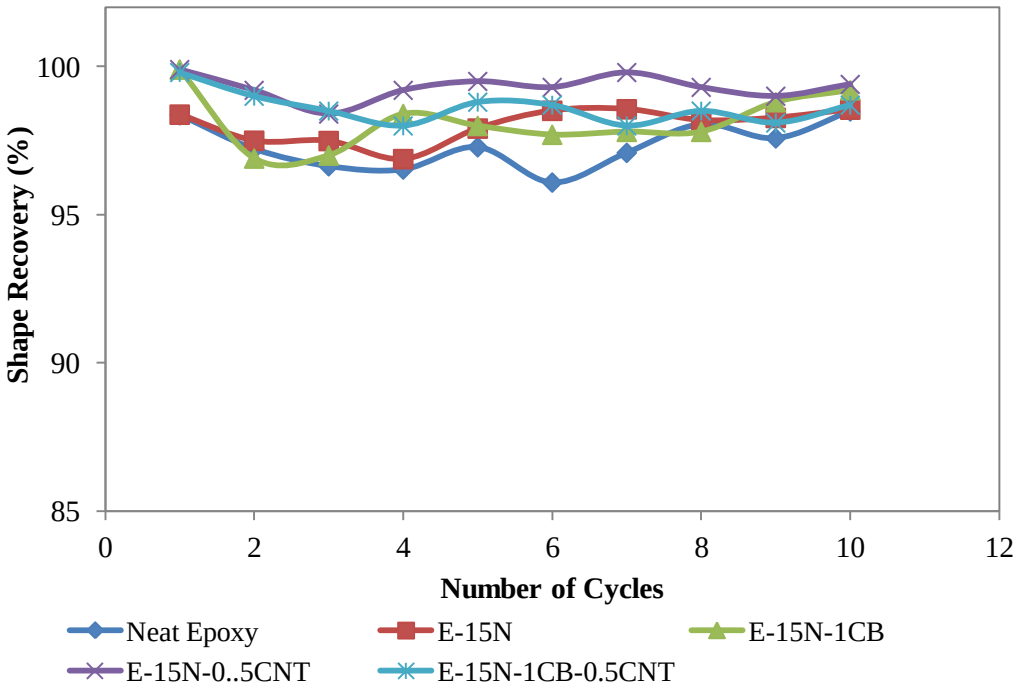

Figure 4.39 Shape recovery values of samples subjected to 10 shape memory cycles

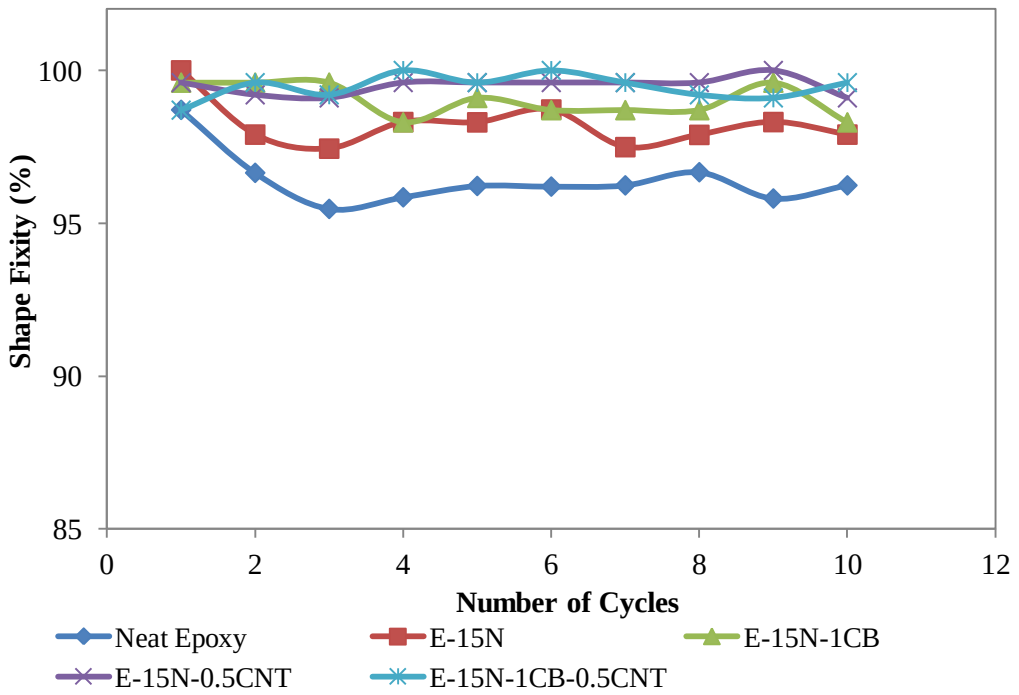

Figure 4.40 Shape fixity values of samples subjected to 10 shape memory cycles

Figure 4.41 shows recovery time values for the samples at each shape memory cycle. For the first cycle recovery time did not show much difference between the samples, however after the second cycle, recovery time almost doubled for neat epoxy sample and continued increasing with successive shape memory cycles. Addition of NGDE and CB to the matrix depressed this effect. On the other hand it was obvious that, presence of CNT in the matrix caused more stable results, and faster recovery than neat samples and the sample containing CB after second cycle. The tabulated results for the performance tests can be seen in Appendix D, Table D-5.

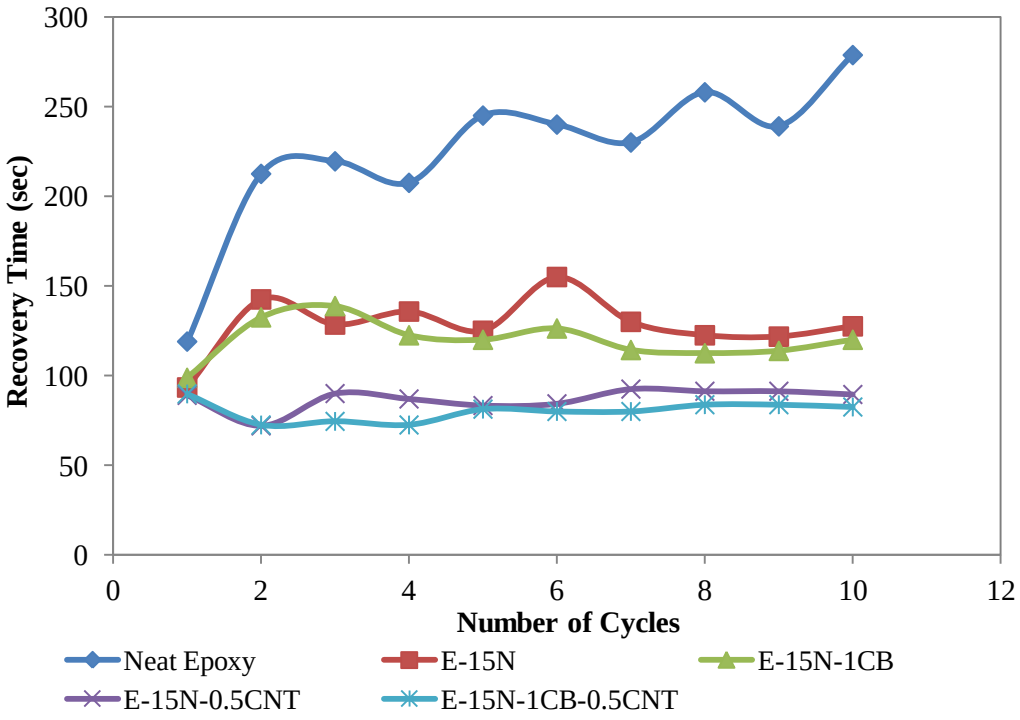

Figure 4.41 Recovery time values of samples subjected to 10 shape memory cycles

CHAPTER 5

CONCLUSIONS

This study consists of the production of epoxy polymer using DGEBA based resin and isophorone diamine based hardener. The matrix was modified by two different monomers; NGDE and RDE. Carbon nanotube and carbon black were used to reinforce the neat epoxy polymer. Mechanical, thermal and electrical characterizations and morphology studies were verified. Shape memory properties were investigated.

Curing study of neat epoxy was carried out. According to the curing percentage values, best curing cycle was selected. Percentage curing was calculated as 95.05 %.

Initial approach was to study the influence of aliphatic amine based NGDE and aromatic amine based RDE monomers. Samples were produced containing 5, 10 and 15 % of each monomer. Results of studies showed that addition of NGDE and RDE did not cause significant changes on tensile strength and modulus. Tensile strength values varied between 57.5 and 67 MPa, Young's Modulus was between 2700 and 3300 MPa and Elongation at break values laid between 4.1 and 5.6 %. Impact strength increased to 18.1 MPa for 15 % NGDE loading from 11.8 MPa for neat epoxy. RDE addition did not cause much difference in impact strength values when compared to NGDE filled samples. Glass transition temperature was found as 88.7°C for neat epoxy and smoothly decreased with NGDE addition to matrix and finally became 71.5°C at 15 % NGDE loading. For RDE loading, glass transition temperature values changed between 88.7 and 82°C. Shape recovery value for neat epoxy was 88 % and it increased to 99 % and 100 % with NGDE and RDE monomer addition respectively. Shape fixity was not affected much by monomer addition; and varied between 95 and 98.5 %. Recovery time of neat epoxy was found as 355 s. With the addition of monomers, this value decreased to 241 s and 224 s for NGDE and RDE monomers, respectively.

The next study was related with the selection of suitable application temperature for thermal activation of shape memory test. Samples of E-15N and E-15R were selected for this test since they show higher shape recovery and fixity values together with fast recovery when compared to the other samples. The samples were subjected to shape memory tests at different temperatures like 90, 100, 110, 120 and 130°C. According to the results of this analysis, shape recovery and shape fixity properties did not change much at different application temperatures for both samples. On the other hand, recovery time of the samples showed a smooth decrease starting from 241 s to 54.2 s for NGDE at 90 and 130°C, respectively and from 224 s to 73 s for RDE at 90 and 130°C, respectively. 110°C was selected as application temperature for further shape memory tests.

In the third part, carbon black and carbon nanotube addition to the neat epoxy matrix was investigated. Moreover, hybrid composites were also prepared using both carbon black

and carbon nanotubes together. Carbon black was added to the polymer in 0.5, 1, 3 and 5 % loadings whereas; carbon nanotubes were filled according to 0.25, 0.5, 1 and 2 % by weight fractions. Fractions of hybrid composites were 1 % CB – 0.25 % CNT, 1 % CB-0.5 % CNT, and 1 % CB-1 % CNT. A general decreasing trend was observed in the tensile strength results. Tensile strength was decreased to 48.5 MPa for CB, to 44.3 MPa for CNT and to 48 MPa for E-1CB-1CNT hybrid composite. Highest tensile strength value was obtained for 0.5 wt. % CNT loading as 77 MPa. Significant changes did not occur for the Young's Modulus results. Elongation at break values decreased in considerable amount; value for neat epoxy was 4.9 %, and it decreased smoothly to 2.2 % for 5 % CB loading and to 1.85 % for 2 % CNT loading and to 1.76 % for 1 % CB and1 % CNT loading at the same time. Impact strength also decreased with the addition of carbon based fillers. For neat epoxy sample, 5.8 kJ/m^2 impact strength was obtained. The value fell down to 0.4 kJ/m^2 for 5 % CB loading and to 1.6 kJ/m^2 for 2 % CNT loading. For hybrid composites, impact strength increased up to 10.9 kJ/m^2 for E-1CB-0.5CNT, however fell down sharply to 1.9 kJ/m^2 for E-1CB-1CNT. According to the differential scanning calorimetry analysis of composites, decreasing trend of 3°C for CB filled samples and a fluctuating trend for CNT filled samples and also for hybrid samples was observed. Shape recovery and shape fixity values did not change at all with the addition of both carbon based fillers, very slight decrease down to 97 %. Recovery time had tendency to increase with filler addition, for neat epoxy recovery time was found as 136 s at 110°C application temperature. This value increased to 167 s for E-3CB, 265 s for E-1CNT and 166 s for E-1CB-1CNT. Drastic decrease in electrical resistivity with respect to increasing carbon based filler content was observed. Log resistivity values of E-5CB, E-2CNT and E-1CB-1CNT were found as 2.61, 2.0 and 2.71 ohm.cm, respectively.

In the fourth part of this thesis, epoxy matrix was both modified with monomer and reinforced with carbon black and carbon nanotube in order to observe the simultaneous effect of monomer and filler. Tensile tests revealed that tensile strength tend to decrease with the addition of monomer to the matrix in the presence of certain amount of filler. Tensile strength did not fall down below 48.6 MPa which is the value for E-15N-1CB-0.5CNT. Young's Modulus values were found to decrease as monomer was introduced to all composites. It can be concluded that, modulus values of E-15N-1CB-0.5CNT and E-15R-1CB-0.5CNT samples; which are 1757 and 1690 MPa respectively, were much lower than the other samples having values in the range of 2500 and 3100 MPa. Elongation at break was observed higher for the samples containing monomer when compared to the samples without monomer. Highest elongation was observed for E-15N-1CB-0.5CNT sample as 4.96 % where the lowest elongation value, which is 2.68 %, was obtained for E-1CB-0.5CNT sample. Impact tests showed that addition of NGDE to the matrix increased the impact strength in a considerable amount. Highest impact strength results were 10.75, 14.58, 15.69, 13.12 kJ/m^2 for E-15N, E-15N-1CB, E-15N-0.5CNT and E-15N-1CB-0.5CNT composites, respectively. DSC test results clearly showed that addition of NGDE into neat samples caused around 20°C drop in glass transition temperature whereas this decline remained as 5-10°C in RDE addition. Lowest glass transition temperature value was obtained for E-15N-1CB-0.5CNT as 63°C. Shape memory tests showed that percent shape recovery was above 98 % for all samples. Addition of monomers enhanced relatively low shape recovery values of CNT containing

samples to above 99.5 %. Likewise, shape fixity was also enhanced with the incorporation of monomers. Generally values above 98.5 % were observed for all samples. Recovery speed analysis showed that, more time was necessary for carbon filled composites to fully recover, on the other hand; introducing monomer inside the composite compensated this effect and caused as much smaller values as it was obtained for the neat samples. Lowest recovery time values were obtained as 88s for E-15N-1CB-0.5CNT. Electrical resistivity values were not affected from addition of monomer to the matrix, throughout the final composite samples, hybrid samples were found to have lowest resistivity to electricity.

Shape memory test with electrical actuation was carried out for E-2CNT sample being the most conductive sample among the others. The sample could be heated to 50°C under the application of 100 V. E-2CNT sample did not have enough conductivity to be heated more than 50°C, however the sample became rubbery at this temperature and shape recovery procedure could be applied. Percent shape recovery was found as 79 % which was not as much as it was observed for the thermal actuation.

Performance tests for five different samples were applied as 10 subsequent cycles of shape memory tests. Results showed that, amount of cycles did not affect shape recovery property negatively, however it can be claimed that, for neat samples, shape fixity values decreased 2-4 % after the 2^{nd} cycle. Composites containing carbon black, nanotube and both fillers together did not show such a decrease in shape fixity. Neat epoxy sample showed continuous increase in shape recovery time. This increase was observed in small amounts for E-15N and E-15N-1CB samples. No change in recovery time was observed for the E-15N-0.5CNT and E-15N-1CB-0.5CNT composites, these two composites may be considered as proper candidates for shape memory applications in industry because of their repeatable shape memory characteristics.

CHAPTER 6

RECOMMENDATIONS

In the future studies, shape memory procedure with electrical triggering should be developed. It is necessary to produce polymers with lower electrical resistivity values in order to be able to heat the sample to the desired temperature by the application of electrical current. Developing electrical conductivity of the polymer can be achieved by different ways.

Initially, the dispersion of conductive fillers could be enhanced either by a different preparation procedure or by applying purification or modification to the filler particles. Surface functionalization may lead to more homogeneous dispersion of conductive fillers throughout the polymer matrix. As a result, the conductive networks and bridges would be more homogeneous resulting in lowered electrical resistivity.

Another approach may be aligning fiber fillers in one direction during the curing cycle of thermoset polymer. Alignment could be done with application of electric field during the curing process, so that fibrous fillers would be aligned inside the cured matrix and they would be forming bridges and conducting electricity much easily. Likewise, magnetic field could be applied if fibrous filler having magnetic properties like nickel is going to be used.

REFERENCES

[1] Hu, J., Zhu, Y., Huang, H., Lu, J. (2012). Recent advances in shape-memory polymers: Structure, mechanism, functionality, modelling and applications. *Progress in Polymer Science, 37, 12,* 1720-1763.

[2] Huang, W. M., Ding, Z., Wang, C. C., Wei, J., Zhao, Y., Purnawaii, H. (2010). Shape Memory Materials. *Materials Today, 13, 7-8,* 54-61.

[3] Liu, C., Qin, H., Mather, P. T. (2007). Review of progress in shape memory polymers. *Journal of Materials Chemistry,* 17, 1543-1558.

[4] Lendlein, A. (2010). Shape-memory polymers. Heidelberg, Germany: Springer

[5] Suzuka NT, Suzuka AT. Heat-shrinkable film. US Pat 7182998; 2007.

[6] Hu, J., Chen, S. (2010). A review of actively moving polymers in textile applicatons. *Journal of Materials Chemistry,* 20, 3346-3355.

[7] Leng, J., Lan, X., Liu, Y., Du, S. (2011). Shape-memory polymers and their composites: Stimulus methods and applications. *Progress in Materials Science,* 56, 1077-1135.

[8] Luo, X., Mather, P. T. (2010). Conductive shape memory nanocomposites for high speed electrical actuation. *Soft Matter,* 6, 2146-2149.

[9] Jeong, H.M., Ahn, B.K., Kim, B.K. (2001). Miscibility and shape memory effect of thermoplastic polyurethane blends with phenoxy resin. *European Polymer Journal,* 37, 2245-2252.

[10] Leng, J., Wu, X., Liu, Y. (2009). Effect of a linear monomer on the thermomechanical properties of epoxy shape-memory polymer. *Smart Materials and Structures,* 18, 095031-1,6.

[11] Song, W.B., Wang, L.Y., Wang, Z.D. (2011). Synthesis and thermomechanical research of shape memory epoxy resins. *Materials Science and Engineering A,* 529, 29-34.

[12] Yu, K., Zhang, Z., Liu, Y., Leng, J. (2011). Carbon nanotubes chains in a shape memory polymer/carbon black composite: To significantly reduce the electrical resistivity. *Applied Physics Letters,* 98, 074102-1,3.

[13] Xie, T., Rousseau, I.A. (2009). Facile tailoring of thermal transition of epoxy shape memory polymers. *Polymer,* 50, 1852-1856.

[14] Mondal, S., Hu, J.L. (2006). Shape memory studies of functionalized MWNT-reinforced polyurethane copolymers. *Iranian Polymer Journal,* 15, 2, 135-142.

[15] Lan, X., Leng, J., Liu, Y., Du, S. (2008). Investigate of electrical conductivity of shape-memory polymer filled with carbon black. *Advanced Materials Research,* 47-50, 714-717.

[16] Callister, W.D. (2007). Materials science and engineering an introduction. New York, USA: John Wiley&Sons, 7th ed.

[17] L. B. Vernon, H. M. Vernon, 'Producing Molded Articles such as Dentures from Thermoplastic Synthetic Resins', *US Pat.*, 2234993, 1941.

[18] Lendlein, A., Kelch, S. (2002). Shape-Memory Polymers. *Angew. Chem. Int. Ed.*, 41, 2034-2057.

[19] Leng, J., Du, S. (2010). Shape-Memory Polymers and Multifunctional Composites. *CRG Press. 1st Ed.* p.3.

[20] Maitland, D.J., Metzger, M.F., Schumann, D., Lee, A., Wilson, T.S. (2002). Photothermal properties of shape memory polymer micro-actuators for treating stroke. *Lasers in surgery and Medicine*, 30, 1-10.

[21] Mohr, R., Kratz, K., Weigel, T., Lucka-Gabor, M., Moneke, M., Lendlein, A. (2006). Initiation of shape-memory effect by inductive heating of magnetic nanoparticles in thermoplastic polymers. *PNAS*, 103, 10, 1-6.

[22] Morshedian, J., Khonakdar, H. A., Mehrabzadeh, M., Eslami, H. (2003). Preparation and properties of heat-shrinkable cross-linked low-density polyethylene. *Advances in Polymer Technology,* 22, 2, 112-119.

[23] Liu, G., Ding, X., Cao, Y., Zheng, Z., Peng, Y. (2005). Novel shape-memory polymer with two transition temperatures. *Macromolecular Rapid Communications*, 26, 649-652.

[24] Thomas, R., Durix, S., Sinturel, C., Omonov, T., Goossens, S., Groeninckx, G., Moldenaers, P., Thomas, S. (2007). Cure kinetics, morphology and miscibility of modified DGEBA-based epoxy resin – Effects of a liquid rubber inclusion. *Polymer*, 48, 1695-1710.

[25] Thermoset resins, Epoxy resins. Retrieved form http://info.smithersrapra. com/downloads/chapters/Thermoset%20Resins.pdf. Retrieved on 17.03.2013.

[26] Pinto, G., Maaroufi, A. K. (2011). Critical filler concentration for electroconductive polymer composites. *Society of Plastics Engineers*, 10.1002/spepro.003521.

[27] Koysuren, O. (2008). Preparation and characterization of conductive polymer composites, and their assessment for electromagnetic interference shielding materials and capacitors. *Ph.D. Thesis, Middle East Technical University*, Ankara, Turkey.

[28] Li, J., Wong, P. S., Kim, J. K. (2008). Hybrid nanocomposites containing carbon nanotubes and graphite nanoplatelets. *Materials Science and Engineering A*, 483-484, 660-663.

[29] Costa, L.C., Henry, F. (2011). DC electrical conductivity of carbon black polymer composites at low temperatures. *Journal of Non-Crystalline Solids,* 357, 1741-1744.

[30] Leng, J., Lan, X., Liu, Y., Du, S. (2009). Electroactive thermoset shape memory polymer nanocomposites filled with nanocarbon powders. *Smart Materials and Structures,* 18, 074003.

[31] Beloshenko, V. A., Varyukhin, V. N., Voznyak, Y. V. (2005). Electrical properties of carbon containing epoxy compositions under shape memory effect realization. *Composites: Part A,* 36, 65-70.

[32] Razzaq, M. Y., Anhalt, M., Frormann, L., Weidenfeller, B. (2007). Thermal, electrical and magnetic studies of magnetite filled polyurethane shape memory polymers. *Materials Science and Engineering A,* 444, 227-235.

[33] Yoo, H. J., Jung, Y. C., Sahoo, N. G., Cho, J. W. (2006). Polyurethane-carbon nanotube nanocomposites prepared by in-situ polymerization with electroactive shape memory. *Journal of Macromolecular Science, Part B: Physics,* 45, 441-451.

[34] Ipolycond Conductive Polymers Project. (2011). An introduction to conductive polymer composites. *ISmithers Rapra Publishing,* 1-8.

[35] Bianco, A. Carbon nanotubes. Retrieved from: http://www-ibmc.u-strasbg.fr/ict/article83.html.

[36] Alway-Cooper, R. M., Anderson, D. P., Ogale, A. A. (2013). Carbon black modification of mesophase pitch- based carbon fibers. *Carbon, 59,* 40-48.

[37] Robisson, A. (2010). A simple analogy between carbon black reinforced rubbers and random three-dimensional open-cells solids. *Mechanics of Materials,* 42, 11, 974-980.

[38] Dang, Z. M., Li, W. K., Xu, H. P. (2009). Origin of remarkable positive temperature coefficient effect in the modified carbon black and carbon fiber cofilled polymer composites. *Journal of Applied Physics,* 106, 024913.

[39] Sumfleth, J., Adroher, X. C. (2009). Synergistic effects in network formation and electrical properties of hybrid epoxy nanocomposites containing multi-wall carbon nanotubes and carbon black. *Journal of Materials Science,* 44, 3241-3247.

[40] Lau, K., Lu, M., Liao, K. (2006). Improved mechanical properties of coiled carbon nanotubes reinforced epoxy nanocomposites. *Composites: Part A,* 37, 1837-1840.

[41] Yesil, S. (2010). Processing and characterization of carbon nanotube based conductive polymer composites, *Ph.D. Thesis, Middle East Technical University,* Ankara, Turkey.

[42] Oh, T., Hassan, M., Beatty, C., El-Shall, H. (2005). The effect of shear forces on the microstructure and mechanical properties of epoxy-clay nanocomposites. *Journal of Applied Polymer Science,* 100, 3465-3473.

[43] Li, Q., Li, X., Meng, Y. (2012). Curing of DGEBA epoxy using a phenol-terminated hyperbranched curing agent: Cure kinetics, gelation, and the TTT cure diagram. *Thermochimica Acta*, 549, 69-80.

[44] Ersarac, F. (2012). Preparation and characterization of shape memory polymer based composite materials for aerospace applications. *Ms. Thesis, Middle East Technical University*, Ankara, Turkey.

[45] Heidolph impellers. Retrieved from: http://www.heidolph-instruments.com/products/overhead-stirrers/impellers/impellers/, Retrieved on: 22.03.2013.

[46] Nielsen, L.E., Landel, R.F. (1994). Mechanical properties of polymers and composites. *Marcel Dekker*, 2nd ed. New York, USA.

[47] MSE 5473, Fall 2008 Utah. Retrieved from: http://www.coursehero.com/file/5075169/11DSC/, Retrieved on: 16.03.2013.

[48] Özkan, N. (2011). PST508, Characterization Techniques for Polymeric Materials; Course notes. *Middle East Technical University Dept.of Polymer Science and Technology*.

[49] Sichina, W.J. Characterization of epoxy resins using DSC. *Thermal analysis, Application note*.

[50] Lee, J. H., Kim, S. K., Kim, N. H. (2006). Effects of the addition of multi-walled carbon nanotubes on the positive temperature coefficient characteristics of carbon-black-filled high-density polyethylene nanocomposites. *Scripta Materialia*, 55, 1119-1122.

[51] Swapp, S. Scanning electron microscopy (SEM). *Carleton College Science and Education Resource Center*. Retrieved from: http://serc.carleton.edu/research_education/geochemsheets/techniques/SEM.html. Retrieved on 26.03.2013.

[52] Liu, Y., Han, C., Tan, H., Du, X. (2010). Thermal, mechanical and shape memory properties of shape memory epoxy resin. *Materials Science and Engineering A*, 527, 2510-2514.

[53] Product Data Sheet, EPIKOTE 828 and EPIKOTE 828-X-90.

[54] Product Data Sheet, EPIKURE F205.

[55] Product data page of Neopentyl glycol diglycidyl ether. *Sigma Aldrich*, Retrieved from:http://www.sigmaaldrich.com/catalog/ProductDetail.do?D7=0&N5=SEARCH_CONCAT_PNO%7CBRAND_KEY&N4=338036%7CALDRICH&N25=0&QS=ON&F=SPEC.

[56] Product data page of Recorcinol diglycidyl ether. *Sigma Aldrich*, Retrieved from: http://www.sigmaaldrich.com/catalog/product/aldrich/470945?lang=en&region=TR.

[57] Product data page of Acetone. *Sigma Aldrich*, Retrieved from: http://www.sigmaaldrich.com/catalog/product/sial/24201?lang=en&region=TR.

[58] Song, W.B., Wang, L.Y., Wang, Z.D. (2011). Synthesis and thermomechanical research of shape memory epoxy systems. *Materials Science and Engineering*, 529, 29-34.

[59] Chen, Z., Yang, G., Yang, J., Fu, S., Ye, L., Huang, Y. (2009). Simultaneously increasing cryogenic strength, ductility and impact resistance of epoxy resins modified by n-butyl glycidyl ether. *Polymer*, 50, 1316-1323.

[60] Lou, C., Xianzhi, K., Jianxin, W., Liqun, M. (2011). Toughening of epoxy resins by modified m-phenylene daimine having soft ether chain. *Journal of Applied Polymer Science*, 125, 578-583.

[61] Wornyo, E., Gall, K., Yang, F., King, W. (2007). Nanoindentation of shape memory polymer Networks. *Polymer*, 48, 3213-3225.

[62] Yao, D., Kuila, T., Sun, K., Kim, N., Lee, J. (2011). Effect of reactive poly(ethyene glycol) flexible chains on curing kinetics and impact properties of bisphenol-a diglycidyl ether epoxy. *Journal of Applied Polymer Science*, 124, 2325-2332.

[63] Yang, X., Huang, W., Yu, Y. (2011). Epoxy toughening using low viscosity liquid diglycidyl ether of ethoxylated bisphenol-a. *Journal of Applied Polymer Science*, 123, 1913-1921.

[64] Gojny, F. H., Wichmann, M. H. G., Fiedler, B., Schulte, K. (2005). Influence of different carbon nanotubes on the mechanical properties of epoxy matrix composites – a comparative study. *Composites Science and Technology*, 65, 2300-2313.

[65] Yeh, M. K., Hsieh, T. H., Tai, N. H. (2008). Fabrication and mechanical properties of multi-walled carbon nanotube epoxy nanocomposites. *Materials Science and Engineering A*, 483-484, 289-292.

[66] Meincke, O., Kaempfer, D., Weickmann, H., Friedrich, C., Vathauer, M., Warth, H. (2003). Mechanical properties and electrical conductivity of carbon-nanotube filled polyamide-6 and its blends with acrylonitrile /butadiene/styrene. *Polymer*, 45, 739-748.

[67] Zhang, H., Zhang, Z. (2007). Impact behaviour of polypropylene filled with multi-walled carbon nanotubes . *European Polymer Journal*, 43, 3197-3207.

[68] Jin, F., Ma, C., Park, S. (2011). Thermal and mechanical interfacial properties of epoxy composites based functionalized carbon nanotubes. *Materials Science and Engineering A*, 528,8517-8522.

[69] Cho, J., Daniel, I.M. (2008). Reinforcement of carbon epoxy composites with multi-walled carbon nanotubes and dispersion enhancing block copolymers. *Scripta Materialia*, 58, 533-536.

[70] Leng, J., Lv, H., Liu, Y., Du, S. (2008). Synergic effect of carbon black and short carbon fiber on shape memory polymer actuation by electricity. *Journal of Applied Physics*, 104, 104917, 1-4.

[71] Li, H., Zhong, J., Meng, J., Xian, G. (2013). The reinforcement efficiency carbon nanotubes/shape memory polymer nanocomposites. *Composites: Part B,* 44, 508-516.

[72] Bokobza, L., Rahmani, M., Belin, C., Bruneel, J., Bounia, N. E. (2008). Blends of carbon blacks and multiwall carbon nanotubes as reinforcing fillers for hydrocarbon rubbers. *Journal of Polymer Science: Part B: Polymer Physics,* 46, 1939-1951.

APPENDIX A

PERCENTAGE CURING of NEAT EPOXY MATRIX

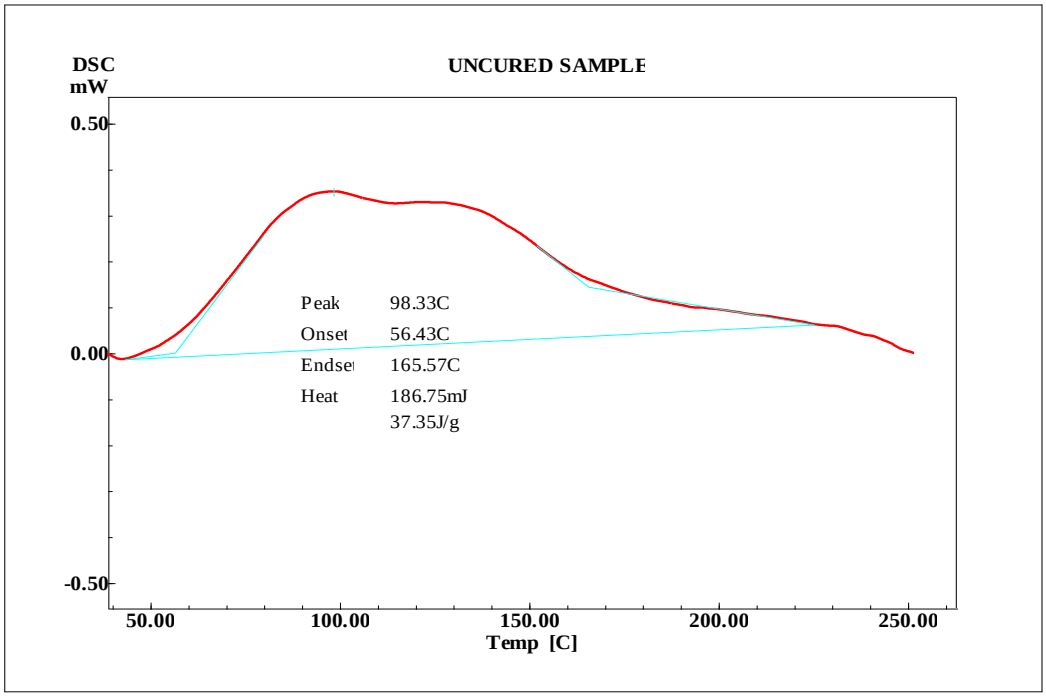

Figure A.1 Amount of heat absorbed by the uncured specimen with increasing temperature

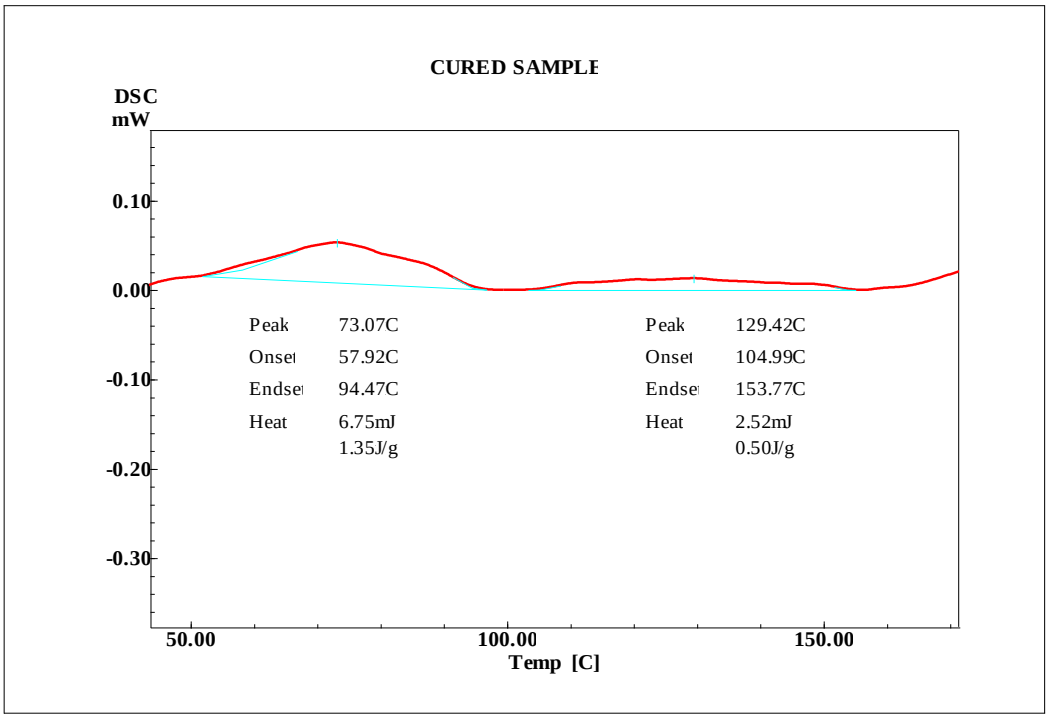

Figure A.2 Amount of heat absorbed by the cured specimen with increasing temperature

$$\%\text{Cure} = \frac{\Delta H_{\text{uncured}} - \Delta H_{\text{cured}}}{\Delta H_{\text{uncured}}} \times 100 \qquad (A.1)$$

$$\%\text{Cure} = \frac{37.35\ \text{J/g} - (1.35 + 0.50)\ \text{J/g}}{37.35\ \text{J/g}} \times 100 = \mathbf{95.05}\ \%$$

APPENDIX B

MECHANICAL PROPERTIES

Table B.1 Tensile strength, Young's modulus, elongation at break and impact strength values of the neat epoxy matrix modified by NGDE and RDE monomers

Sample	Tensile Strength (MPa)	Elongation at Break (%)	Young's Modulus (MPa)	Impact Strength (MPa)
Neat Epoxy	63.05±4.3	5.64±0.3	2720.07±169.6	11.884±1.0
E-5N	62.72±4.3	4.48±0.7	2847.36±132.6	14.373±0.5
E-10N	57.48±2.9	4.09±1.6	2964.58±197.5	11.545±1.2
E-15N	56.70±3.0	5.63±1.6	2352.28±103.7	18.116±1.3
E-5R	67.28±3.1	4.16±0.2	3222.52±136.5	9.085±0.8
E-10R	64.85±1.8	4.82±0.2	3185.62±57.0	10.509±2.1
E-15R	63.72±2.8	5.33±0.44	3298.22±74.0	11.161±2.1

Table B.2 Tensile strength, Young's modulus, elongation at break and impact strength values of carbon black and carbon nanotube reinforced epoxy composites

Sample	Tensile Strength (MPa)	Elongation at Break (%)	Young's Modulus (MPa)	Impact Strength (MPa)
Neat Epoxy	61.37±2.5	4.94±0.6	2867.44±80.9	5.865±0.9
E-0.5CB	55.27±3.5	3.70±0.5	2967.20±67.2	6.225±0.9
E-1CB	54.75±4.1	3.01±0.5	3017.00±51.9	5.115±1.1
E-3CB	54.54±5.0	2.54±0.4	3091.36±118.3	3.218±1.2
E-5CB	48.54±4.9	2.20±0.5	3052.70±130.2	0.364±0.3
E-0.25CNT	53.48±2.4	2.34±0.5	3125.55±96.3	5.192±0.9
E-0.5CNT	77.19±5.2	3.66±0.7	3470.58±85.4	3.134±0.9
E-1CNT	62.76±7.0	3.22±0.7	3110.94±69.5	2.435±1.2
E-2CNT	44.28±7.2	1.85±0.5	2911.82±37.9	1.588±0.6
E-1CB-0.25CNT	60.47±11.0	2.62±0.7	3238.38±101.5	8.41±1.7
E-1CB-0.5CNT	56.22±8.4	2.68±0.9	3071.24±47.3	10.973±1.9
E-1CB-1CNT	47.96±7.3	1.76±0.3	3232.56±95.7	1.991±0.9

Table B.3 Tensile strength, Young's modulus, elongation at break and impact strength values of final composites containing monomer and carbon based fillers

Sample	Tensile Strength (MPa)	Elongation at Break (%)	Young's Modulus (MPa)	Impact Strength (MPa)
Neat Epoxy	61.37±2.5	4.94±0.6	2867.44±80.9	5.865±0.9
E-15N	61.05±1.8	3.84±0.5	2835.08±104.4	10.745±1.4
E-15N-1CB	49.24±4.4	3.80±0.6	2633.00±215.9	14.581±3.1
E-15N-0.5CNT	54.11±4.0	4.36±1.3	2833.96±111.9	15.694±4.0
E-15N-1CB-0.5CNT	48.62±4.8	4.96±1.4	1757.82±263.1	13.124±4.0
E-15R	62.76±1.7	3.57±0.7	3121.54±146.7	6.875±0.6
E-15R-1CB	49.09±1.3	4.35±0.3	2538.28±183.1	10.966±2.3
E-15R-0.5CNT	62.35±3.5	3.82±0.7	3102.56±114.5	6.655±1.0
E-15R-1CB-0.5CNT	45.49±6.0	3.65±0.9	1690.44±239.4	3.743±1.7

APPENDIX C

THERMAL PROPERTIES

Table C.1 Glass transition temperature values of the neat epoxy matrix modified by NGDE and RDE monomers

Sample	Glass Transition Temperature (°C)
Neat Epoxy	88.73±0.8
E-5N	84.21±3.9
E-10N	77.56±3.4
E-15N	71.56±2.1
E-5R	88.08±0.5
E-10R	82.85±0.8
E-15R	86.48±1.0

Table C.2 Glass transition temperature values of carbon black and carbon nanotube reinforced epoxy composites

Sample	Glass Transition Temperature (°C)
Neat Epoxy	87.33±0.6
E-0.5CB	84.15±1.0
E-1CB	83.61±1.4
E-3CB	85.78±1.0
E-5CB	84.08±2.4
E-0.25CNT	81.13±0.9
E-0.5CNT	86.63±0.3
E-1CNT	84.46±1.1
E-2CNT	87.78±1.9
E-1CB-0.25CNT	87.39±1.2
E-1CB-0.5CNT	83.87±0.4
E-1CB-1CNT	83.75±2.3

Table C.3 Glass transition temperature values of final composites containing monomer and carbon based fillers

Sample	Glass Transition Temperature (°C)
Neat Epoxy	87.33±0.6
E-15N	68.22±0.6
E-15N-1CB	64.66±3.8
E-15N-0.5CNT	65.06±3.7
E-15N-1CB-0.5CNT	62.98±1.1
E-15R	79.85±0.6
E-15R-1CB	74.96±0.7
E-15R-0.5CNT	77.91±1.4
E-15R-1CB-0.5CNT	78.22±2.4

APPENDIX D

SHAPE MEMORY PROPERTIES

Table D.1 Shape recovery, shape fixity and recovery time values of the neat epoxy matrix modified by NGDE and RDE monomers at 90°C

Sample	Shape Recovery (%)	Shape Fixity (%)	Recovery Time (s)
Neat Epoxy	88.2±3.3	97.3±0.9	355.0±22.4
E-5N	91.0±3.5	95.0±0.8	262.0±24.2
E-10N	96.0±1.9	96.8±2.1	282.5±28.2
E-15N	98.9±0.8	98.3±1.2	241.0±16.0
E-5R	86.1±2.8	95.8±1.4	317.0±21.9
E-10R	98.9±0.6	97.8±2.7	319.0±36.7
E-15R	99.7±0.4	98.5±1.2	224.0±32.6

Table D.2 Shape recovery, shape fixity and recovery time values of E-15N and E-15R samples at different temperatures

Sample	Activation Temperature (°C)	Shape Recovery (%)	Shape Fixity (%)	Recovery Time (s)
E-15N	90	98.9±0.8	98.3±1.2	241.0±16.0
	100	95.6±1.3	97.9±0.8	159.0±10.0
	110	97.6±1.2	98.2±1.2	91.0±9.9
	120	99.0±1.1	99.3±0.9	78±2.8
	130	98.9±1.0	99.1±0.9	54.2±8.5
E-15R	90	99.7±0.4	98.5±1.2	224.0±32.6
	100	96.4±0.7	97.5±1.0	223.8±41.3
	110	98.8±1.0	98.6±0.8	121.6±10.5
	120	99.5±0.7	98.3±1.2	94.8±14.6
	130	99.8±0.3	99.8±0.4	73.4±10.3

Table D.3 Shape recovery, shape fixity and recovery time values of carbon black and carbon nanotube reinforced epoxy composites at 110°C

Sample	Shape Recovery (%)	Shape Fixity (%)	Recovery Time (s)
Neat Epoxy	98.0±1.0	98.8±1.3	136.2±20.6
E-0.5CB	99.8±0.3	97.6±0.9	147.0±24.5
E-1CB	99.4±0.6	97.8±0.8	165.8±36.4
E-3CB	100±0	97.6±0.9	166.8±17.0
E-5CB	100±0	97.0±0.7	148.8±17.6
E-0.25CNT	98.9±0.4	98.6±0.8	151.2±13.2
E-0.5CNT	96.8±0.7	97.6±0.9	259.0±21.0
E-1CNT	98.0±0.8	97.6±0.9	265.0±61.0
E-2CNT	98.4±0.4	97.6±0.9	185.6±6.8
E-1CB-0.25CNT	97.2±0.8	99.7±0.8	146.4±40.2
E-1CB-0.5CNT	97.2±0.8	99.7±0.8	122.8±22.0
E-1CB-1CNT	98.6±0.9	100.0±0	166.2±18.5

Table D.4 Shape recovery, shape fixity and recovery time values of final composites containing monomer and carbon based fillers at 110°C

Sample	Shape Recovery (%)	Shape Fixity (%)	Recovery Time (s)
Neat Epoxy	98.0±1.0	98.8±1.3	136.2±20.6
E-15N	99.2±1.2	100.0±0	93.4±14.7
E-15N-1CB	99.9±0.3	99.6±0.8	98.6±4.4
E-15N-0.5CNT	99.8±0.3	99.6±0.8	89.6±4.6
E-15N-1CB-0.5CNT	99.7±0.4	98.9±1.0	88.0±9.9
E-15R	98.4±1.1	98.6±0.8	133.8±11.2
E-15R-1CB	99.5±0.5	100.0±0	118.2±7.2
E-15R-0.5CNT	99.4±0.8	99.3±1.0	125.6±12.7
E-15R-1CB-0.5CNT	99.5±0.8	100.0±0	158.2±15.1

Table D.5 Shape recovery, shape fixity and recovery time values of some samples at 110°C subjected to 10 consecutive cycles of shape recovery procedure

	Cycle number	Shape Recovery (%)	Shape Fixity (%)	Recovery Time (s)
Neat Epoxy	1	98.4±1.2	98.7±1.6	119.0±18.8
	2	97.2±1.0	96.7±0.1	212.5±32.0
	3	96.6±0.8	95.5±0.8	219.5±31.8
	4	96.5±0.9	95.9±0.9	207.5±43.0
	5	97.3±1.1	96.2±0.8	245.0±10.0
	6	96.1±0.5	96.2±0.8	240.0±51.6
	7	97.1±1.6	96.2±0.8	230.0±42.4
	8	98.1±1.1	96.7±0.1	258.0±46.9
	9	97.6±1.4	95.8±1.0	239.0±44.3
	10	98.5±1.2	96.2±0.8	278.8±45.9
E-15N	1	98.4±1.1	100.0±0	93.4±14.7
	2	97.5±2.4	97.9±0.8	142.5±36.1
	3	97.5±0.9	97.4±1.0	128.5±28.4
	4	96.9±2.3	98.3±2.0	135.8±40.4
	5	97.9±1.8	98.3±1.4	125.0±28.0
	6	98.5±1.8	98.7±0.9	155.0±37.0
	7	98.6±1.8	97.5±1.0	130.0±42.6
	8	98.2±1.1	97.9±0.8	122.5±26.3
	9	98.3±2.0	98.3±0	121.8±21.1
	10	98.6±1.7	97.9±1.6	127.5±33.0
E-15N-1CB	1	99.9±0.3	99.6±0.9	98.8±5.3
	2	96.9±2.0	99.6±0.9	132.5±25.0
	3	97.0±2.0	99.6±0.9	138.8±28.4
	4	98.4±1.6	98.3±0	122.5±25.0
	5	98.0±2.0	99.1±1.0	120.0±14.7
	6	97.7±1.3	98.7±0.9	126.3±13.8
	7	97.8±2.0	98.7±0.8	114.3±10.2
	8	97.8±1.0	98.7±0.9	112.5±25.0
	9	98.8±2.5	99.6±0.8	113.8±24.3
	10	99.2±1.5	98.3±0	120.0±27.1

Table D.5 (Continued) Shape recovery, shape fixity and recovery time values of some samples at 110°C subjected to 10 consecutive cycles of shape recovery procedure

	Cycle number	Shape Recovery (%)	Shape Fixity (%)	Recovery Time (s)
E-15N-0.5CNT	1	99.9±0.3	99.6±0.9	89.0±4.8
	2	99.2±1.2	99.2±1.7	72.0±21.1
	3	98.4±1.5	99.1±1.0	90.0±7.1
	4	99.2±1.6	99.6±0.8	87.0±6.3
	5	99.5±1.0	99.6±0.8	83.3±12.3
	6	99.3±0.6	99.6±0.9	84.3±7.1
	7	99.8±0.4	99.6±0.9	92.5±6.5
	8	99.3±0.6	99.6±0.9	91.3±10.3
	9	99.0±0.8	100.0±0.0	91.3±7.5
	10	99.4±0.9	99.1±1.0	89.5±9.2
E-15N-1CB-0.5CNT	1	99.8±0.3	98.7±0.9	89.8±10.5
	2	99.0±1.3	99.6±0.8	72.5±9.6
	3	98.5±1.0	99.2±1.0	74.5±11.7
	4	98.0±1.5	100.0±0	72.5±2.9
	5	98.8±1.3	99.6±0.9	81.3±8.5
	6	98.7±1.0	100.0±0	80.0±12.2
	7	98.0±1.4	99.6±0.9	80.0±7.1
	8	98.5±1.0	99.2±0.9	83.8±9.5
	9	98.1±1.1	99.1±1.0	83.8±12.5
	10	98.7±1.7	99.6±0.9	82.5± 6.5

APPENDIX E

ELECTRICAL PROPERTIES

Table E.1 Electrical resistivity values of carbon black and carbon nanotube reinforced epoxy composites

Sample	Log Electrical Resistivity (ohm.cm)
Neat Epoxy	16.00
E-0.5CB	8.92
E-1CB	5.83
E-3CB	2.96
E-5CB	2.61
E-0.25CNT	4.40
E-0.5CNT	3.60
E-1CNT	3.40
E-2CNT	2.00
E-1CB-0.25CNT	4.34
E-1CB-0.5CNT	2.72
E-1CB-1CNT	2.71

Table E.2 Electrical resistivity values of final composites containing monomer and carbon based fillers

Sample	Log Electrical Resistivity (ohm.cm)
Neat Epoxy	16.00
E-15N-1CB	3.59
E-15N-0.5CNT	3.30
E-15N-1CB-0.5CNT	3.03
E-15R-1CB	3.73
E-15R-0.5CNT	3.18
E-15R-1CB-0.5CNT	2.78